Western Graduate&PostdoctoralStudies

Western University
Scholarship@Western

Electronic Thesis and Dissertation Repository

1-8-2018 2:00 PM

Chromatin organizer CTCF in brain development and behaviour

Adrienne Elbert, *The University of Western Ontario*

Supervisor: Berube, Nathalie G., *The University of Western Ontario*

A thesis submitted in partial fulfillment of the requirements for the Doctor of Philosophy degree in Biochemistry

© Adrienne Elbert 2018

Follow this and additional works at: https://ir.lib.uwo.ca/etd

Part of the Developmental Neuroscience Commons

Recommended Citation
Elbert, Adrienne, "Chromatin organizer CTCF in brain development and behaviour" (2018). *Electronic Thesis and Dissertation Repository*. 5215.
https://ir.lib.uwo.ca/etd/5215

This Dissertation/Thesis is brought to you for free and open access by Scholarship@Western. It has been accepted for inclusion in Electronic Thesis and Dissertation Repository by an authorized administrator of Scholarship@Western. For more information, please contact wlswadmin@uwo.ca.

Abstract

Chromatin architecture is an important regulator of gene expression, which dictates development. Mutations in one copy of the *CTCF* chromatin organizer gene cause intellectual disability and autism. Polymorphisms in *CTCF* have also been associated with increased risk for schizophrenia, a condition that overlaps in biological etiology with autism and intellectual disability. In this thesis, we sought to understand the role of CTCF in neurodevelopment using brain-specific conditional knockout and heterozygote mouse models. Using the *Ctcf*-null animals, we identify a cell-autonomous role for CTCF in regulating cortical interneuron development in the medial ganglionic eminence (MGE) through the transcriptional control of *Lhx6.* In the absence of CTCF, MGE-derived cortical interneuron subtypes are inappropriately specified such that their cortical laminar position is altered and there is a reduction in the number of cells expressing PV and SST. These features are rescued with viral-mediated re-expression of *Lhx6*. In addition, there is a concomitant increase in the expression of *Lhx8,* which specifies ventral telencephalic cell types in the MGE, indicating CTCF is an important regulator of cell fate choice in the MGE. To model the human condition associated with *CTCF* mutation, we generated mice heterozygous for *Ctcf* deletion in the developing brain (*Ctcf*$^{\text{NestinHet}}$). These mice had spontaneous hyperactivity and impaired spatial learning on behavioural testing. In addition to these behaviours, male mice had decreased sociability, altered aggression, and decreased anxiety. Together, this constellation of behaviours is reminiscent of other mouse models of schizophrenia, autism and intellectual disability. In addition, structural MRI revealed that *Ctcf*$^{\text{NestinHet}}$ mouse brains had decreased white matter volume, suggestive of hypoconnectivity, a feature commonly attributed to the pathophysiology of autism. There were also significant volume decreases in the cerebellar nuclei, and an increase in the anterior cerebellar lobe. These findings provide further evidence for the emerging role of the cerebellum in cognition and in neurodevelopmental disorders. In summary, this work addresses the consequence of reduced CTCF expression in the developing brain at cellular, structural and behaviour levels, and thus significantly furthers our understanding of chromatin architecture regulation in neurodevelopmental disease.

Words: 338

Keywords

CTCF, chromatin organization, Autism Spectrum Disorder, Intellectual Disability, schizophrenia, epigenetics, medial ganglionic eminence, cortical interneurons, mouse model

Epigraph

“What is it that we rat runners [psychologists who work with rats] still have to contribute to the understanding of the deeds and misdeeds, the absurdities and the tragedies of our friend, and our enemy-homo sapiens? The answer is that, whereas man’s successes, persistences, and socially unacceptable divagations—that is, his intelligences, his motivations, and his instabilities—are all ultimately shaped and materialised by specific cultures, it is still true that most of the formal underlying laws of intelligence, motivation, and instability can still be studied in rats as well as, and more easily than, in men.”

E.C. Tolman (1945)

"P.S. please if you get a chance put some flowers on Algernon's grave in the back yard."

Daniel Keyes, *Flowers for Algernon*

Co-Authorship Statement

Chapter 2:

The project conception was the joint thought product of myself and my supervisor, Dr. Nathalie Bérubé. I completed the majority of the experimental work and analysis, with the exception of the following:

Dr. Daniel Vogt completed the experiments conducted in San Francisco, California involving viral transduction of MGE-cells and MGE-cell transplantation (Figure 7 and Figure 8) in the lab of Dr. John Rubenstein.

Dr. L. Ashley Watson performed the quantitative real time PCR of the *Pcdh* genes (Figure S1) and aided in the generation of *Nestin-Cre* mediated *Ctcf* knockout animals, including those with concomitant PUMA deletion. She also prepared the tissue used for RNA-sequencing.

Dr. Michael Levy performed the analysis of the E14 telencephalon transcriptomes (Figure 1A-B) and of the overlap between CTCF and NKX2.1 ChIP-seq (Figure 3D).

Yan Jiang performed the western blot and Co-IP experiments for NKX2.1 (Figure 3A, C).

Emilie Brûlé assisted with the ISH and quantitative real time PCR of *Gbx2* (Figure 8).

Megan Rowland performed the quantification of serum T4.

Chapter 3:

The project conception was the joint thought product of myself and my supervisor, Dr. Nathalie Bérubé. I completed the majority of the experimental work and analysis, with the exception of the following:

Dr. Michael Levy and Dr. L. Ashley Watson assisted with weighing and measuring clasping. Dr. Michael Levy performed part of the quantitative PCR of *Ctcf* in brain tissues (Figure 1).

Dr. Susanne Schmid assisted with the experimental design examining sensory filtering.

Dr. Jason Lerch performed the MRI and its analysis.

Acknowledgements

I am very grateful for the generous mentorship of my supervisor Dr. Nathalie Bérubé. She provided me with the perfect balance of guidance and intellectual challenges to best promote my growth as a scientist over the last few years. She gave me a fun and unique PhD opportunity, through setting up collaborations and following the results down novel scientific avenues. I not only consider her my role model as a scientist, but also as a person. I am also thankful for the support and knowledge of my committee members Dr. Mellissa Mann and Dr. Thomas Drysdale, and other scientists at the VRL including Dr. Fred Dick, Dr. Andy Babwah and Dr. David Rodenhiser. I always felt their respect and faith in me. These scientists, including my supervisor, motivated me to learn and achieve so as to be continuously deserving of this honour. I feel a tremendous thankfulness to have had the opportunity to do my PhD in the Bérubé lab. I would also like to thank the other students of the Bérubé lab for sharing in the joys and tribulations of graduate work, and for their continued friendship once I returned to medical school. In addition, I would like to acknowledge the assistance and friendship of our technician Yan Jiang, the manager of the VRL mouse facility, Robert Gauthier, and the manager of the Robarts mouse behaviour facility, Matthew Cowan. I am also very cognizant and appreciative of the animal sacrifice that was inherent to the completion of this project. I hope that the significance of the work justifies the loss of animal life. I would also like to thank the groups and agencies that provided me with their generous funding including the CIHR, the OMHF and Schulich School of Medicine and Dentistry. Finally, I would like to thank my parents for their love and support, which came in so many forms over the years, including physical, emotional, and financial … I will also always appreciate their interest in my scientific endeavours.

Table of Contents

Abstract i

Epigraph iii

Co-Authorship Statement iv

Acknowledgements v

Table of Contents vi

List of Tables x

List of Figures xi

1 Introduction 1

1.1 Brain Development 1

1.1.1 General overview 1

1.1.2 Cortical excitatory neurons 2

1.1.3 Cortical inhibitory neurons 6

1.1.4 Ventral forebrain cells specified by the MGE 12

1.2 Chromatin structure and CTCF 14

1.2.1 Basics of chromatin 14

1.2.2 CTCF regulates chromatin higher order structure and gene expression ... 17

1.2.3 CTCF in development 21

1.3 Neurodevelopmental Disorders 23

1.3.1 Overview of Intellectual Disability, Autism Spectrum Disorder, and schizophrenia 23

1.3.2 Regulators of chromatin structure cause neurodevelopmental disorders . 26

1.3.3 CTCF causes autosomal dominant ID and ASD 29

1.3.4 CTCF is associated with SCZ 31

1.3.5 Evidence for cortical interneurons in neurodevelopmental disorders 32

1.4 Mouse models of neurodevelopmental disorders 34

1.4.1 Behavioural phenotyping of SCZ and ID/ASD mouse models 34

1.5 Rationale 38

1.6 Hypothesis.. 38

1.7 Objectives 39

1.8 References.. 39

2 Chapter 2 66

The CTCF chromatin organizer directs the fate of cortical interneurons derived from the MGE... 66

2.1 Abstract 66

2.2 Introduction.. 67

2.3 Results.. 69

2.3.1 RNA-seq of CTCF-null telencephalon identifies clustered protocadherins and genes involved in GABAergic neuron differentiation 69

2.3.2 Ctcf regulates the expression of Lhx6 and Lhx8 in the MGE 71

2.3.3 CTCF acts in parallel to, or downstream of NKX2.1 to regulate Lhx6 and Lhx8 expression 75

2.3.4 CTCF regulates MGE development cell-autonomously........................... 76

2.3.5 MGE-specific deletion of Ctcf leads to a reduction of cortical interneurons expressing Pv and Sst.. 79

2.3.6 Deletion of Ctcf results in altered fate and distribution of MGE-derived cells 80

2.3.7 Forced Lhx6 expression in CTCF-null MGE-derived cells restores SST-expressing interneurons upon transplantation in the cortex of wildtype mice.. 82

2.3.8 CTCF-null MGE cells acquire a GABAergic projection neuron fate....... 84

2.4 Discussion.. 87

2.5 Materials and methods 95

2.6 References.. 102

Chapter 3 111

3 Brain dysmorphology and sexually dimorphic behaviour impairments induced by embryonic CTCF haploinsufficiency 111

3.1 Abstract 111

3.2 Introduction 112

3.3 Results 114

3.3.1 Evidence of allelic compensation in the brain of Ctcf$^{\text{Nestinhet}}$ mice. 114

3.3.2 Ctcf$^{\text{Nestinhet}}$ and NestinCre control mice are smaller and display hind-limb clasping 116

3.3.3 Reduced brain volume in adult Ctcf$^{\text{Nestinhet}}$ mice 116

3.3.4 Abnormal behaviours are observed in Ctcf$^{\text{Nestinhet}}$ mice 119

3.3.5 Anxiety, sociability and aggressive behaviour were observed in male Ctcf$^{\text{NestinCre}}$ mice. 125

3.4 Discussion 127

3.5 Methods 134

3.6 References: 139

Chapter 4 148

4 Discussion 148

4.1 4.1 General overview 148

4.2 The role of CTCF in MGE development 149

4.3 Implication to human disease 161

4.4 Implications to disease treatment 152

4.5 Face validity of the *Ctcf*$^{\text{Nestinhet}}$ mice as a model of the associated human syndrome and SCZ 153

4.6 The male brain is more susceptible to neurological perturbation 154

4.7 The phenotype of *Ctcf*$^{\text{Nestinhet}}$ mice resemble other mutant mouse models of chromatin factors 156

4.8 Construct validity of the *Ctcf*$^{\text{Nestinhet}}$ mice and further evidence for the cerebellum in cognition 158

4.9 Future investigation of GABAergic neurons in *Ctcf*$^{\text{Nestinhet}}$ mice 159

4.10 Limitations of the mouse models 160

4.11 References 163

Curriculum Vitae 172

List of Acronyms

Autism Spectrum Disorder (ASD)
Calretinin (Cr)
Caudal ganglionic eminence (CGE)
CCCTC-binding factor (CTCF)
Choline acetyl transferase (ChAT).
Conditional knockout (cKO)
Cornelia de Lange Syndrome (CdLs)
Dorsal lateral prefrontal cortex (DLPC)
Embryonic Day (E)
Gamma-aminobutyric acid (GABA)
Glutamate decarboxylases (GAD)
Histone acetyltransferases (HAT)
Histone deacetylases (HDAC)
Intellectual Disability (ID)
Interstitial neurons in the white matter (IWMN)
Lateral ganglionic eminence (LGE)
Medial ganglionic eminence (MGE)
Mediator complex (MED)
Morris Water Maze (MWM)
Parvalbumin (Pv)
Post-translational modifications (PTM),
Preoptic area (POA)
Prepulse inhibition (PPI)
Protocadherin (Pdch)
Radial glia cells (RGC)
Reelin (RLN)
Schizophrenia (SCZ)
Serotonin receptor (5HT3aR)
Somatostatin (Sst)
Sonic Hedgehog (SHH)
Subventricular zone (SVZ)
Topologically associating domains (TAD)
Vasointestinal peptide (Vip)
Ventricular zone (VZ)

List of Tables

Table 1: Summary of behaviours of common ASD, ID and SCZ rodent models 34

Table 2: Number of GFP+ cells observed 35 days after MGE cell transplantation for each genotype 94

Table 3: Primer sequences used for genotyping, RT-qPCR, and ISH probe synthesis 95

Table 4: Summary of *Ctcf*^{Nestinhet} behaviours 155

List of Figures

Figure 1: Overview of brain development in mice. 3

Figure 2: Summary of interneuron subtype classification characteristics. 7

Figure 3 Transcriptional profiling of Ctcf-null E14 telencephalon. 71

Figure 4: The *Ctcf*-null embryonic MGE exhibits altered expression of genes implicated in fate specification. 74

Figure 5: CTCF functions in parallel or downstream of Nkx2.1 to regulate *Lhx6* and *Lhx8* . 77

Figure 6: MGE-specific inactivation of Ctcf replicates gene expression changes and extends postnatal survival. 78

Figure 7: Fewer CTCF-null MGE-derived cells reach their destination in the cortex. 79

Figure 8: CTCF is required for final cortical lamination of interneurons.............................. 81

Figure 9: Analysis of transplanted CTCF-null MGE cells and rescue by ectopic *Lhx6* expression. 85

Figure 10: Specification of CTCF-null MGE cells to Lhx8+Gbx2+ GABAergic projection neurons of the globus pallidus. 86

Figure 11: Early deletion of *Ctcf* from neuroprogenitors results in dysregulated expression of Protocadherin (*Pcdh*) clusters. 91

Figure 12: CTCF expression is lost early in conditional knockouts but does not impact number of proliferative cells at peak interneuron-genesis. 92

Figure 13: $Ctcf^{Nkx\text{-}Cre}$ mice have low serum T4 levels... 93

Figure 14: Reduced expression of the *Lhx6* downstream effector *Cxcr4* in the CTCF-null E14 telencephalon. 93

Figure 15: Deletion of Ctcf does not promote fate switch to SP8+ interneuron subtype. 94

Figure 16: CTCF expression in *Ctcf*^{NestinCre} brain suggests significant compensation from the wildtype allele. 115

Figure 17: *Ctcf*^{NestinCre} and *NestinCre* control mice are smaller and develop hind-limb clasping. 117

Figure 18: *Ctcf*^{NestinCre} mice have altered brain anatomy on MRI 118

Figure 19: *Ctcf*^{NestinCre} mice are hyperactive, and male *Ctcf*^{NestinCre} mice have reduced anxiety, compared to control siblings. 121

Figure 20: *Ctcf*^{NestinCre} mice have delays in spatial learning but impairments in short and long-term memory. 122

Figure 21: Figure 6. *Ctcf*^{NestinCre} mice have normal sensory gating. 123

Figure 22: Male *Ctcf*^{NestinCre} have decreased sociability and altered aggression behaviour. . 124

Figure 23: *Ctcf*^{NestinCre} do not have stereotyped or repetitive behaviours. 125

Figure 24: *Ctcf*^{NestinCre} mice display sex differences in hyperactivity and anxiety. 132

Figure 25: *Ctcf*^{NestinCre} mice have normal reversal and motor learning 133

Figure 26: Smaller size of *Ctcf*^{NestinCre} is not correlated with aggression. 133

roduction

n Development

eral overview

Early processes in brain patterning are conserved among vertebrates (reviewed in [1,2]). The nervous system is derived from the ectoderm by inhibition of BMP/TGF-beta signalling (reviewed in [3]). Through the process of neurulation, the neuro-ectoderm forms a hollow tube that divides into three major parts, the forebrain (prosencephalon), midbrain (mesencephalon) and the hindbrain (rhombencephalon), with a central fluid-filled ventricular system. The forebrain is further subdivided into the telencephalon and diencephalon. The cerebral cortex, which is responsible for higher functions such as thought and language in humans, is a large part of the mature telencephalon. The hippocampi (involved in memory formation) and basal ganglia (which function in voluntary movement) are also located in the telencephalon.

The brain consists of neurons and non-neuronal cells called glia. Neurons are a heterogeneous group of electrically-responsive cells that receive and transmit electrical and chemical information. They have specialized cellular structure for this function: the **soma** is the cell body, which houses the nucleus; the **dendrites** are branched extensions that receive signal from another neuron and transmit it to the soma; and the **axon** which is a slender projection that typically transmits signal away from the cell body. In addition, the dendrites can harbour hundreds of spines that function in synaptic transmission.

The telencephalon is the most diverse brain region with respect to neuronal variety[4]. Part of this diversity results from early molecular signals that induce and maintain anterior-posterior and dorso-ventral patterning in the telencephalon[1,3–5], summarized in Figure 1. All neurons are generated from progenitors of specific positional identity, which then migrate to their final position in the mature brain and form the appropriate connections to integrate into functional networks. The final position and functional identity of the mature neuron is based on intrinsic and extrinsic factors. Fate-mapping experiments *in vivo* through cell-labeling, historically through [^{3}H] thymidine and then by genetic means, have revealed the origins and movements of neuron subtypes.

tical excitatory neurons

The cerebral cortex contains a large variety of excitatory neurons (pyramidal and projection) that release the excitatory neurotransmitter glutamate. Cortical excitatory neurons are generated from dorsal progenitors known as radial glia cells (RGC), typically situated in the ventricular zone (VZ), and intermediate progenitors in the subventricular zone (SVZ) (reviewed in [6,7]) between gestational week 5 and 20 (humans) and embryonic day (E) 11 to 19 (mice) (reviewed in [6]). Symmetric division of RGC results in self-renewal of these progenitors, and has been implicated in determining final brain size[5,8]. Retinoic acid signalling induces a switch of RGC to asymmetric, neurogenic divisions. Recently, a subtype of RGC, outer radial glia, that loses the apical process and moves out of the VZ, was also described. Outer radial glia are present in mice, but exist in greater number in the primate cortex. Asymmetric RGC divisions generate one daughter cell identical to the parent cell, and another daughter cell that is an excitatory neuron or an intermediate progenitor (reviewed in [8,9]). Intermediate progenitors typically undergo one division to produce two excitatory neurons.

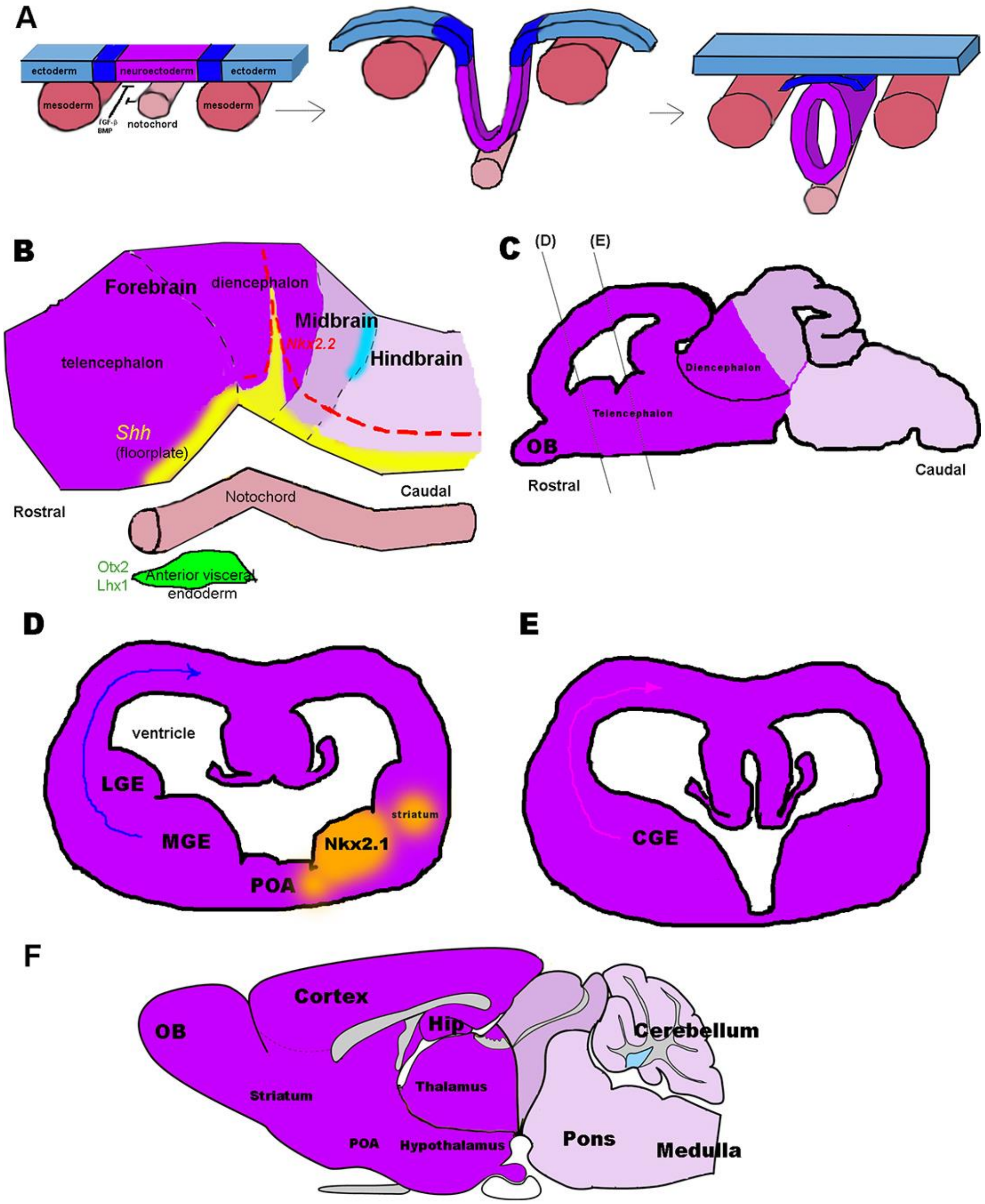
A
ectoderm
neuroectoderm
ectoderm
mesoderm
TGF-β
BMP
notochord
mesoderm
B
Forebrain
diencephalon
Midbrain
Nkx2.2
telencephalon
Hindbrain
Shh
(floorplate)
Rostral
Notochord
Caudal
Otx2
Lhx1
Anterior visceral
endoderm
C
(D)
(E)
Diencephalon
Telencephalon
OB
Rostral
Caudal
D
ventricle
LGE
MGE
POA
Nkx2.1
striatum
E
CGE
F
Cortex
OB
Hip
Cerebellum
Striatum
Thalamus
POA
Hypothalamus
Pons
Medulla

Figure 1: Overview of brain development in mice.

(A) Transverse image of the mesoderm-derived (pink) notochord, which induces neurulation (purple) in the overlying ectoderm (blue). This occurs through the inhibition of TGF-beta / BMP signalling. Some of the implicated molecules include SIP1, SMAD7, and Noggin. The neuroectoderm (purple), also called the neural plate, invaginates and the centre hollows to form the neural tube (secondary neurulation), from which forms the future brain and spinal cord. (B) Sagittal view of the neural tube, which becomes specified from rostral to caudal as forebrain (telencephalon & diencephalon), midbrain, hindbrain, and spinal cord. Organizers, such as the zona limitans intrathalamica (diencephalon) and the isthmus (midbrain-hindbrain junction) secrete morphogens to create boundaries between developing brain regions. The zona limitans intrathalamica is a strong source of SHH (yellow), while the isthmus secretes the dorsalizing morphogen FGF8 (turquoise). Other dorsalizing signals include Retinoic Acid, other FGFs, and WNT. Anterior fate is generated in the absence of dorsalizing signals. Also, the head does not form without influence of the anterior-lying anterior visceral endoderm (AVE) which expresses *Otx2* and *Lhx1,* among other transcription factors. The floor or basal plate of the neural tube expresses the diffusible morphogen SHH (yellow), the major ventralizing signal in the neural tube. *Nkx2.2* (red) expression is induced at high concentrations of SHH, and creates the alar-basal boundary from the hindbrain to the diencephalon. (C) Sagittal view of the embryonic brain (E13.5). Different shades of purple correspond to forebrain, midbrain, and hindbrain. Black lines indicate the two levels at which coronal sections are shown in (D) and (E). (D) Rostral coronal section through the embryonic (E13.5) mouse telencephalon, depicting the POA, MGE and LGE on both sides. NKX2.1 expression (orange) is located in the MGE (depicted only on one half for simplicity), and in the striatum, to where MGE-cells have begun to migrate by E13.5. The arrow indicates the path of tangential migration of MGE cells destined to the cortex. (E) Caudal coronal section through the embryonic (E13.5) mouse telencephalon, depicting the CGE. The arrow indicates the path of tangential migration of CGE cells to the cortex. (F) Sagittal view of the adult murine brain coloured different shades of purple to indicate the forebrain, midbrain and hindbrain. Some major structures are indicated. OB= olfactory bulb, Hip= hippocampus. Adapted from Puelles and Rubenstein 2015[1].

With the exception of the olfactory cortex and part of the temporal lobe, the human cerebral cortex is organized into six functionally and anatomically distinct layers of excitatory neurons. The layers are generated such that layer VI is closest to the SVZ, and is formed first. Successive layers of excitatory neurons are formed in an inside-out manner by tightly controlled progenitor divisions and radial migration of daughter-cells (reviewed in [6]). Not only do RGCs act as progenitors, but their basal processes also form a scaffold for the migration of excitatory neurons. Migration is guided, therefore, by interactions with the radial glial process, along with other intrinsic and extrinsic factors[10]. One such extrinsic factor is REELIN (RLN), a glycoprotein secreted by the Cajal-Retzius cells in the marginal zone (layer I) (reviewed in [5,11]).

Transplant experiments indicate that layer identity of the neuron is determined at the level of the progenitor cell, which responds to extrinsic cues to generate the neuron subtype for the appropriate developmental age (reviewed in [9]). Moreover, retroviral-labeling experiments suggest the existence of two different progenitor populations, one generating layers II-IV, and the other V-VI, and this remains incompletely understood[6]. One proposed explanation is the coexistence of both multipotent and restricted progenitors.

The vast majority of excitatory neurons (reviewed in [6,9]) are pyramidal neurons, characterized by their single long apical dendrite. Pyramidal neurons are found in all cortical layers except layer I. In contrast, spiny stellate neurons are a locally-connecting excitatory neuron with several dendrites of similar lengths. Spiny stellate neurons are specialized in receiving the majority of thalamic inputs and are found exclusively in layer IV. The majority of locally targeting pyramidal neurons are located in layers II and III. Some pyramidal neurons can be sub-classified as projection neurons if they connect i) to distant cortex (associative or commissural projection neurons), or ii) to non-cortical brain regions (corticofugal projection neurons). Commissural projection neurons connect via either the corpus callosum or the anterior commissure. Cortifugal projection neurons (reviewed in [12]) can be sub-divided by hodology, into i) corticothalamic (layer VI), ii) corticopontine, corticospinal, and corticotectal (layer V), and ii) corticostriatal neurons.

tical inhibitory neurons

The second major class of cortical neurons are inhibitory neurons that release gamma-aminobutyric acid (GABA), which is the main inhibitory neurotransmitter of the adult brain. They comprise 20-30% of cortical neurons in primates[13] and 10-15% in rodents[14]. In the adult mammalian brain, GABAergic cells are identified by the expression of two isoforms of glutamate decarboxylases (GAD), GAD 67 or 65, expressed from *Gad1* and *Gad2* genes, respectively. They are also called *interneurons* as they form local connections, where there role is to gate signal flow, shape and synchronize network outputs, and generate cortical rhythms[15].

Many different subtypes of cortical interneurons exist, but there is currently no consensus on a formal classification system[15]. Cortical interneurons can be classified by marker expression, firing properties, and morphology (Figure 2). Morphologically, they can be grouped by the laminar position of their soma, and shape of their dendrites and axon, and can even be described by the preferred targeted subcellular domain of their axons (ie soma, dendrite or axon)[15]. Electro-physiologically, firing capacity can vary due to differences in processing of signals from other cells, including other interneurons through different GABA receptor subunit expression[16]. In terms of markers, nearly 100% of *Gad1*-expressing cells in the cortex can be captured by staining for the markers *somatostatin* (*Sst), Parvalbumin* (*Pv),* and *serotonin receptor* (*5HT3aR*)[17,18] (reviewed in [15]). In the past, *Calretinin* (*Cr*) has also been used with *Sst* and *Pv* to classify nearly all cortical interneurons, albeit both *Cr* and *5HT3aR* have some overlap with *Sst*[19].

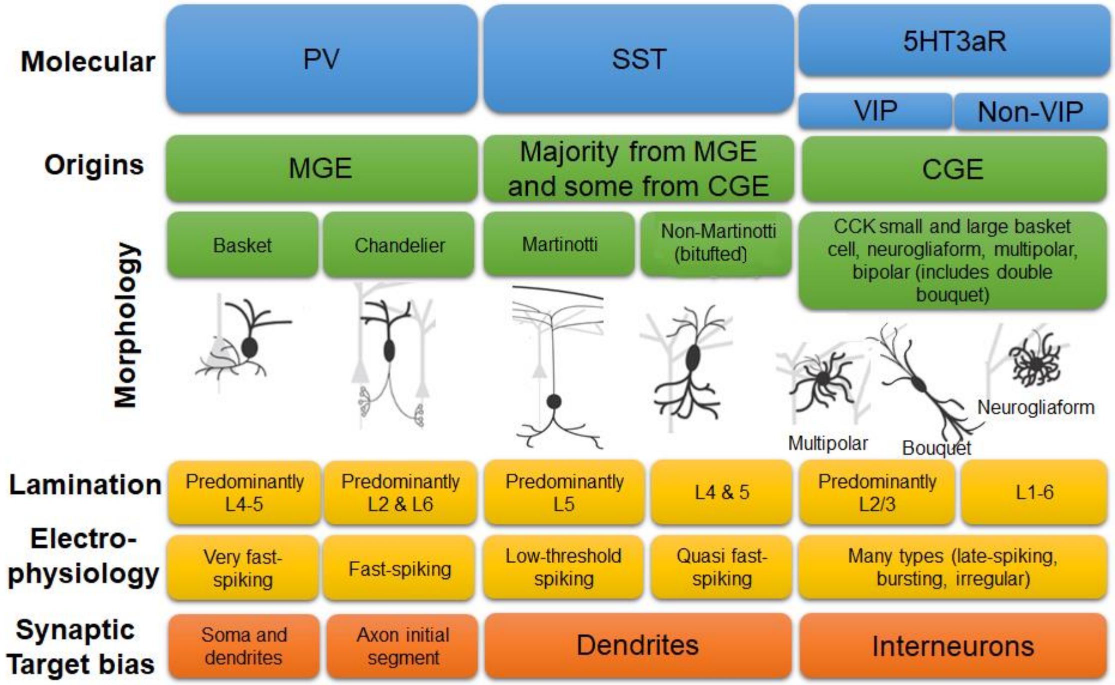
Molecular
PV
SST
5HT3aR
VIP
Non-VIP
Origins
MGE
Majority from MGE and some from CGE
CGE
Morphology
Basket
Chandelier
Martinotti
Non-Martinotti (bitufted)
CCK small and large basket cell, neurogliaform, multipolar, bipolar (includes double bouquet)
Multipolar
Bouquet
Neurogliaform
Lamination
Predominantly L4-5
Predominantly L2 & L6
Predominantly L5
L4 & 5
Predominantly L2/3
L1-6
Electro-physiology
Very fast-spiking
Fast-spiking
Low-threshold spiking
Quasi fast-spiking
Many types (late-spiking, bursting, irregular)
Synaptic Target bias
Soma and dendrites
Axon initial segment
Dendrites
Interneurons

Figure 2: Summary of interneuron subtype classification characteristics.

Adapted from Tremblay, et al. 2016; and morphology images from Themes, 2016.
1. Tremblay, R., Lee, S. & Rudy, B. GABAergic Interneurons in the Neocortex: From Cellular Properties to Circuits. Neuron 91, 260–292 (2016).
2. Themes, U. F. O. Neocortical Anatomy and Physiology. Neupsy Key (2016).

Unlike the excitatory neurons of the cortex, which are generated *in situ*, the interneurons are generated outside of the future neocortex. Cortical interneurons are generated from neuroprogenitors in the ventral telencephalon, and then migrate tangentially into the forming cortical layers during development. In rodents, they are generated in the preoptic area (POA), and transient embryonic structures known as the medial ganglionic eminence (MGE) and the caudal ganglionic eminence (CGE), between E12-14[20] (Figure 1). In humans, there is some evidence that cortical radial glia have the potential to generate GABAergic neurons[21], however the vast majority of interneurons are also produced in the

VZ and SVZ of ganglionic eminences, rather than from the cortex, and many are derived from a non-epithelial neural stem cell in the SVZ, during the early second trimester (weeks 8 to 14)[22]. The MGE produces the majority (approximately 70%) of the cortical interneurons in rodents[23] (reviewed in[20]). In contrast, it appears that the majority of human cortical interneurons are generated in the CGE rather than the MGE[22]. The POA in mice contributes to less than 10% of interneurons[24].

Early specification of interneurons

As a class, cortical interneurons can be recognized in the cortex by early expression (E10.5) of the *Distal-less homebox (Dlx)* genes, which are arranged in bigenic clusters, and drive expression of *Gad1/2*, required for GABA production[25,26]. *Dlx* genes are also expressed in GABAergic projection neurons in the ventral forebrain discussed in a later section. *Dlx1/2* appear to be required for early differentiation, as they are already expressed in the VZ and SVZ of the ganglionic eminences, whereas *Dlx5/6* are turned on in the migrating interneurons[27]. Inactivation of both *Dlx1/2* is perinatal lethal, and results in a failure of cortical interneurons to migrate tangentially to the cortex[28]. The neurons stay as ectopia in the basal ganglia, resulting in a 75% reduction of interneurons in the cortex[28,29]. In these double-knockout mice, *Dlx5/6* expression is also reduced[28], most likely due to their failed activation by DLX2, which binds at the intergenic enhancer, I56i[30]. *Dlx1/2* have at least two intergenic regulatory elements, I12a and I12b[31,32]. The migratory function associated with *Dlx1/2* is thought to be regulated in part due to DLX2 activation of *Aristaless related homeobox* (*Arx*). ARX is expressed in tangentially migrating cortical interneurons and activates the expression of cell surface receptors implicated in interneuron migration, including C-X-C chemokine receptor type 4 (CXCR4)[33,34].

CGE-derived cortical interneurons

The CGE consists of two subdomains: the ventral CGE is the caudal extension of the MGE and the dorsal part is an extension of the lateral ganglionic eminence (LGE)[29,35] (Figure 1). The CGE can however be distinguished from both the MGE and LGE by marker expression, such as COUP-TFII[29,36,37]. The cortical interneurons derived from the CGE have a distinct pattern of tangential migration, preferentially contribute to different cortical laminar positions, and have different marker expression[36]. Transplant experiments suggest these features are intrinsic, rather than induced by local cues, suggesting that the CGE is more than just an extension of other structures, but represents a unique group of progenitors with diverse potential[36].

All CGE-derived cortical interneurons express 5HT3aR[18]. These can be further divided into those that express *Vasointestinal peptide* (*Vip*) and those that do not. About 40% of the 5HT3aR subtype of interneurons express *Vip,* and there is no overlap between *Vip* and *Pv* or *Sst*[18]. About 27% of E13.5 CGE cells go on to express *Sst*, whereas less than 3% have detectable *Pv* expression[36]. Other markers expressed by a large portion of CGE-derived interneurons are *Cr, Rln, Prox1* and *Sp8*[38]. Morphologically, CGE-derived interneurons can have radially-oriented processes, multipolar-shape, or neurogliaform shape[18]. CGE-derived cortical interneurons can occupy any laminar position, but are preferentially positioned in more superficial layers[36,39].

In terms of their migration, CGE-derived interneurons tend to migrate into the cortex later than those from the MGE[38]. The ability of CGE-derived interneurons to tangentially migrate along the posterior cortex is in part due to COUP-TFII expression[37]. In addition, CGE-derived interneurons were found to travel along two novel other caudo-rostral streams, one laterally towards the LGE (requiring COUP-TFI expression), and one medially towards the POA[38].

MGE-derived cortical interneurons

The MGE is a source of cortical interneurons, striatal neurons, globus pallidus cells, amygdala cells, oligodendrocytes, and to a lesser extent, hippocampal interneurons[29,36,40,41]. Specification of the MGE is dependent on the expression of NKX2.1 which is detectable in the telencephalon from approximately E9.5[42]. NKX2.1 is present in the proliferating cells of the MGE and its expression depends on sonic hedgehog (SHH) signalling[43]. Homozygous targeted deletion of *Nkx2.1* in mice results in perinatal death, and although an MGE-like structure forms, it appears to be re-specified to LGE fate, which generates GABAergic medium spiny neurons destined for the striatum[44]. Therefore, in *Nkx2.1* mutant mice, the early migrating MGE-derived cortical interneurons are not generated, whereas the late-migrating CGE-derived cortical interneurons are unaffected[44,45].

The function of NKX2.1 was further studied by its conditional deletion at E10.5, and at E12.5, which allows the initial formation of the MGE[46]. Under both conditions, the authors observed that the cortical interneurons generated from the MGE were re-specified to CGE-like cortical interneurons. For example, the neurons preferentially expressed CGE markers VIP and CR at the expense of PV and SST, and had firing patterns of late-spiking neurogliaform-type interneurons. In addition, earlier deletion of *Nkx2.1* reproduced previous work; there was a reduction in total cortical interneuron numbers and a concomitant increase in the generation of LGE-type, GABAergic medium spiny neurons destined for the striatum. These results highlight the dual function of NKX2.1 as i) specifying MGE versus LGE fate in early forebrain cells, and ii) specifying PV and SST interneuron subtypes over the seemingly default CGE-like subtypes later in development. This second role of NKX2.1 was eventually shown to be due to the downstream activation of the LIM homeodomain transcription factor LHX6[47], discussed in detail below. As cells exit the cell cycle and reposition in the SVZ of the MGE, NKX2.1 directly induces the expression of *Lhx6*[35,48], through binding to a site 240 bases upstream of the transcription start site[49]. The immature *Lhx6*-expressing neurons of the MGE SVZ produce GABA[40,48] and are referred to as proto-GABAergic neurons.

Counter-intuitively, down-regulation of *Nkx2.1* is required in post-mitotic LHX6-positive MGE-derived cells for their migration to the cortex[50]. The ectopic expression of NKX2.1 in these cells leads to their accumulation in the striatum. The cortical interneurons from the MGE were shown to express Neuropilin-1 and 2, receptors for the migratory-repellents semaphorin-3A and F, respectively, present in the developing striatum[51]. NKX2.1 inhibits the expression of Neuropilin transcripts, and therefore its down-regulation in MGE-derived cortical interneurons is required for their avoidance of the striatum and continued tangential migration into the neocortex[50]. In addition to semaphorins, MGE-derived cells destined for the cortex are guided through a ventral permissive corridor by ERBB4/ neuregulin-1 (NRGN1) signalling[52].

As mentioned above, deletion of *Nkx2.1* specifically results in a loss of PV and SST cortical interneuron subtypes. Du *et al.*[49] performed elegant experiments in which electroporation of *Nkx2.1* or *Lhx6* cDNA into *Nkx2.1*-null cultured embryonic brain slices, followed by transplantation into wildtype neocortex, rescued the number of SST and PV positive interneurons. As expected, *Lhx6* mutant animals also do not produce PV and SST cortical interneuron subtypes[48,53]. PV-expressing cortical interneurons are typically described as Chandelier cells (also called axo-axonic) and Basket cells (the majority of which are fast-spiking). This fast-spiking property allows PV-positive interneurons to contribute to synchronizing excitatory neuron firing into gamma oscillatory waves[15,54]. SST-expressing interneurons are typically categorized as Martinotti cells and bitufted cells[15].

Lhx6-null MGE cells appear to lose the ability to become PV and SST subtypes, while acquiring a CGE-like fate[47]. Electro-physiologically, *Lhx6*-null MGE cells were no longer fast-spiking, but instead had late-spiking properties of neurogliaform interneurons. In addition, there was an increase in the expression of CGE-cell marker SP8, and a preference to laminate to superficial cortical layers, especially layer I.

In addition, LHX6 was shown to bind and activate the *Arx* and *Cxcr7* genes involved in interneuron migration[47]. Transduction of *Lhx6*-null cells with *Arx* cDNA partially rescued the expression of PV and SST, but did not significantly alter the number of *Lhx6*-null cells that ended up ectopically in layer I of the cortex. Alternatively, transduction with *Cxcr7* cDNA partially rescued the lamination defect but not PV or SST expression, suggesting these downstream effectors of LHX6 are required for different downstream functions.

tral forebrain cells specified by the MGE

The MGE-derived cells that are destined to remain in the ventral forebrain maintain the expression of NKX2.1 to become striatal cholinergic and GABAergic interneurons, as well as GABAergic projection neurons of the basal forebrain[55]. Cholinergic neurons release acetylcholine and are identified by the expression of the rate limiting enzyme in its synthesis, choline acetyl transferase (ChAT). These cholinergic and GABAergic interneurons of the striatum were shown to mature from the proto-GABAergic neurons[41]. The specification to cholinergic versus GABAergic fate was shown to depend on the combinatorial expression of LHX6, and two other LIM homeodomain transcription factors, ISLET-1 (ISL1) and LHX8[41].

Like LHX6, LHX8 is also induced in post-mitotic cells of the MGE SVZ. However, LHX8 is down-regulated in MGE-derived cells destined for the cortex. The MGE cells that maintain dual expression of LHX6 and LHX8 migrate tangentially and become the GABAergic striatal interneurons, which constitute approximately 1-2% of striatal neurons[41]. In contrast, some of the proto-GABAergic neurons down-regulate *Lhx6* and maintain the expression of LHX8 and ISL1, specifying these cells to the cholinergic fate, constituting approximately 0.3% of the striatal neurons[41]. Interestingly, when *Lhx8* was deleted, there was a reduction in cholinergic forebrain interneurons in exchange for an increased number of GABAergic striatal interneurons expressing LHX6[41,56]. Another transcription factor, gastrulation brain homeobox 2 (GBX2), functions downstream of LHX8, and is required for the specification of the cholinergic striatal interneurons[57].

Despite the seemingly oppositional roles of LHX6 and LHX8 in specifying GABAergic versus cholinergic fate, there is evidence that these transcription factors have overlapping function. For example, when *Lhx6*-null MGE cells are transduced with ectopic *Lhx8* cDNA before transplantation into the cortex, this partially rescues PV and SST expression, as well as cortical lamination defects[47].

In addition, *Lhx8* mutant mice not only had a loss of cholinergic interneurons, but also had a loss of basal forebrain projection neurons, which are non-cholinergic, and typically GABAergic[58]. The cells destined to become basal forebrain projection neurons migrate radially from the MGE and require not only LHX8, but also GBX2 expression[57].

omatin structure and CTCF

cs of chromatin

In the eukaryotic cell, DNA is organized with associated proteins, and this complex is referred to as chromatin. The organization of DNA is dependent on the dynamic nature and modification of these proteins, termed chromatin remodeling, which in turn governs virtually all cellular function through precise regulation of gene expression[59].

The basic unit of DNA organization is known as the nucleosome, in which the negatively-charged linear DNA is tightly packaged with four pairs of positively-charged histones[60]. In the canonical nucleosome these four histones are H2A, H2B, H3 and H4, but these can be replaced by others in specific contexts (reviewed in [61]).

Histone H1 coats the so-called “linker DNA” between adjacent nucleosomes, and stabilizes the next levels of chromatin folding. The nucleosome-wrapped DNA is then thought to coil on itself into a 30 nm wide fiber, which can then be folded and looped into higher order tertiary structures. Epigenetics refers to the molecular determinants influencing chromatin structure, and this includes DNA methylation, nucleosome composition, histone post-translational modifications (PTM), and any non-coding RNAs and protein factors that regulate these.

Methylation of cytosine residues in DNA occurs through methyltransferases, and high levels of 5-methylcytosine residues are correlated with gene silencing (reviewed in [62]). However, DNA methylation also occurs in exons of actively transcribed genes, and is thought to influence mRNA splicing[63]. There are also *in vivo* derivatives of 5-methylcytosine with unknown function; 5-formylcytosine, 5-carboxylcytosine, and 5-hydroxymethylcytosine. In particular 5-hydroxymethylcytosine may be relevant to brain function, as it is enriched at intron-exon boundaries of genes encoding synapse proteins[64].

Histone PTM occurs at the N-terminal tails, which protrude from the nucleosome, and is an essential epigenetic mechanisms of gene regulation (reviewed in [65]). PTM include, but are not limited to, methylation, acetylation, ubiquitination and phosphorylation. For example, histone acetylation is dynamically introduced and erased by histone acetyltransferases (HAT) and histone deacetylases (HDAC), respectively. These PTM are recognized by “reader” proteins and complexes that can execute further changes to chromatin organization.

Many studies have attempted to decode the language of histone PTM (the histone code), and there has been some consensus in this realm. Acetylation of lysine residues (in particular at H3K9, H3K14) is associated with accessible, active genes (euchromatin)[65]. Trimethylation at H3K4 also tends to mark promoters of active genes[66], whereas H3K9 and H3K27 trimethylation are associated with repressed genes (reviewed in [67]). Recently, attempts have been made to direct functional states of chromatin through the synthesis of defined, modified histones in order to better interrogate the role of specific PTM in chromatin regulation (reviewed in [68]). However, there appears to be exceptions to every rule, and the so-called histone code is elaborate and cell-context dependent, with the significance of different combination of PTM still being a topic of research, and the number of novel PTM still growing (reviewed in [69]).

The readers of PTM are often associated with ATPase function to allow for ATP-dependent remodeling of chromatin at the target site. One of the functions of ATP-dependent chromatin remodelers (reviewed in [70]) is to displace nucleosomes to expose DNA sequences to DNA binding factors.

Higher order chromatin structure refers to the three-dimensional, looped organization of the chromatin in the nucleus. The techniques of fluorescent in situ hybridization (FISH), chromosome conformation capture (3C), and techniques derived from 3C (reviewed in [71]) have allowed scientists to begin to characterize higher order chromatin structure, and understand the factors that regulate it. Ubiquitous factors such as the mediator complex (MED), CCCTC-binding factor (CTCF, discussed in next section), and a complex of proteins called cohesin, have been implicated in loop formation (reviewed in [72]). MED is a complex of up to 26 subunits that is involved in gene activation, and can mediate loop structure formation through interacting simultaneously with multiple proteins at different, distant chromatin sites[72]. Cohesin is a ring-shaped complex of proteins that was originally characterized for its role in sister chromatid cohesion during mitosis and meiosis and double-strand DNA break repair (reviewed in [73]). The cohesin complex is thought to stabilize loop structures by encircling chromatin strands[74]. The ring shape is formed by SMC1, SMC3, and RAD21, whereas SA1/2 interacts with RAD21 to target cohesin to appropriate genomic sites (reviewed in [73]).

Although incompletely understood, Hi-C experiments have shown that chromosomes are further compartmentalized into topologically associating domains (TAD), which are regions of chromatin with distinct epigenetic signatures that are characterized by a high number of intra-domain interactions[75]. Intra-domain chromatin loops allow for communication between promoters and enhancers that may be hundreds of kilobases apart. TAD boundaries represent transitions between differing epigenetic signatures, and are marked by insulator sequences bound by cohesin and CTCF[76]. Many aspects of TADs are concordant across multiple cell types, and even shared between human and mouse[77].

CF regulates chromatin higher order structure and gene expression

CTCF is a highly conserved, ubiquitously expressed, eleven zinc finger protein that has multiple functions (reviewed in [78,79]). The mammalian CTCF coding sequence is nearly identical to that of chicken (93% shared amino-acids), indicating conservation of protein structure, and likely function, over the past 300 million years (reviewed in [80]). In the mammalian *CTCF* gene, exons 4 through 10 encode the eleven zinc fingers, which allow for DNA and protein binding. CTCF binding is methylation sensitive, and it can bind to a variety of unmethylated DNA sequences through different combinatorial participation of its zinc fingers. CTCF binds to approximately 50,000 sites across the mammalian genome[81–84].

CTCF-mediated chromatin looping has been shown to regulate gene expression by promoting promoter-enhancer interactions and by maintaining topological boundaries between chromatin regions with differing epigenetic signatures[85–87]. Up to one third of CTCF occupied sites are concordant across different cell types (ie constitutive sites)[88]. These sites map to TAD boundaries, suggesting these sites contribute to general genomic structure either TAD maintenance or establishment[88]. In support of this, the depletion of CTCF caused a reduction in within-domain interactions and an increase in inter-domain ones[76]. The non-constitutive binding sites, which account for between 30 to 60% (depending on the mammalian species), vary among cell types[81,82,84,85]. These cell-type specific CTCF sites are enriched in enhancer elements and are suggested to be involved in cell fate or lineage specifying programs by regulation of gene expression[89,90]. However, only a handful of CTCF occupied sites participate in chromatin looping at a given time in a cell, indicating that these chromatin interactions are dynamic[91].

Chromatin looping not only functions to mediate enhancer-promoter interactions, but also to physically block a gene from activating regulatory elements; this mechanism of regulation is known as insulation. In vertebrates, CTCF is the only protein known to bind insulator sequences to elicit this blocking effect[92]. This function occurs through the formation of a loop structure in which the gene promoter can no longer physically interact with regulatory elements required for its expression[93,94].

The zinc fingers of CTCF allow for its interaction with a huge diversity of protein binding partners and PTM[95]. As CTCF mediates chromatin loop structures through simultaneous interaction with DNA and chromatin-bound proteins at distant sites, its promiscuity in protein-binding partners allows for looping specific to cell-types and developmental contexts[78,79]. As with MED, stabilization of the CTCF-based loop structure often also involves cohesin. The cooperation of cohesin and CTCF in chromatin loop formation and gene regulation has been demonstrated at multiple loci (the HOXA cluster[96,97]; the H19/Igf2 locus[98], the IFNG locus[99], the beta-globin locus[100], and the MHC class II locus[101]), some of which are discussed below. Cohesin and CTCF binding sites largely overlap across the genome, especially near active genes[74,102], and multiple studies have shown altered gene expression with the depletion of either CTCF or cohesin at specific loci[94,98–101].

To summarize, CTCF has both ubiquitous and cell-specific functions in higher order chromatin organization, which are mediated by chromatin looping. These functions often occur in cooperation with cohesin and regulate gene expression, through physically promoting or impeding interaction between distant loci[93]

CTCF and imprinted gene regulation

CTCF has been extensively studied at the imprinted H19/ Igf2 locus[98,103–107]. In genomic imprinting, one of two parental alleles of the gene is repressed though epigenetic mechanisms[108]. Imprinted genes are regulated in clusters by imprinting control regions with allele-specific methylation patterns. At the *H19/ Igf2* locus, CTCF binding at the unmethylated maternal imprinting control region has multiple functions (reviewed in [106]). First of all, CTCF binding has insulator function, as it prevents the activation of the maternal *Igf2* allele by a downstream enhancer. This is hypothesized to occur through chromatin interactions that place Igf2 in a repressive loop (reviewed in [106]). CTCF is also implicated in the allelic differences in replication timing at the *H19/ Igf2* locus and in influencing the chromatin marks in the region[109]. In the mouse postnatal brain, the chromatin remodeling protein ATRX has been shown to be required for CTCF recruitment and appropriate expression of the maternal allele of *H19*[105]. ATRX is thought to displace nucleosomes at the site through its translocase function and expose binding sites for CTCF[107]. CTCF has also been shown to regulate allele-specific chromatin changes at the

11p15 imprinted locus, where defects result in Silver-Russell and Beckwith-Wiedemann Syndromes (reviewed in [110]).

CTCF and PUMA/ *Bbc3* regulation

The *Bbc3* gene encodes a pro-apototic factor called P53-upregulated modulator of apoptosis (PUMA). Upon P53 activation, PUMA is expressed (exons 1b, 1a, 2, 3, 4) and causes caspase-mediated cell death. Interestingly, when P53 signaling is not active, the middle exons of the *Bbc3* gene (exons 1a, 2 and 3) are constitutively expressed as a long RNA with no known protein coding function[111]. The boundaries of the constitutively transcribed portion are demarcated by CTCF and cohesin binding, as well as by a sharp transition from permissive epigenetic marks (H3K9Ac and H3K4me3) to silencing ones (H3K9me3). Upon CTCF knockdown, the cohesin complex was not recruited and chromatin boundary signature was reduced, leading to expression of PUMA-coding RNA[111]. *In vivo*, deletion of *Ctcf* from the murine limb bud resulted in PUMA expression and was accompanied by apoptosis and deformity of limb structures, a feature common in Cornelia de Lange Syndrome (CdLS)[112]. Together this suggests that CTCF and cohesin function together to repress PUMA expression in the absence of P53.

CTCF and protocadherin gene regulation

The accuracy of neuron connectivity is intimately tied with neuronal diversity at the level of the individual cell. In particular, the independent, stochastic mono-allelic autosomal expression of clustered *protocadherin* (*Pdch*) genes has been implicated. Whether the expression of the variable exon is from the maternal or paternal allele is independently regulated for each *Pcdh* gene, creating a unique combination at the level of the neuron (reviewed in [113]). The combinatorial expression of approximately 50 *Pcdh* genes (α-, β-, and γ- clusters), which are members of the cadherin superfamily of homophilic cell-adhesion molecules, guides neuronal connections by creating a large number of possible selective binding units for neuron-neuron interactions and by allowing dendrite self-avoidance (reviewed in [113]). *Pcdh* promoter choice is determined by promoter/ enhancer interactions, through CTCF and RAD21 (member of the cohesin complex) binding. CTCF binding at a *Pcdh* promoter occurs in association with its activation and is dependent on the binding-site orientation, which is evidence that this function is mediated through loop structures.

CF in development

In vivo, RNAi-mediated knock-down of *Ctcf* in oocytes leads to transcriptional dysregulation, mitotic defects and apoptosis in 4-cell stage embryos[114]. In a later study, Moore *et al*.[115] generated embryos with loss-of-function *Ctcf* alleles to distinguish effects of maternal *Ctcf* loss from those of zygotic. These embryos developed up to the blastocyst stage but then underwent cell death as maternal stores of *Ctcf* transcript became depleted. Together, these results indicate that CTCF is an essential protein that is necessary for embryonic development. Conditional deletion of *Ctcf* in the developing limb bud results in widespread apoptosis, recapitulating the effects of *Ctcf* loss in the embryo[112]. However when *Ctcf* is ablated in thymocytes, these cells do not undergo cell death, but instead undergo cell cycle arrest due to increased expression of p21 and p27, and are unable to differentiate into mature αβ T cells[116]. These findings show that the tissue-specific function of CTCF is diverse, but that roles in cell survival and mitosis are likely shared functions in many cell types.

CTCF in brain development

Hirayama *et al.*[117] generated a *Ctcf* conditional knockout (cKO) mouse in projection neurons using the *Nex-Cre* driver line and *floxed Ctcf* mice. These cKO mice had postnatal growth retardation and displayed abnormal hind-limb clasping, which is a sign of neurologic dysfunction. Expression studies revealed that nearly all clustered *Pcdh* genes were down-regulated. The cKO neurons managed to form synapses, but with reduced dendritic arborisation and spine density. In addition, these cKO mice had disorganized somatosensory cortices. Normally, the pathway from each whisker to the somatosensory cortex is organized into "barrelettes". In the *Ctcf* cKO mice, staining revealed that the barrel segmentation pattern was completely lost, indicative of impaired somatosensory mapping during development.

Watson *et al.* [118] generated two additional *Ctcf* cKO mice in embryonic brain tissue. In the first, *Ctcf* is deleted using the *Foxg1-Cre* driver line at E8.5 in the forebrain and anterior retina. This resulted in massive expression of PUMA, and associated apoptosis. The second *Ctcf* cKO model made use of the *Nestin-Cre* driver line, which mediates deletion of *Ctcf* at approximately E11 in neuroprogenitors across the CNS. Deletion of *Ctcf* in embryonic neuroprogenitors resulted in microcephaly, and perinatal death of resultant pups. The apoptosis was rescued by concomitant deletion of *Bbc3*, the gene encoding PUMA, but microcephaly and perinatal lethality were not. These were found to result from aberrant proliferation of *Ctcf*-null radial glia in the VZ/ SVZ and IZ, resulting in premature depletion of the neuroprogenitor pool. The effects of *Ctcf* loss on proliferation in this cell population are likely in part due to DNA damage (unpublished data, [119,120]).

Another group created *Ctcf* cKO mice using the *CamKIIa-Cre* driver line, which deletes *Ctcf* in excitatory neurons starting at post-natal day (P) 5, to determine the role of CTCF in learning and memory[121]. These cKO mice had growth similar to controls, but lifespan was shortened to about 4 months of age, after massive apoptosis in the hippocampus. The dendritic morphology in the hippocampi of 10-week old cKO mice was intact, with the exception of the CA1 region, where there was a reduction in spine density with the loss of *Ctcf.* This was associated with deficits in long-term potentiation, the physiological driver of learning & memory, as measured from the CA1 in cultured slices. Unsurprisingly, 10 week old *Ctcf* cKO had impaired contextual and cued fear memory and impaired spatial memory in the MWM paradigm. In addition, these cKO mice had normal sociability but had no preference for a novel versus familiar mouse, suggestive of a social memory deficit. Next Sams *et al* performed RNA-sequencing in 10 week old *Ctcf* cKO and control hippocampus and found that *Pcdh* were down-regulated, similarly to other studies.

rodevelopmental Disorders

rview of Intellectual Disability, Autism Spectrum Disorder, and schizophrenia

Autism spectrum disorder (ASD) is a persistent neurodevelopmental condition beginning in childhood, characterized by i) restricted, repetitive behaviour, and ii) problems with social and adaptive functioning, and communication. These behaviours can present as motor stereotypies, compulsions, insistence on sameness, reduced eye gaze, literal use of words, and poor pragmatic skills. Individuals with ASD also often have Intellectual Disability (ID), although either condition can occur without the other. ID typically corresponds to an IQ below 70 with deficits in adaptive skills, and affects about 1% of the population[122].

Schizophrenia (SCZ) typically onsets in young adulthood and is a disease that leads to altered perception of reality [123]. SCZ is characterized by positive and negative symptoms, in addition to disordered thoughts and impaired cognition[123]. Cognitive dysfunction in SCZ can manifest as sensory-gating abnormalities, which result in the inability to filter irrelevant sensory information (reviewed in [124]). Cognitive dysfunction can also manifest as a decrease in working memory, measured traditionally using the Wisconsin card sorting task[125]. The dorsal lateral prefrontal cortex (DLPC) is critical for working memory, and post-mortem studies have repeatedly found gray matter loss and reductions in spine density in this brain region[126,127]. Positive symptoms include hallucinations and delusions, and these are typically responsive to medications which block dopamine receptors (reviewed in [128]). Negative symptoms pertain to a loss of motivation, impaired emotional expressivity, and social dysfunction.

Evidence suggests that ASD, ID and SCZ have common causal biological factors and may exist on a genetic and clinical continuum[129,130]. Both disorders result from perturbations of shared genetic pathways and insults during vulnerable periods of brain development from *in utero* through to early adulthood, converging on mechanisms that lead to altered brain connectivity, such as migration and lamination defects, altered cell proliferation, and abnormal synapse function and number (reviewed in [131]). In the case of SCZ, these insults seem to perturb three neurotransmitter systems: the excitatory glutamatergic system, the inhibitory GABAergic, and the modulating dopaminergic pathway[132]. There is also evidence for imbalance between excitatory and inhibitory systems in ASD[133].

As there are several single-gene disorders have ASD and ID as core features, most of the ASD research has focused on characterizing these genes' functions. Some of these genes include *MECP2*; the postsynaptic cell adhesion proteins known as Neuroligins (*NLGN* ; reviewed in [134]); Neurexins (*NRXN*) which are interactors of *NLGN*; Contactin-associated protein-like 2 (CNTNAP2; reviewed in [135]), which is also a *NRXN* family member; and SH3 and multiple ankyrin repeat domains 3 (SHANK3). Genes associated with SCZ risk include *Disrupted In Schizophrenia 1* (*DISC1*)[136,137], *ERBB4* and its binding partner, *NRG1* (reviewed in [138]), among others. There have also been *de novo* loss of function mutations implicated as causal for SCZ, including in SHANK1[130].

In general structural abnormalities on brain imaging for both ASD and SCZ are subtle or difficult to reproduce. On MRI, group-wise changes associated with SCZ include smaller total brain volume with ventricular enlargement (reviewed in [139]). Region-specific changes include reduced cortical, hippocampal, and thalamic volumes, and increased globus pallidus volume. Others have also found reduced cerebellar volumes in SCZ by MRI, and right cerebellar volume was inversely correlated with "neurological soft signs", which include abnormalities in sensory and motor performance[140]. These are measured by changes in speech articulation, finger-to-thumb opposition, finger-to-nose test, tandem walking, and right/ left orientation. Connectivity modeling in SCZ has implicated the cortico- cerebellar–thalamic–cortical circuit[141]. Dysfunction in this circuitry is thought to cause "cognitive dysmetria", described as impaired processing and response to information.

ASD is very heterogeneous, and is associated with both macrocephaly and microcephaly[142], and structural MRI in ASD patients found evidence for increased parieto-temporal lobe and cerebellar volumes[143]. Structural MRI of 26 different ASD mouse models recapitulated this heterogeneity in brain volume, and when volume-normalized, the parieto-temporal lobe, cerebellum, frontal lobe, hypothalamus and striatum were found to be structurally abnormal across all models[144]. Studies in ASD using functional MRI have reported patterns consistent with hypo-connectivity dominating across brain regions, and some over-connectivity locally[145].

ulators of chromatin structure cause neurodevelopmental disorders

Mutations in genes involved in regulating chromatin structure, such as subunits of chromatin remodeling complexes, are a major cause of ID, ASD and SCZ ([146,147], reviewed in [148]). In addition, genes encoding proteins involved in chromatin loop formation are also implicated in causing these disorders[149–152]. Whitton and colleagues sought to identify shared genetic etiology between SCZ and ID among epigenetic factors, and identified eight candidate genes: *BCL11B, CHD7, EP300, EPC2, GATAD2A, KDM3B, RERE,* and *SATB2*[153]. Evidence suggests that the function of chromatin structure regulators converges on similar biological processes in the brain, in particular gene regulation.

Rubinstein-Taybi syndrome: This multisystem disorder is heterogeneous but moderate to severe ID is always present (reviewed in [154]). This disorder is caused by *de novo* mutation of a single copy of the cAMP response element binding protein (CREB)-binding protein, (*CREBBP*), which encodes transcriptional cofactor called CBP. A milder form of the disorder also results from mutation of the paralog of CBP, the E1A-associated protein 300 gene (*EP300*), which encodes P300. Both CBP and P300 are ubiquitous factors that function in transcriptional regulation through intrinsic HAT activity as well as by recruiting a multitude of transcription factors through protein-binding domains. Enhancers are typically enriched with H3K4me1 or H3K27ac and CBP or P300[155,156], but only a subset are actively regulating transcription at a given time[157]. Neuronal activity has been shown to increase CBP binding to H3K4me1-enriched sites in cultured mouse cortical neurons[158]. Further experiments[159] revealed that acetylation of H3K27 increased at a subset of these sites and many of these neuronal activity-regulated enhancers became bound by the early-response factor FOS. Although these tests were performed *in vitro*¸ there was 65% overlap of these sites with DNaseI hypersensitive sites in murine adult cortex, suggesting these regions are functional enhancers *in vivo.*

Rett Syndrome: Mutations in *MECP2* gene cause a well-studied condition in females known as Rett syndrome, a neurodevelopmental disorder that presents at around 6 to 18 months of age and is characterized by ID, features of ASD, and an increased risk of seizure disorder[160]. MECP2, is a ubiquitous nuclear protein that binds to methylated cytosine residues through its methyl binding domain. Emerging evidence suggests MECP2 affects transcription by influencing global chromatin organization, as it has been shown to coat DNA like a histone[161], and even compete with histone H1 for binding sites[162]. In addition, MECP2 functions in heterochromatin condensation[163]. In the brain, MECP2 recruits repressive complexes (HDAC1, HDAC2 and Sin3A) to methylated loci. MECP2 not only functions in gene repression, in fact the majority of genes bound by MECP2 in wildtype brain showed decreased expression in *Mecp2*-deficient tissues[164]. MECP2, like CBP, interacts with CREB1 at active promoters. Some of the targets MECP2 activates include the brain-derived neurotrophic factor (*Bdnf*)[164], *Sst*[164] and Dlx5[165].

Alpha-thalassemia, mental retardation X-liked (ATR-X) syndrome: This rare disorder affects males and is characterized by moderate to severe ID, skeletal and urogenital defects, seizures, and mild alpha-thalassemia[166]. ATR-X syndrome is caused by hypomorphic mutations in the X-linked ATP-dependent chromatin remodeling protein (ATRX), typically in either the ADD domain at the N-terminus or SWI/ SNF translocase domain at the C-terminus[167]. The ADD domain allows ATRX to selectively bind the combinatorial readout of H3K9me3 and H3K4me0[168,169]. ATRX is enriched at repetitive, heterochromatic GC-rich sequences, and is targeted there by histone marks and through protein-protein interactions (reviewed in [170]). The translocase domain is theorized to allow for ATP-dependent chromatin remodelling[171], which has been shown to regulate transcription through making specific chromatin regions available for deposition of histone variant H3.3[172]. Deposition of H3.3 may be important for transcription and replication machinery to pass through GC-rich domains[173]. Deletion of *Atrx* from forebrain results in widespread P53-dependent apoptosis[174], which is likely secondary to replication damage in the neuroprogenitors[175].

In addition, ATRX has been shown to be recruited by MECP2 to pericentromeric heterochromatin in neurons[176], suggesting ATRX may be required as a downstream effector of MECP2. The *H19* gene is genetically imprinted, which means in some tissues it is expressed preferentially from one parental allele (in this case the maternal), and carries parent of origin-specific DNA methylation patterns which are stably inherited by daughter cells (reviewed in [108]). MECP2 was shown to recruit ATRX to the maternal *H19* imprinting control region in the neonatal mouse brain[105,107]. Without ATRX or MECP2, repression of a network of imprinted alleles is lost in the brain, and may contribute to the overlap of ID in the two human disorders[105].

Cornelia de Lange Syndrome (CdLs): This is a multi-system disorder that causes ID, short stature and limb defects, but milder cases can have features of ASD[177]. CdLS is caused by mutations in members and regulators of the Cohesin complex (*NIPBL, SMC1A, SMC3, RAD21*, and *HDAC8*) (reviewed in [178,179]). The cohesin complex is an important transcriptional regulator through its role in chromatin loop stabilization, and it is this role that has been implicated in the symptomology of CdLS[180,181]. Transcriptional profiling in embryonic brain tissue from *Nipbl* mutant mice showed altered expression of the clustered *Pcdh-β* genes[181], involved in synapse formation and dendrite avoidance (reviewed in [113]). The cohesin complex also interacts with MECP2 and ATRX at imprinted loci[105].

Mutations in MED cause ID: Mutations in the X-linked *MED12* gene causes at least three different conditions associated with moderate to severe ID, and varying other clinical features such as heart defects, hypotonia and macrocephaly. Mutations in the *MED13L* gene also cause a similar disorder. These genes encode subunits of MED, and as with cohesin, MED is an important regulator of gene expression through its role in loop stabilization between promoters and enhancers[152].

CF causes autosomal dominant ID and ASD

Gregor et al[149] identified a *de novo* frameshift mutation in *CTCF* by performing trio exome sequencing for a 9 year-old Caucasian boy with ID (IQ 64), congenital cardiac defects, microcephaly, short stature and delayed walking. After identifying this mutation in a novel ID gene, they proceeded with unidirectional sequencing of all coding exons and exon-intron boundaries of CTCF in a cohort of 399 children with ID. Two other boys with mutations in *CTCF* were identified, one with a *de novo* frameshift mutation and the other with a *de novo* missense mutation. The boy with the frameshift had mild ID (IQ 79–

86), global developmental delay, muscular hypotonia, microcephaly, cryptorchidism and recurrent infections. The second proband, carrying the missense mutation, was a boy with severe ID (no IQ score available), global developmental delay, microcephaly, autistic behaviour, feeding difficulties and cryptorchidism.

Whole transcriptome sequencing was performed on lymphocytes from these three individuals and 8 healthy controls. The expression patterns were more similar between those individuals with frameshift mutations, than the missense, but the three individuals still had significant overlap of up- and downregulated genes, indicating common pathogenic transcriptional changes. The authors evaluated a set of 698 downregulated genes for Gene Ontology (GO) terms, finding enrichment in biological processes of inflammatory response, signal transduction, and chemotaxis. Upregulated genes (set of 118) were enriched for GO terms implicated in protein translation and processing.

To date there have been three studies describing patients with ID and disruption or mutation of the *CTCF* gene, a syndrome described as Autosomal Dominant Mental Retardation 21 (MRD21)[149,182,183]. Along with the three individuals from their own database, Gregor *et al.* identified a fourth individual with ID and a 280 kb deletion spanning eight genes including *CTCF*[149]. Another group performed whole-exome sequencing of 2508 children with ASD to identify *de novo* mutations[183]. Of note, there was significantly more males in the screened affected population than females, as commonly is the case with ASD, by a ratio of 1 female to every 7 males. There were two ASD probands identified with mutations in *CTCF;* one with a frameshift mutation (a female), and the other with a missense mutation (a male). Both of these individuals had reduced non-verbal IQ, with scores of 61 and 51, respectively.

The third study was a case report that described a female with a *de novo* frameshift mutation in the CTCF gene, identified by whole exome sequencing[182]. She was extremely small for gestational age, and at birth weighed below the 3rd percentile, while head circumference was under the 10th percentile, consistent with previous findings that CTCF haploinsufficiency leads to short stature and microcephaly. Along with global developmental delay, she suffered repeated respiratory infections and had minor heart abnormalities (small atrial septal defect), all of which were reported previously with CTCF mutation.

CF is associated with SCZ

Juraeva and colleagues[150] sought to investigate the joint effects of multiple functionally related pathways (pathway-based analysis of GWAS), which provides more power to genetic association studies. They applied a hierarchical approach, using the Global Test, to identify altered gene pathways[184]. Next, they used FORGE[185] to identify important risk genes within the Global Test- selected pathways. They increased the robustness of their study by using two separate datasets, one containing 5040 individuals with SCZ, and the other consisting of 5082.

The Global Test yielded 27 significantly associated pathways, of which 14 pathways were significantly associated with SCZ in the replication dataset. Using FORGE to perform gene-based analysis on these results identified 100 genes, of which 8 genes overlapped with 4 or more of the 14 replicated significant pathways (FOXP2, BCL11A, PCDH7, RPL36P13, CACNB2, CTCF, MECOM, and RIMS1). The 100 genes were tested for association, which yielded 18 genes significantly associated with SCZ. Among these were multiple known SCZ susceptibility genes. CTCF and CACNB2 were among this set of genes as well, and were tested separately in the replication sample, where CTCF again was strongly associated with SCZ, and CACNB2 showed a trend toward association.

lence for cortical interneurons in neurodevelopmental disorders

Most of the evidence for cortical interneuron dysfunction in ASD comes from studying the genes associated with monogenic syndromic ASD (*MECP2,* and members of the *NLGN*, *NRXN* and *SHANK* molecular families). Deletion of *Mecp2* from forebrain GABAergic interneurons is sufficient for mice to recapitulate ASD phenotypes (repetitive behaviours, altered sociability, cognitive deficits), suggesting these behaviours are mediated by interneuron dysfunction[186]. In addition, when NRXN family member *Cntnap2* is deleted in mice, this results in a reduced number of PV interneurons[187]. Post-mortem studies in ASD are limited, but some samples from ASD patients have shown reduced GAD65/67 in cortex[188]. One study also implicates altered interneuron subtype ratios in the cortex of ASD patients[133].

In SCZ, reductions in cortical interneurons as measured by *Gad1* mRNA have been found across several cortical regions[189,190], reviewed in [191]. In addition, there are reports of increased GABA receptor (A) α2 subunit[192,193] and decreases in GABA receptor (A) sub-units α1 and α5[189,193] in SCZ, suggesting that GABAergic signaling in general is altered.

It has been suggested that reductions in GABAergic cell numbers in the cortex of SCZ may occur due to defects in migration from the ganglionic eminence. In support of this, an increased number of interstitial neurons in the white matter (IWMN) have been found in post-mortem SCZ samples[194–199]. These IWMN could represent cortical interneurons that have lost their way during tangential migration[200]. Others have suggested that although cortical interneuron number may be affected in some patients with SCZ, interneuron dysfunction is more relevant to the spectrum of the disease (reviewed in [201]).

As mentioned in a prior section, cortical interneurons influence synchronicity of activity to generate oscillation. PV-expressing interneurons give rise to gamma oscillatory activity, described in the frequency range of 30-80 Hz[202]. Gamma oscillatory patterns are reproducibly abnormal in the brains of SCZ patients, suggesting a role for PV-expressing interneuron dysfunction[203–205]. In support of this, reduced staining for PV has been found in SCZ[206–209]. Others have found reduced GAD67 staining in specific subclasses of interneurons of the DPFC in SCZ, suggesting a decreased potential to secrete GABA[194,210]. It has been suggested that these deficits in PV interneurons can stem from dysfunction of their NMDARs. Neurons, including interneurons, can respond to excitatory glutamate through NMDAR. Taking antagonists of NMDAR (eg. PCP) produces a phenotype similar to SCZ and alters gamma oscillations (reviewed in [211]). Culturing neurons with NMDAR antagonists results in reduced *Gad1* and *Pv* mRNA[212], and animal studies also support that down-regulation by blocking NMDAR in PV interneurons is sufficient to generate SCZ phenotypes, such as altered gamma oscillations[213].

Studies of SCZ risk-genes (*DISC1*, *ERBB4*, and *NRG1*), provide further evidence for PV interneuron dysfunction in SCZ. Outside of guiding interneuron tangential migration, ERBB4 has important roles in the function of mature interneurons[214]. Deletion of *ErbB4* from PV interneurons in mice resulted in reduced synapsing between chandelier and excitatory neurons[214,215]. Transgenic mice that express mutant forms of *Disc1* also have PV interneuron abnormalities, including reduced PV expression[216], and reduced or mal-positioned PV interneurons[217,218].

Although the evidence for PV interneuron dysfunction in SCZ is strong, the loss of SST staining is also robustly reported[189,209,219], suggesting that there may be alterations occurring at the level of MGE development. In support of this, both *LHX6*[220] and *NKX2.1*[221] have been implicated in schizophrenia. *LHX6* mRNA levels were lower in schizophrenia cortex and correlated with lower *GAD67* levels as well.

se models of neurodevelopmental disorders

avioural phenotyping of SCZ and ID/ASD mouse models

Animal models are evaluated based on face validity (reproduce phenotypes of human syndrome), construct validity (demonstrate the same underlying biological dysfunction as in human condition), and predictive validity (have analogous response to treatment as in patients). Common mouse models for ASD, ID and SCZ and their behavioural deficits are presented in Table 1.

Table 1: Summary of behaviours of common ASD, ID and SCZ rodent models

Rodent Model/ Gene	Disorder Modeled	Behaviour	References
Post-weaning social isolation (rats)	Attention Deficit/ Hyperactivity Disorder (ADHD) SCZ	Hyperactivity, enhanced responses to novelty, impaired PPI, cognitive inflexibility, impaired fear learning, and increased aggression	Reviewed in [1]

Maternal immune activation (rats)	SCZ ASD	Abnormal communication, decreased sociability, increased repetitive behaviors, impaired PPI, impaired working memory, cognitive inflexibility, increased anxiety, and enhanced reactivity to amphetamines	Reviewed in [2]
***Disc1* mutants** (mice) Haplo-insufficiency: i) exon 8 Termination, (∆25 bp); ii) ∆ex 2/3; iii) ∆ex1-3 (Disc1-LI) Point mutation: i) L100P homozygote; ii) Q31L homozygote Transgenic: Dominant-negative (DN) DISC1 expression	SCZ ASD Mood Disorder	∆25 bp: Impaired working memory ∆ex 2/3: Increased impulsivity *Disc1*-LI: Normal behaviour L100P: Impaired PPI and decreased acoustic startle, hyperactivity, impaired working memory. Normal sociability (Note: On other genetic background, this mutant was indistinguishable from controls). Q31L: Decreased sociability and social memory, impaired PPI, and depressive-like traits DN-DISC1[3]: Hyperactivity, impaired PPI, and depressive-like traits. Normal working memory. Sociability not tested DN-DISC1[4]: Depressive-like traits, impaired working memory, and decreased sociability DN-DISC1[5]: Hyperactivity. Males: Decreased social approach, increased aggression. Normal spatial learning and memory. Females: Impaired spatial memory	Point mutations[6] Reviewed in [7] Transgenics: [3–5]
***Erbb4* / *Nrg1* mutants** (mice)	SCZ	*Erbb4*-null, *Erbb4* cKO (*Pv*-Cre) and *Nrg1* hypomorphs[8]: Hyperactivity, and impaired PPI. In addition, *Errb4*-null have decreased anxiety. *Erbb4* cKO (*Lhx6*-Cre)[9]: Hyperactivity, reduced anxiety, decreased sociability, disorganized nests, impaired working memory, and impaired PPI	[8–10]
Neuroligin (*Nlgn*) mutants (mice)	ASD and ID (NLGN 3, 4) SCZ (NLGN 2)	*Nlgn1* KO: Decreased sociability, impaired spatial learning and memory, and increased repetitive behavior. *Nlgn2* KO: Normal	Reviewed in [11]

		social approach, increased anxiety, decreased pain sensitivity and poor motor coordination. *Nlgn3* KO: Decreased sociability, altered communication, repetitive behaviour, and hyperactivity. *Nlgn4* KO: Decreased sociability, altered communication, and repetitive behaviour	
Shank 1, 2, 3 mutants	ASD SCZ ID ADHD Bipolar Disorder	*Shank1*-null: Impaired fear memory. Altered male-female social interactions and vocalizations, increased self-grooming, and increased anxiety. *Shank2*-null: Decreased sociability, altered communication, repetitive jumping, decreased digging, impaired spatial learning, hyperactivity and increased anxiety. *Shank3*-null: Altered social approach/ communication, and increased self-grooming	Reviewed in [11,12]
Mecp2 i) Δ exon ¾ (*Mecp2*$^{tm1.1Bird}$), ii) 308X; iii) *Pv*-Cre *Mecp2* cKO	ASD ID Rett Syndrome	Female *Mecp2*$^{tm1.1Bird}$ develop uncoordinated gait, reduced spontaneous movement, hind-limb clasping and irregular breathing between 3-9 months of age. Male *Mecp2*^{308X} similar, with altered social interactions, increased anxiety, and stereotypies at 6 weeks of age. *Pv*-Cre cKO: Impaired motor, impaired acoustic startle, impaired cued fear memory, and increased social novelty preference	*Mecp2*$^{tm1.1Bird}$ [13] *Mecp2*^{308X} [14] *Pv*-Cre *Mecp2* cKO[15]

Modeling ASD

As ASD diagnosis is based on behavioural criteria, phenotyping these correlates in mice became essential for developing mouse models to study ASD-implicated genes (reviewed in [222]). There are currently over 70 mouse models of ASD[223], and behaviour testing focuses on abnormal social behaviour, altered communication, and repetitive /

perseverative behaviours. Mice have spontaneous stereotypies such as jumping, backflips and self-grooming[224]. Altered social behaviour typically presents as decreased sociability and decreased social memory in the *social choice assay*[222], but the opposite has also been observed[225]. The way mice communicate is not well understood, but some have used olfactory cues and olfactory habituation testing in ASD mouse models (reviewed in[222]). Complex ultrasonic vocalizations[226], for example in pups separated from the dam and nest, have been shown to be abnormal in ASD mouse models[227].

In addition, learning and memory deficits are often observed in ASD mouse models[228]. Mice have a well-developed ability to navigate in space as part of their natural ethology. Therefore, spatial memory acquisition, which is dependent on the hippocampus and entorhinal cortex (reviewed in [229]), is typically used to test learning in mice.

Modeling SCZ

In SCZ, creating mice with face validity has been more challenging[230,231]. Here the behaviours usually model i) the negative symptoms by abnormal social behaviour, ii) impaired cognition by decreased working memory and cognitive inflexibility, and iii) positive symptoms by hyperactivity at baseline or in response to psychotomimetic drugs.

SCZ mouse models tend to show decreased sociability[231]. Decreased aggression, representing social withdrawal, as well as increased aggression, have also been observed in SCZ mouse models[232]. In mice, behavioural inflexibility can be tested with *reversal learning tasks* (reviewed in [233]) and is relevant to both ASD and SCZ. Working memory can also be tested in rodents using maze paradigms which require short term-memory and manipulation of the stored information to perform (reviewed in [234]).

Hyperactivity has been observed in many SCZ animal models at baseline, or in response to novelty, while others have detected increased locomotor activity in response to NMDAR antagonists, dopamimetic drugs, amphetamine, or cocaine compared to control animals (reviewed in [231]). In addition, sensory-gating abnormalities have been observed in SCZ patients, and are readily modeled in animals[232]. In SCZ mouse models, there is often a reduction in PPI due to abnormal sensory filtering of the prepulse stimulus.

onale

Genes encoding regulators of chromatin higher order structure are being increasingly implicated in ASD, ID and SCZ (see section 3.2), however our understanding of how they influence brain development and behaviour remains poorly understood. CTCF functions in the regulation of gene expression through influencing higher order chromatin structure. It has an irrefutably important role in brain development, as its mutation results in intellectual disability and ASD[149,183]. In addition, *CTCF* has been associated with SCZ in two patient samples[150]. Despite this, there have only been a handful of studies exploring the role of CTCF in the brain, in particular during development.

othesis

The over-arching hypothesis of this thesis is that CTCF is required for the development of normal cell type composition, brain structure and behaviour by regulating gene expression at the embryonic stage. In addition, because of the syndrome associated with single copy mutation of *CTCF*, I hypothesize that haplo-insufficiency of *Ctcf* in the mouse brain will resemble other rodent models of ASD, ID and SCZ in behaviour and brain structure.

ectives

(1) Identify genes important during brain development that are affected by loss of *Ctcf*.

This will involve the generation of appropriate mouse models to explore the outcome of *Ctcf* loss and examine differential transcriptional profiles in the developing forebrain. Based on this transcriptional screen, we will focus on specific genes implicated in key events during brain development and that potentially could be linked to ID, ASD or SCZ etiology. Cellular effects will be examined using *in vivo* models and causality of phenotypes verified by rescue experiments.

(2) Determine the effect of *Ctcf* haplo-insufficiency on brain morphology and behaviour.

To achieve this, I will generate mice with conditional deletion of a single copy of *Ctcf* in the embryonic central nervous system. If the mutant mice survive to adulthood, they will be subjected to a battery of behavioural tasks relevant to ASD, ID, and SCZ and brain morphological changes will be evaluated by MRI.

rences

1. Wilson, S. W. & Houart, C. Early Steps in the Development of the Forebrain. *Dev. Cell* **6,** 167–181 (2004).
2. Gilbert, S. F. *Developmental Biology*. (Sinauer Associates, 2000).
3. Andoniadou, C. L. & Martinez-Barbera, J. P. Developmental mechanisms directing early anterior forebrain specification in vertebrates. *Cell. Mol. Life Sci. CMLS* **70,** 3739–3752 (2013).
4. Campbell, K. Dorsal-ventral patterning in the mammalian telencephalon. *Curr. Opin. Neurobiol.* **13,** 50–56 (2003).

5. Pierani, A. & Wassef, M. Cerebral cortex development: From progenitors patterning to neocortical size during evolution. *Dev. Growth Differ.* **51,** 325–342 (2009).
6. Costa, M. R. & Müller, U. Specification of excitatory neurons in the developing cerebral cortex: progenitor diversity and environmental influences. *Front. Cell. Neurosci.* **8,** (2015).
7. Lodato, S. & Arlotta, P. Generating Neuronal Diversity in the Mammalian Cerebral Cortex. *Annu. Rev. Cell Dev. Biol.* **31,** 699–720 (2015).
8. Matsuzaki, F. & Shitamukai, A. Cell Division Modes and Cleavage Planes of Neural Progenitors during Mammalian Cortical Development. *Cold Spring Harb. Perspect. Biol.* **7,** a015719 (2015).
9. Lodato, S., Shetty, A. S. & Arlotta, P. Cerebral cortex assembly: generating and reprogramming projection neuron diversity. *Trends Neurosci.* **38,** 117–125 (2015).
10. Kwan, K. Y., Sestan, N. & Anton, E. S. Transcriptional co-regulation of neuronal migration and laminar identity in the neocortex. *Dev. Camb. Engl.* **139,** 1535–1546 (2012).
11. Borello, U. & Pierani, A. Patterning the cerebral cortex: traveling with morphogens. *Curr. Opin. Genet. Dev.* **20,** 408–415 (2010).
12. Leyva-Díaz, E. & López-Bendito, G. In and out from the cortex: Development of major forebrain connections. *Neuroscience* **254,** 26–44 (2013).
13. Jones, E. G. GABAergic neurons and their role in cortical plasticity in primates. *Cereb. Cortex N. Y. N 1991* **3,** 361–372 (1993).
14. Meyer, H. S. *et al.* Inhibitory interneurons in a cortical column form hot zones of inhibition in layers 2 and 5A. *Proc. Natl. Acad. Sci.* **108,** 16807–16812 (2011).

15. Tremblay, R., Lee, S. & Rudy, B. GABAergic Interneurons in the Neocortex: From Cellular Properties to Circuits. *Neuron* **91,** 260–292 (2016).
16. Ali, A. B. & Thomson, A. M. Synaptic α5 Subunit–Containing GABAA Receptors Mediate IPSPs Elicited by Dendrite-Preferring Cells in Rat Neocortex. *Cereb. Cortex* **18,** 1260–1271 (2008).
17. Rudy, B., Fishell, G., Lee, S. & Hjerling-Leffler, J. Three groups of interneurons account for nearly 100% of neocortical GABAergic neurons. *Dev. Neurobiol.* **71,** 45–61 (2011).
18. Lee, S., Hjerling-Leffler, J., Zagha, E., Fishell, G. & Rudy, B. The Largest Group of Superficial Neocortical GABAergic Interneurons Expresses Ionotropic Serotonin Receptors. *J. Neurosci.* **30,** 16796–16808 (2010).
19. Xu, Q., Cobos, I., De La Cruz, E., Rubenstein, J. L. & Anderson, S. A. Origins of cortical interneuron subtypes. *J. Neurosci. Off. J. Soc. Neurosci.* **24,** 2612–2622 (2004).
20. Wonders, C. & Anderson, S. A. Cortical Interneurons and Their Origins. *The Neuroscientist* **11,** 199–205 (2005).
21. Yu, X. & Zecevic, N. Dorsal Radial Glial Cells Have the Potential to Generate Cortical Interneurons in Human But Not in Mouse Brain. *J. Neurosci.* **31,** 2413–2420 (2011).
22. Hansen, D. V. *et al.* Non-epithelial stem cells and cortical interneuron production in the human ganglionic eminences. *Nat. Neurosci.* **16,** 1576–1587 (2013).
23. Fishell, G. Perspectives on the developmental origins of cortical interneuron diversity. *Novartis Found. Symp.* **288,** 21-35; discussion 35-44, 96–98 (2007).

24. Gelman, D. M. *et al.* The embryonic preoptic area is a novel source of cortical GABAergic interneurons. *J. Neurosci. Off. J. Soc. Neurosci.* **29,** 9380–9389 (2009).

25. Fazel Darbandi, S. *et al.* Functional consequences of I56ii Dlx enhancer deletion in the developing mouse forebrain. *Dev. Biol.* **420,** 32–42 (2016).

26. Le, T. N. *et al.* GABAergic Interneuron Differentiation in the Basal Forebrain Is Mediated through Direct Regulation of Glutamic Acid Decarboxylase Isoforms by Dlx Homeobox Transcription Factors. *J. Neurosci.* **37,** 8816–8829 (2017).

27. Eisenstat, D. D. *et al.* DLX-1, DLX-2, and DLX-5 expression define distinct stages of basal forebrain differentiation. *J. Comp. Neurol.* **414,** 217–237 (1999).

28. Anderson, S. A., Eisenstat, D. D., Shi, L. & Rubenstein, J. L. R. Interneuron Migration from Basal Forebrain to Neocortex: Dependence on Dlx Genes. *Science* **278,** 474–476 (1997).

29. Long, J. E., Cobos, I., Potter, G. B. & Rubenstein, J. L. R. Dlx1&2 and Mash1 Transcription Factors Control MGE and CGE Patterning and Differentiation through Parallel and Overlapping Pathways. *Cereb. Cortex* **19,** i96–i106 (2009).

30. Zerucha, T. *et al.* A Highly Conserved Enhancer in the Dlx5/Dlx6Intergenic Region is the Site of Cross-Regulatory Interactions betweenDlx Genes in the Embryonic Forebrain. *J. Neurosci.* **20,** 709–721 (2000).

31. Ghanem, N. *et al.* Regulatory Roles of Conserved Intergenic Domains in Vertebrate Dlx Bigene Clusters. *Genome Res.* **13,** 533–543 (2003).

32. Park, B. K. *et al.* Intergenic enhancers with distinct activities regulate Dlx gene expression in the mesenchyme of the branchial arches. *Dev. Biol.* **268,** 532–545 (2004).

33. Fulp, C. T. *et al.* Identification of Arx transcriptional targets in the developing basal forebrain. *Hum. Mol. Genet.* **17,** 3740–3760 (2008).

34. Mattiske, T., Lee, K., Gecz, J., Friocourt, G. & Shoubridge, C. Embryonic forebrain transcriptome of mice with polyalanine expansion mutations in the ARX homeobox gene. *Hum. Mol. Genet.* **25,** 5433–5443 (2016).

35. Flames, N. *et al.* Delineation of Multiple Subpallial Progenitor Domains by the Combinatorial Expression of Transcriptional Codes. *J. Neurosci.* **27,** 9682–9695 (2007).

36. Nery, S., Fishell, G. & Corbin, J. G. The caudal ganglionic eminence is a source of distinct cortical and subcortical cell populations. *Nat. Neurosci.* **5,** 1279–1287 (2002).

37. Kanatani, S., Yozu, M., Tabata, H. & Nakajima, K. COUP-TFII Is Preferentially Expressed in the Caudal Ganglionic Eminence and Is Involved in the Caudal Migratory Stream. *J. Neurosci.* **28,** 13582–13591 (2008).

38. Touzot, A., Ruiz-Reig, N., Vitalis, T. & Studer, M. Molecular control of two novel migratory paths for CGE-derived interneurons in the developing mouse brain. *Development* **143,** 1753–1765 (2016).

39. Torigoe, M., Yamauchi, K., Kimura, T., Uemura, Y. & Murakami, F. Evidence That the Laminar Fate of LGE/CGE-Derived Neocortical Interneurons Is Dependent on Their Progenitor Domains. *J. Neurosci.* **36,** 2044–2056 (2016).

40. Marin, O., Anderson, S. A. & Rubenstein, J. L. Origin and molecular specification of striatal interneurons. *J. Neurosci. Off. J. Soc. Neurosci.* **20,** 6063–6076 (2000).

41. Fragkouli, A., van Wijk, N. V., Lopes, R., Kessaris, N. & Pachnis, V. LIM homeodomain transcription factor-dependent specification of bipotential MGE

progenitors into cholinergic and GABAergic striatal interneurons. *Dev. Camb. Engl.* **136,** 3841–3851 (2009).

42. Lazzaro, D., Price, M., Felice, M. de & Lauro, R. D. The transcription factor TTF-1 is expressed at the onset of thyroid and lung morphogenesis and in restricted regions of the foetal brain. *Development* **113,** 1093–1104 (1991).
43. Xu, Q., Wonders, C. P. & Anderson, S. A. Sonic hedgehog maintains the identity of cortical interneuron progenitors in the ventral telencephalon. *Dev. Camb. Engl.* **132,** 4987–4998 (2005).
44. Sussel, L., Marin, O., Kimura, S. & Rubenstein, J. L. Loss of Nkx2.1 homeobox gene function results in a ventral to dorsal molecular respecification within the basal telencephalon: evidence for a transformation of the pallidum into the striatum. *Development* **126,** 3359–3370 (1999).
45. Nery, S., Corbin, J. G. & Fishell, G. Dlx2 progenitor migration in wild type and Nkx2.1 mutant telencephalon. *Cereb. Cortex N. Y. N 1991* **13,** 895–903 (2003).
46. Butt, S. J. B. *et al.* The Requirement of Nkx2-1 in the Temporal Specification of Cortical Interneuron Subtypes. *Neuron* **59,** 722–732 (2008).
47. Vogt, D. *et al.* Lhx6 Directly Regulates Arx and CXCR7 to Determine Cortical Interneuron Fate and Laminar Position. *Neuron* **82,** 350–364 (2014).
48. Liodis, P. *et al.* Lhx6 Activity Is Required for the Normal Migration and Specification of Cortical Interneuron Subtypes. *J. Neurosci.* **27,** 3078–3089 (2007).
49. Du, T., Xu, Q., Ocbina, P. J. & Anderson, S. A. NKX2.1 specifies cortical interneuron fate by activating Lhx6. *Development* **135,** 1559–1567 (2008).

50. Nóbrega-Pereira, S. *et al.* Postmitotic Nkx2-1 Controls the Migration of Telencephalic Interneurons by Direct Repression of Guidance Receptors. *Neuron* **59,** 733–745 (2008).
51. Marín, O., Yaron, A., Bagri, A., Tessier-Lavigne, M. & Rubenstein, J. L. R. Sorting of Striatal and Cortical Interneurons Regulated by Semaphorin-Neuropilin Interactions. *Science* **293,** 872–875 (2001).
52. Flames, N. *et al.* Short- and Long-Range Attraction of Cortical GABAergic Interneurons by Neuregulin-1. *Neuron* **44,** 251–261 (2004).
53. Zhao, Y. *et al.* Distinct Molecular Pathways for Development of Telencephalic Interneuron Subtypes Revealed Through Analysis of Lhx6 Mutants. *J. Comp. Neurol.* **510,** 79–99 (2008).
54. Hu, H., Gan, J. & Jonas, P. Fast-spiking, parvalbumin+ GABAergic interneurons: From cellular design to microcircuit function. *Science* **345,** 1255263 (2014).
55. Magno, L., Catanzariti, V., Nitsch, R., Krude, H. & Naumann, T. Ongoing expression of Nkx2.1 in the postnatal mouse forebrain: Potential for understanding NKX2.1 haploinsufficiency in humans? *Brain Res.* **1304,** 164–186 (2009).
56. Zhao, Y. *et al.* The LIM-homeobox gene Lhx8 is required for the development of many cholinergic neurons in the mouse forebrain. *Proc. Natl. Acad. Sci. U. S. A.* **100,** 9005–9010 (2003).
57. Chen, L., Chatterjee, M. & Li, J. Y. H. The Mouse Homeobox Gene Gbx2 Is Required for the Development of Cholinergic Interneurons in the Striatum. *J. Neurosci.* **30,** 14824–14834 (2010).

58. Fragkouli, A. *et al.* Loss of forebrain cholinergic neurons and impairment in spatial learning and memory in LHX7-deficient mice. *Eur. J. Neurosci.* **21,** 2923–2938 (2005).
59. Brunner, A. M., Tweedie-Cullen, R. Y. & Mansuy, I. M. Epigenetic modifications of the neuroproteome. *Proteomics* **12,** 2404–2420 (2012).
60. Kornberg, R. D. Chromatin structure: a repeating unit of histones and DNA. *Science* **184,** 868–871 (1974).
61. Millau, J.-F. & Gaudreau, L. CTCF, cohesin, and histone variants: connecting the genome. *Biochem. Cell Biol. Biochim. Biol. Cell.* **89,** 505–513 (2011).
62. Yeivin, A. & Razin, A. Gene methylation patterns and expression. *EXS* **64,** 523–568 (1993).
63. Oberdoerffer, S. A conserved role for intragenic DNA methylation in alternative pre-mRNA splicing. *Transcription* **3,** 106–109 (2012).
64. Khare, T. *et al.* 5-hmC in the brain is abundant in synaptic genes and shows differences at the exon-intron boundary. *Nat. Struct. Mol. Biol.* **19,** 1037–1043 (2012).
65. Jenuwein, T. & Allis, C. D. Translating the histone code. *Science* **293,** 1074–1080 (2001).
66. Guenther, M. G., Levine, S. S., Boyer, L. A., Jaenisch, R. & Young, R. A. A chromatin landmark and transcription initiation at most promoters in human cells. *Cell* **130,** 77–88 (2007).
67. Farooq, Z., Banday, S., Pandita, T. K. & Altaf, M. The many faces of histone H3K79 methylation. *Mutat. Res. Rev. Mutat. Res.* **768,** 46–52 (2016).

68. Fischle, W., Mootz, H. D. & Schwarzer, D. Synthetic histone code. *Curr. Opin. Chem. Biol.* **28,** 131–140 (2015).
69. Huang, H., Sabari, B. R., Garcia, B. A., Allis, C. D. & Zhao, Y. SnapShot: histone modifications. *Cell* **159,** 458–458.e1 (2014).
70. Tyler, J. K. Chromatin assembly. *Eur. J. Biochem.* **269,** 2268–2274 (2002).
71. Denker, A. & Laat, W. de. The second decade of 3C technologies: detailed insights into nuclear organization. *Genes Dev.* **30,** 1357–1382 (2016).
72. Kagey, M. H. *et al.* Mediator and cohesin connect gene expression and chromatin architecture. *Nature* **467,** 430–435 (2010).
73. Mehta, G. D., Rizvi, S. M. A. & Ghosh, S. K. Cohesin: a guardian of genome integrity. *Biochim. Biophys. Acta* **1823,** 1324–1342 (2012).
74. Wendt, K. S. *et al.* Cohesin mediates transcriptional insulation by CCCTC-binding factor. *Nature* **451,** 796–801 (2008).
75. Dixon, J. R. *et al.* Topological domains in mammalian genomes identified by analysis of chromatin interactions. *Nature* **485,** 376–380 (2012).
76. Zuin, J. *et al.* Cohesin and CTCF differentially affect chromatin architecture and gene expression in human cells. *Proc. Natl. Acad. Sci.* **111,** 996–1001 (2014).
77. Chambers, E. V., Bickmore, W. A. & Semple, C. A. Divergence of mammalian higher order chromatin structure is associated with developmental loci. *PLoS Comput. Biol.* **9,** e1003017 (2013).
78. Phillips, J. E. & Corces, V. G. CTCF: Master Weaver of the Genome. *Cell* **137,** 1194–1211 (2009).

79. Ong, C.-T. & Corces, V. G. CTCF: an architectural protein bridging genome topology and function. *Nat. Rev. Genet.* **15,** nrg3663 (2014).
80. Ohlsson, R., Renkawitz, R. & Lobanenkov, V. CTCF is a uniquely versatile transcription regulator linked to epigenetics and disease. *Trends Genet.* **17,** 520–527 (2001).
81. Kim, T. H. *et al.* Analysis of the Vertebrate Insulator Protein CTCF-Binding Sites in the Human Genome. *Cell* **128,** 1231–1245 (2007).
82. Barski, A. *et al.* High-Resolution Profiling of Histone Methylations in the Human Genome. *Cell* **129,** 823–837 (2007).
83. Bao, L., Zhou, M. & Cui, Y. CTCFBSDB: a CTCF-binding site database for characterization of vertebrate genomic insulators. *Nucleic Acids Res.* **36,** D83–D87 (2008).
84. Chen, H., Tian, Y., Shu, W., Bo, X. & Wang, S. Comprehensive Identification and Annotation of Cell Type-Specific and Ubiquitous CTCF-Binding Sites in the Human Genome. *PLOS ONE* **7,** e41374 (2012).
85. Cuddapah, S. *et al.* Global analysis of the insulator binding protein CTCF in chromatin barrier regions reveals demarcation of active and repressive domains. *Genome Res.* **19,** 24–32 (2009).
86. Wang, J., Lunyak, V. V. & Jordan, I. K. Genome-wide prediction and analysis of human chromatin boundary elements. *Nucleic Acids Res.* **40,** 511–529 (2012).
87. Merkenschlager, M. & Odom, D. T. CTCF and Cohesin: Linking Gene Regulatory Elements with Their Targets. *Cell* **152,** 1285–1297 (2013).

88. Li, Y. *et al.* Characterization of constitutive CTCF/cohesin loci: a possible role in establishing topological domains in mammalian genomes. *BMC Genomics* **14,** 553 (2013).
89. DeMare, L. E. *et al.* The genomic landscape of cohesin-associated chromatin interactions. *Genome Res.* **23,** 1224–1234 (2013).
90. Song, L. *et al.* Open chromatin defined by DNaseI and FAIRE identifies regulatory elements that shape cell-type identity. *Genome Res.* **21,** 1757–1767 (2011).
91. Botta, M., Haider, S., Leung, I. X. Y., Lio, P. & Mozziconacci, J. Intra- and inter-chromosomal interactions correlate with CTCF binding genome wide. *Mol. Syst. Biol.* **6,** 426 (2010).
92. Bell, A. C., West, A. G. & Felsenfeld, G. The Protein CTCF Is Required for the Enhancer Blocking Activity of Vertebrate Insulators. *Cell* **98,** 387–396 (1999).
93. Hou, C., Zhao, H., Tanimoto, K. & Dean, A. CTCF-dependent enhancer-blocking by alternative chromatin loop formation. *Proc. Natl. Acad. Sci. U. S. A.* **105,** 20398–20403 (2008).
94. Nativio, R. *et al.* Cohesin is required for higher-order chromatin conformation at the imprinted IGF2-H19 locus. *PLoS Genet.* **5,** e1000739 (2009).
95. Chernukhin, I. V. *et al.* Physical and functional interaction between two pluripotent proteins, the Y-box DNA/RNA-binding factor, YB-1, and the multivalent zinc finger factor, CTCF. *J. Biol. Chem.* **275,** 29915–29921 (2000).
96. Rousseau, M. *et al.* Hox in motion: tracking HoxA cluster conformation during differentiation. *Nucleic Acids Res.* **42,** 1524–1540 (2014).

97. Xu, M. *et al.* CTCF Controls HOXA Cluster Silencing and Mediates PRC2-Repressive Higher-Order Chromatin Structure in NT2/D1 Cells. *Mol. Cell. Biol.* **34,** 3867–3879 (2014).

98. Guibert, S. *et al.* CTCF-binding sites within the H19 ICR differentially regulate local chromatin structures and cis-acting functions. *Epigenetics* **7,** 361–369 (2012).

99. Hadjur, S. *et al.* Cohesins form chromosomal cis-interactions at the developmentally regulated IFNG locus. *Nature* **460,** 410–413 (2009).

100. Chien, R. *et al.* Cohesin mediates chromatin interactions that regulate mammalian β-globin expression. *J. Biol. Chem.* **286,** 17870–17878 (2011).

101. Majumder, P. & Boss, J. M. Cohesin regulates MHC class II genes through interactions with MHC class II insulators. *J. Immunol. Baltim. Md 1950* **187,** 4236–4244 (2011).

102. Parelho, V. *et al.* Cohesins functionally associate with CTCF on mammalian chromosome arms. *Cell* **132,** 422–433 (2008).

103. Beygo, J. *et al.* The molecular function and clinical phenotype of partial deletions of the IGF2/H19 imprinting control region depends on the spatial arrangement of the remaining CTCF-binding sites. *Hum. Mol. Genet.* **22,** 544–557 (2013).

104. Fedoriw, A. M., Stein, P., Svoboda, P., Schultz, R. M. & Bartolomei, M. S. Transgenic RNAi Reveals Essential Function for CTCF in H19 Gene Imprinting. *Science* **303,** 238–240 (2004).

105. Kernohan, K. D. *et al.* ATRX Partners with Cohesin and MeCP2 and Contributes to Developmental Silencing of Imprinted Genes in the Brain. *Dev. Cell* **18,** 191–202 (2010).

106. Singh, P., Lee, D.-H. & Szabó, P. E. More than insulator: multiple roles of CTCF at the H19-Igf2 imprinted domain. *Front. Genet.* **3,** 214 (2012).

107. Kernohan, K. D., Vernimmen, D., Gloor, G. B. & Bérubé, N. G. Analysis of neonatal brain lacking ATRX or MeCP2 reveals changes in nucleosome density, CTCF binding and chromatin looping. *Nucleic Acids Res.* **42,** 8356–8368 (2014).

108. Kacem, S. & Feil, R. Chromatin mechanisms in genomic imprinting. *Mamm. Genome* **20,** 544–556 (2009).

109. Bergström, R., Whitehead, J., Kurukuti, S. & Ohlsson, R. CTCF regulates asynchronous replication of the imprinted H19/Igf2 domain. *Cell Cycle Georget. Tex* **6,** 450–454 (2007).

110. Demars, J. & Gicquel, C. Epigenetic and genetic disturbance of the imprinted 11p15 region in Beckwith–Wiedemann and Silver–Russell syndromes. *Clin. Genet.* **81,** 350–361 (2012).

111. Gomes, N. P. & Espinosa, J. M. Gene-specific repression of the p53 target gene PUMA via intragenic CTCF–Cohesin binding. *Genes Dev.* **24,** 1022–1034 (2010).

112. Soshnikova, N., Montavon, T., Leleu, M., Galjart, N. & Duboule, D. Functional analysis of CTCF during mammalian limb development. *Dev. Cell* **19,** 819–830 (2010).

113. Hirayama, T. & Yagi, T. Regulation of clustered protocadherin genes in individual neurons. *Semin. Cell Dev. Biol.* **69,** 122–130 (2017).

114. Wan, L.-B. *et al.* Maternal depletion of CTCF reveals multiple functions during oocyte and preimplantation embryo development. *Development* **135,** 2729–2738 (2008).

115. Moore, J. M. *et al.* Loss of maternal CTCF is associated with peri-implantation lethality of Ctcf null embryos. *PloS One* **7,** e34915 (2012).

116. Heath, H. *et al.* CTCF regulates cell cycle progression of αβ T cells in the thymus. *EMBO J.* **27,** 2839–2850 (2008).

117. Hirayama, T., Tarusawa, E., Yoshimura, Y., Galjart, N. & Yagi, T. CTCF is required for neural development and stochastic expression of clustered Pcdh genes in neurons. *Cell Rep.* **2,** 345–357 (2012).

118. Watson, L. A. *et al.* Dual Effect of CTCF Loss on Neuroprogenitor Differentiation and Survival. *J. Neurosci.* **34,** 2860–2870 (2014).

119. Lang, F. *et al.* CTCF prevents genomic instability by promoting homologous recombination-directed DNA double-strand break repair. *Proc. Natl. Acad. Sci. U. S. A.* (2017). doi:10.1073/pnas.1704076114

120. Hilmi, K. *et al.* CTCF facilitates DNA double-strand break repair by enhancing homologous recombination repair. *Sci. Adv.* **3,** e1601898 (2017).

121. Sams, D. S. *et al.* Neuronal CTCF Is Necessary for Basal and Experience-Dependent Gene Regulation, Memory Formation, and Genomic Structure of BDNF and Arc. *Cell Rep.* **17,** 2418–2430 (2016).

122. Tassé, M. J., Luckasson, R. & Schalock, R. L. The Relation Between Intellectual Functioning and Adaptive Behavior in the Diagnosis of Intellectual Disability. *Intellect. Dev. Disabil.* **54,** 381–390 (2016).

123. Diagnostic and statistical manual of mental disorders : DSM-5. - NLM Catalog - NCBI. Available at: https://www-ncbi-nlm-nih-gov.proxy1.lib.uwo.ca/nlmcatalog/101604226. (Accessed: 6th March 2017)

124. Javitt, D. C. Sensory processing in schizophrenia: neither simple nor intact. *Schizophr. Bull.* **35,** 1059–1064 (2009).

125. Lysaker, P., Bell, M. & Beam-Goulet, J. Wisconsin card sorting test and work performance in schizophrenia. *Psychiatry Res.* **56,** 45–51 (1995).

126. Vita, A., De Peri, L., Deste, G. & Sacchetti, E. Progressive loss of cortical gray matter in schizophrenia: a meta-analysis and meta-regression of longitudinal MRI studies. *Transl. Psychiatry* **2,** e190 (2012).

127. Glantz, L. A. & Lewis, D. A. Decreased dendritic spine density on prefrontal cortical pyramidal neurons in schizophrenia. *Arch. Gen. Psychiatry* **57,** 65–73 (2000).

128. Kapur, S., Mizrahi, R. & Li, M. From dopamine to salience to psychosis--linking biology, pharmacology and phenomenology of psychosis. *Schizophr. Res.* **79,** 59–68 (2005).

129. de Lacy, N. & King, B. H. Revisiting the relationship between autism and schizophrenia: toward an integrated neurobiology. *Annu. Rev. Clin. Psychol.* **9,** 555–587 (2013).

130. Fromer, M. *et al.* De novo mutations in schizophrenia implicate synaptic networks. *Nature* **506,** 179 (2014).

131. Insel, T. R. Rethinking schizophrenia. *Nature* **468,** 187–193 (2010).

132. Seshadri, S., Zeledon, M. & Sawa, A. Synapse-specific contributions in the cortical pathology of schizophrenia. *Neurobiol. Dis.* **53,** 26–35 (2013).

133. Zikopoulos, B. & Barbas, H. Altered neural connectivity in excitatory and inhibitory cortical circuits in autism. *Front. Hum. Neurosci.* **7,** 609 (2013).

134. Singh, S. K. & Eroglu, C. Neuroligins provide molecular links between syndromic and nonsyndromic autism. *Sci. Signal.* **6,** re4 (2013).

135. Poot, M. Connecting the CNTNAP2 Networks with Neurodevelopmental Disorders. *Mol. Syndromol.* **6,** 7–22 (2015).

136. Millar, J. K. *et al.* Disruption of two novel genes by a translocation co-segregating with schizophrenia. *Hum. Mol. Genet.* **9,** 1415–1423 (2000).

137. Schumacher, J. *et al.* The DISC locus and schizophrenia: evidence from an association study in a central European sample and from a meta-analysis across different European populations. *Hum. Mol. Genet.* **18,** 2719–2727 (2009).

138. Mei, L. & Xiong, W.-C. Neuregulin 1 in neural development, synaptic plasticity and schizophrenia. *Nat. Rev. Neurosci.* **9,** 437–452 (2008).

139. Haukvik, U. K., Hartberg, C. B. & Agartz, I. Schizophrenia--what does structural MRI show? *Tidsskr. Den Nor. Laegeforening Tidsskr. Prakt. Med. Ny Raekke* **133,** 850–853 (2013).

140. Bottmer, C. *et al.* Reduced cerebellar volume and neurological soft signs in first-episode schizophrenia. *Psychiatry Res. Neuroimaging* **140,** 239–250 (2005).

141. Andreasen, N. C., Paradiso, S. & O’Leary, D. S. ‘Cognitive dysmetria’ as an integrative theory of schizophrenia: a dysfunction in cortical-subcortical-cerebellar circuitry? *Schizophr. Bull.* **24,** 203–218 (1998).

142. Courchesne, E., Campbell, K. & Solso, S. Brain growth across the life span in autism: age-specific changes in anatomical pathology. *Brain Res.* **1380,** 138–145 (2011).

143. Brambilla, P. *et al.* Brain anatomy and development in autism: review of structural MRI studies. *Brain Res. Bull.* **61,** 557–569 (2003).

144. Ellegood, J. *et al.* Clustering autism - using neuroanatomical differences in 26 mouse models to gain insight into the heterogeneity. *Mol. Psychiatry* **20,** 118–125 (2015).

145. Wass, S. Distortions and disconnections: Disrupted brain connectivity in autism. *Brain Cogn.* **75,** 18–28 (2011).

146. Vogel-Ciernia, A. & Wood, M. A. Neuron-specific chromatin remodeling: A missing link in epigenetic mechanisms underlying synaptic plasticity, memory, and intellectual disability disorders. *Neuropharmacology* **80,** 18–27 (2014).

147. López, A. J. & Wood, M. A. Role of nucleosome remodeling in neurodevelopmental and intellectual disability disorders. *Front. Behav. Neurosci.* **9,** (2015).

148. van Bokhoven, H. & Kramer, J. M. Disruption of the epigenetic code: an emerging mechanism in mental retardation. *Neurobiol. Dis.* **39,** 3–12 (2010).

149. Gregor, A. *et al.* De novo mutations in the genome organizer CTCF cause intellectual disability. *Am. J. Hum. Genet.* **93,** 124–131 (2013).

150. Juraeva, D. *et al.* Integrated Pathway-Based Approach Identifies Association between Genomic Regions at CTCF and CACNB2 and Schizophrenia. *PLOS Genet* **10,** e1004345 (2014).

151. Watrin, E., Kaiser, F. J. & Wendt, K. S. Gene regulation and chromatin organization: relevance of cohesin mutations to human disease. *Curr. Opin. Genet. Dev.* **37,** 59–66 (2016).

152. Caro-Llopis, A. *et al.* De novo mutations in genes of mediator complex causing syndromic intellectual disability: mediatorpathy or transcriptomopathy? *Pediatr. Res.* **80,** 809–815 (2016).

153. Whitton, L. *et al.* Cognitive analysis of schizophrenia risk genes that function as epigenetic regulators of gene expression. *Am. J. Med. Genet. Part B Neuropsychiatr. Genet. Off. Publ. Int. Soc. Psychiatr. Genet.* **171,** 1170–1179 (2016).

154. Spena, S., Gervasini, C. & Milani, D. Genetic Advances in Intellectual Disability: Ultra-Rare Syndromes: The Example of Rubinstein–Taybi Syndrome. *J. Pediatr. Genet.* **4,** 177 (2015).

155. Heintzman, N. D. *et al.* Distinct and predictive chromatin signatures of transcriptional promoters and enhancers in the human genome. *Nat. Genet.* **39,** 311–318 (2007).

156. Visel, A. *et al.* ChIP-seq accurately predicts tissue-specific activity of enhancers. *Nature* **457,** 854–858 (2009).

157. Creyghton, M. P. *et al.* Histone H3K27ac separates active from poised enhancers and predicts developmental state. *Proc. Natl. Acad. Sci. U. S. A.* **107,** 21931–21936 (2010).

158. Kim, T.-K. *et al.* Widespread transcription at neuronal activity-regulated enhancers. *Nature* **465,** 182–187 (2010).

159. Malik, A. N. *et al.* Genome-wide identification and characterization of functional neuronal activity-dependent enhancers. *Nat. Neurosci.* **17,** 1330–1339 (2014).

160. Amir, R. E. *et al.* Rett syndrome is caused by mutations in X-linked MECP2, encoding methyl-CpG-binding protein 2. *Nat. Genet.* **23,** 185–188 (1999).

161. Skene, P. J. *et al.* Neuronal MeCP2 is expressed at near histone-octamer levels and globally alters the chromatin state. *Mol. Cell* **37,** 457–468 (2010).

162. Ghosh, R. P., Horowitz-Scherer, R. A., Nikitina, T., Shlyakhtenko, L. S. & Woodcock, C. L. MeCP2 binds cooperatively to its substrate and competes with histone H1 for chromatin binding sites. *Mol. Cell. Biol.* **30,** 4656–4670 (2010).

163. Casas-Delucchi, C. S., Becker, A., Bolius, J. J. & Cardoso, M. C. Targeted manipulation of heterochromatin rescues MeCP2 Rett mutants and re-establishes higher order chromatin organization. *Nucleic Acids Res.* **40,** e176 (2012).

164. Chahrour, M. *et al.* MeCP2, a Key Contributor to Neurological Disease, Activates and Represses Transcription. *Science* **320,** 1224–1229 (2008).

165. Horike, S., Cai, S., Miyano, M., Cheng, J.-F. & Kohwi-Shigematsu, T. Loss of silent-chromatin looping and impaired imprinting of DLX5 in Rett syndrome. *Nat. Genet.* **37,** 31–40 (2005).

166. Gibbons, R. J., Wilkie, A. O., Weatherall, D. J. & Higgs, D. R. A newly defined X linked mental retardation syndrome associated with alpha thalassaemia. *J. Med. Genet.* **28,** 729–733 (1991).

167. Gibbons, R. J., Picketts, D. J., Villard, L. & Higgs, D. R. Mutations in a putative global transcriptional regulator cause X-linked mental retardation with alpha-thalassemia (ATR-X syndrome). *Cell* **80,** 837–845 (1995).

168. Iwase, S. *et al.* ATRX ADD domain links an atypical histone methylation recognition mechanism to human mental-retardation syndrome. *Nat. Struct. Mol. Biol.* **18,** 769–776 (2011).

169. Dhayalan, A. *et al.* The ATRX-ADD domain binds to H3 tail peptides and reads the combined methylation state of K4 and K9. *Hum. Mol. Genet.* **20,** 2195–2203 (2011).

170. Elbert, A. & Bérubé, N. G. Chromatin Structure and Intellectual Disability Syndromes. (2013). doi:10.5772/55730

171. Richmond, E. & Peterson, C. L. Functional analysis of the DNA-stimulated ATPase domain of yeast SWI2/SNF2. *Nucleic Acids Res.* **24,** 3685–3692 (1996).

172. Lewis, P. W., Elsaesser, S. J., Noh, K.-M., Stadler, S. C. & Allis, C. D. Daxx is an H3.3-specific histone chaperone and cooperates with ATRX in replication-independent chromatin assembly at telomeres. *Proc. Natl. Acad. Sci.* **107,** 14075–14080 (2010).

173. Levy, M. A., Kernohan, K. D., Jiang, Y. & Bérubé, N. G. ATRX promotes gene expression by facilitating transcriptional elongation through guanine-rich coding regions. *Hum. Mol. Genet.* **24,** 1824–1835 (2015).

174. Bérubé, N. G. *et al.* The chromatin-remodeling protein ATRX is critical for neuronal survival during corticogenesis. *J. Clin. Invest.* **115,** 258–267 (2005).

175. Watson, L. A. *et al.* Atrx deficiency induces telomere dysfunction, endocrine defects, and reduced life span. *J. Clin. Invest.* **123,** 2049–2063 (2013).

176. Nan, X. *et al.* Interaction between chromatin proteins MECP2 and ATRX is disrupted by mutations that cause inherited mental retardation. *Proc. Natl. Acad. Sci. U. S. A.* **104,** 2709–2714 (2007).

177. Nakanishi, M. *et al.* Investigation of autistic features among individuals with mild to moderate Cornelia de Lange syndrome. *Am. J. Med. Genet. A.* **158A,** 1841–1847 (2012).

178. Dorsett, D. & Krantz, I. D. On the molecular etiology of Cornelia de Lange syndrome. *Ann. N. Y. Acad. Sci.* **1151,** 22–37 (2009).

179. Parenti, I. *et al.* Mutations in chromatin regulators functionally link Cornelia de Lange syndrome and clinically overlapping phenotypes. *Hum. Genet.* **136,** 307–320 (2017).

180. Muto, A., Calof, A. L., Lander, A. D. & Schilling, T. F. Multifactorial origins of heart and gut defects in nipbl-deficient zebrafish, a model of Cornelia de Lange Syndrome. *PLoS Biol.* **9,** e1001181 (2011).

181. Kawauchi, S. *et al.* Multiple organ system defects and transcriptional dysregulation in the Nipbl(+/-) mouse, a model of Cornelia de Lange Syndrome. *PLoS Genet.* **5,** e1000650 (2009).

182. Bastaki, F. *et al.* Identification of a novel CTCF mutation responsible for syndromic intellectual disability – a case report. *BMC Med. Genet.* **18,** 68 (2017).

183. Iossifov, I. *et al.* The contribution of de novo coding mutations to autism spectrum disorder. *Nature* **515,** 216–221 (2014).

184. Goeman, J. J., van de Geer, S. A., de Kort, F. & van Houwelingen, H. C. A global test for groups of genes: testing association with a clinical outcome. *Bioinforma. Oxf. Engl.* **20,** 93–99 (2004).

185. Pedroso, I. & Breen, G. Gene set analysis and network analysis for genome-wide association studies. *Cold Spring Harb. Protoc.* **2011,** (2011).

186. Chao, H.-T. *et al.* Dysfunction in GABA signalling mediates autism-like stereotypies and Rett syndrome phenotypes. *Nature* **468,** 263–269 (2010).

187. Peñagarikano, O. *et al.* Absence of CNTNAP2 leads to epilepsy, neuronal migration abnormalities, and core autism-related deficits. *Cell* **147,** 235–246 (2011).

188. Fatemi, S. H. *et al.* Glutamic acid decarboxylase 65 and 67 kDa proteins are reduced in autistic parietal and cerebellar cortices. *Biol. Psychiatry* **52,** 805–810 (2002).

189. Hashimoto, T. *et al.* Alterations in GABA-related transcriptome in the dorsolateral prefrontal cortex of subjects with schizophrenia. *Mol. Psychiatry* **13,** 147–161 (2007).

190. Thompson, M., Weickert, C. S., Wyatt, E. & Webster, M. J. Decreased glutamic acid decarboxylase67 mRNA expression in multiple brain areas of patients with schizophrenia and mood disorders. *J. Psychiatr. Res.* **43,** 970–977 (2009).

191. Gonzalez-Burgos, G., Hashimoto, T. & Lewis, D. A. Alterations of Cortical GABA Neurons and Network Oscillations in Schizophrenia. *Curr. Psychiatry Rep.* **12,** 335–344 (2010).

192. Volk, D. W. *et al.* Reciprocal alterations in pre- and postsynaptic inhibitory markers at chandelier cell inputs to pyramidal neurons in schizophrenia. *Cereb. Cortex N. Y. N 1991* **12,** 1063–1070 (2002).

193. Beneyto, M., Abbott, A., Hashimoto, T. & Lewis, D. A. Lamina-specific alterations in cortical GABA(A) receptor subunit expression in schizophrenia. *Cereb. Cortex N. Y. N 1991* **21,** 999–1011 (2011).

194. Akbarian, S. *et al.* Gene expression for glutamic acid decarboxylase is reduced without loss of neurons in prefrontal cortex of schizophrenics. *Arch. Gen. Psychiatry* **52,** 258–266 (1995).

195. Anderson, S. A., Volk, D. W. & Lewis, D. A. Increased density of microtubule associated protein 2-immunoreactive neurons in the prefrontal white matter of schizophrenic subjects. *Schizophr. Res.* **19,** 111–119 (1996).

196. Eastwood, S. L. & Harrison, P. J. Interstitial white matter neurons express less reelin and are abnormally distributed in schizophrenia: towards an integration of molecular and morphologic aspects of the neurodevelopmental hypothesis. *Mol. Psychiatry* **8,** 769, 821–831 (2003).

197. Eastwood, S. L. & Harrison, P. J. Interstitial white matter neuron density in the dorsolateral prefrontal cortex and parahippocampal gyrus in schizophrenia. *Schizophr. Res.* **79,** 181–188 (2005).

198. Kirkpatrick, B., Conley, R. C., Kakoyannis, A., Reep, R. L. & Roberts, R. C. Interstitial cells of the white matter in the inferior parietal cortex in schizophrenia: An unbiased cell-counting study. *Synap. N. Y. N* **34,** 95–102 (1999).

199. Yang, Y., Fung, S. J., Rothwell, A., Tianmei, S. & Weickert, C. S. Increased interstitial white matter neuron density in the dorsolateral prefrontal cortex of people with schizophrenia. *Biol. Psychiatry* **69,** 63–70 (2011).

200. Catts, V. S. *et al.* Rethinking schizophrenia in the context of normal neurodevelopment. *Front. Cell. Neurosci.* **7,** 60 (2013).

201. Marín, O. Interneuron dysfunction in psychiatric disorders. *Nat. Rev. Neurosci.* **13,** 107–120 (2012).

202. Buzsáki, G. & Draguhn, A. Neuronal Oscillations in Cortical Networks. *Science* **304,** 1926–1929 (2004).

203. Haenschel, C. *et al.* Cortical Oscillatory Activity Is Critical for Working Memory as Revealed by Deficits in Early-Onset Schizophrenia. *J. Neurosci.* **29,** 9481–9489 (2009).

204. Barr, M. S. *et al.* Evidence for excessive frontal evoked gamma oscillatory activity in schizophrenia during working memory. *Schizophr. Res.* **121,** 146–152 (2010).

205. Uhlhaas, P. J. High-Frequency Oscillations in Schizophrenia. *Clin. EEG Neurosci.* **42,** 77–82 (2011).

206. Beasley, C. L. & Reynolds, G. P. Parvalbumin-immunoreactive neurons are reduced in the prefrontal cortex of schizophrenics. *Schizophr. Res.* **24,** 349–355 (1997).

207. Sakai, T. *et al.* Changes in density of calcium-binding-protein-immunoreactive GABAergic neurons in prefrontal cortex in schizophrenia and bipolar disorder. *Neuropathol. Off. J. Jpn. Soc. Neuropathol.* **28,** 143–150 (2008).

208. Mellios, N. *et al.* Molecular determinants of dysregulated GABAergic gene expression in the prefrontal cortex of subjects with schizophrenia. *Biol. Psychiatry* **65,** 1006–1014 (2009).

209. Fung, S. J. *et al.* Expression of interneuron markers in the dorsolateral prefrontal cortex of the developing human and in schizophrenia. *Am. J. Psychiatry* **167,** 1479–1488 (2010).

210. Hashimoto, T. *et al.* Gene Expression Deficits in a Subclass of GABA Neurons in the Prefrontal Cortex of Subjects with Schizophrenia. *J. Neurosci.* **23,** 6315–6326 (2003).

211. Morris, B. J., Cochran, S. M. & Pratt, J. A. PCP: from pharmacology to modelling schizophrenia. *Curr. Opin. Pharmacol.* **5,** 101–106 (2005).

212. Kinney, J. W. *et al.* A specific role for NR2A-containing NMDA receptors in the maintenance of parvalbumin and GAD67 immunoreactivity in cultured interneurons. *J. Neurosci. Off. J. Soc. Neurosci.* **26,** 1604–1615 (2006).

213. Carlén, M. *et al.* A critical role for NMDA receptors in parvalbumin interneurons for gamma rhythm induction and behavior. *Mol. Psychiatry* **17,** 537–548 (2012).

214. Fazzari, P. *et al.* Control of cortical GABA circuitry development by Nrg1 and ErbB4 signalling. *Nature* **464,** 1376–1380 (2010).

215. Ting, A. K. *et al.* Neuregulin 1 promotes excitatory synapse development and function in GABAergic interneurons. *J. Neurosci. Off. J. Soc. Neurosci.* **31,** 15–25 (2011).

216. Hikida, T. *et al.* Dominant-negative DISC1 transgenic mice display schizophrenia-associated phenotypes detected by measures translatable to humans. *Proc. Natl. Acad. Sci.* **104,** 14501–14506 (2007).

217. Lee, F. H. F., Zai, C. C., Cordes, S. P., Roder, J. C. & Wong, A. H. C. Abnormal interneuron development in disrupted-in-schizophrenia-1 L100P mutant mice. *Mol. Brain* **6,** 20 (2013).

218. Shen, S. *et al.* Schizophrenia-Related Neural and Behavioral Phenotypes in Transgenic Mice Expressing Truncated Disc1. *J. Neurosci.* **28,** 10893–10904 (2008).

219. Morris, H. M., Hashimoto, T. & Lewis, D. A. Alterations in somatostatin mRNA expression in the dorsolateral prefrontal cortex of subjects with schizophrenia or schizoaffective disorder. *Cereb. Cortex N. Y. N 1991* **18,** 1575–1587 (2008).

220. Volk, D. W., Edelson, J. R. & Lewis, D. A. Cortical Inhibitory Neuron Disturbances in Schizophrenia: Role of the Ontogenetic Transcription Factor Lhx6. *Schizophr. Bull.* **40,** 1053–1061 (2014).

221. Malt, E. A., Juhasz, K., Malt, U. F. & Naumann, T. A Role for the Transcription Factor Nk2 Homeobox 1 in Schizophrenia: Convergent Evidence from Animal and Human Studies. *Front. Behav. Neurosci.* 59 (2016). doi:10.3389/fnbeh.2016.00059

222. Silverman, J. L., Yang, M., Lord, C. & Crawley, J. N. Behavioural phenotyping assays for mouse models of autism. *Nat. Rev. Neurosci.* **11,** 490–502 (2010).

223. Banerjee-Basu, S. & Packer, A. SFARI Gene: an evolving database for the autism research community. *Dis. Model. Mech.* **3,** 133–135 (2010).

224. Lewis, M. H., Tanimura, Y., Lee, L. W. & Bodfish, J. W. Animal models of restricted repetitive behavior in autism. *Behav. Brain Res.* **176,** 66–74 (2007).

225. Spencer, C. M., Graham, D. F., Yuva-Paylor, L. A., Nelson, D. L. & Paylor, R. Social behavior in Fmr1 knockout mice carrying a human FMR1 transgene. *Behav. Neurosci.* **122,** 710–715 (2008).

226. Branchi, I., Santucci, D. & Alleva, E. Ultrasonic vocalisation emitted by infant rodents: a tool for assessment of neurobehavioural development. *Behav. Brain Res.* **125,** 49–56 (2001).

227. Jamain, S. *et al.* Reduced social interaction and ultrasonic communication in a mouse model of monogenic heritable autism. *Proc. Natl. Acad. Sci.* **105,** 1710–1715 (2008).

228. Bey, A. L. & Jiang, Y. Current Protocols in Pharmacology: Overview of Mouse Models of Autism Spectrum Disorders. *Curr. Protoc. Pharmacol. Editor. Board SJ Enna Ed.--Chief Al* **66,** 5.66.1 (2014).

229. Vorhees, C. V. & Williams, M. T. Assessing Spatial Learning and Memory in Rodents. *ILAR J.* **55,** 310–332 (2014).

230. Wong, A. H. C. & Josselyn, S. A. Caution When Diagnosing Your Mouse With Schizophrenia: The Use and Misuse of Model Animals for Understanding Psychiatric Disorders. *Biol. Psychiatry* **79,** 32–38 (2016).

231. Powell, C. M. & Miyakawa, T. Schizophrenia-Relevant Behavioral Testing in Rodent Models: A Uniquely Human Disorder? *Biol. Psychiatry* **59,** 1198–1207 (2006).

232. Jones, C., Watson, D. & Fone, K. Animal models of schizophrenia. *Br. J. Pharmacol.* **164,** 1162–1194 (2011).

233. Bissonette, G. B. & Powell, E. M. Reversal learning and attentional set-shifting in mice. *Neuropharmacology* **62,** 1168–1174 (2012).

234. Dudchenko, P. A. An overview of the tasks used to test working memory in rodents. *Neurosci. Biobehav. Rev.* **28,** 699–709 (2004).

apter 2

The work in this chapter originates from the following submitted article:

The CTCF chromatin organizer directs the fate of cortical interneurons derived from the MGE

Elbert, A.[1,2], Vogt, D.[3], Watson, L.A.[1,2], Levy, M. [1,2], Jiang, Y. [1,2], Brûlé, E. [1,2], Rowland, M. E. [1,2], Rubenstein, J. L. R.[3] and Bérubé, N.G.[1,2,*]

Affiliations: [1]Children's Health Research Institute, London, Ontario, Canada.
[2]Departments of Paediatrics, Schulich School of Medicine and Dentistry, the University of Western Ontario, Victoria Research Laboratories, London, Ontario, Canada.
[3]Department of Psychiatry, Neuroscience Program and the Nina Ireland Laboratory of Developmental Neurobiology, University of California San Francisco, San Francisco, USA

tract

CTCF is a chromatin organizer linked to schizophrenia, intellectual disability and autism spectrum disorder. Here we show that loss of *Ctcf* disrupts the dichotomy between *Lhx6* and *Lhx8* transcriptional cascades in the MGE, which is critical for fate determination of cortical PV and SST expressing interneurons. Conditional *Ctcf* ablation MGE led to a marked reduction of these cell types in the postnatal neocortex and to cortical interneuron lamination defects. Re-expression of *Lhx6* in *Ctcf*-null MGE cells in transplantation experiments rescued cortical SST interneuron number and interneuron lamination defects, indicating that these particular outcomes of *Ctcf* deletion are due to decreased expression of *Lhx6* in the MGE. Conversely, we detected a surplus of MGE cells expressing *Lhx8*

that gain markers of GABAergic projection neurons of the basal forebrain, indicative of a fate switch. Collectively, these findings suggest that CTCF-mediated chromatin organization in embryonic progenitor cells of the MGE is essential for the fate and differentiation of cortical interneurons and the establishment of functional inhibitory networks.

oduction

Interneurons that produce γ-aminobutyric acid (GABA) provide the rhythmic inhibitory activity that synchronizes pyramidal cell firing in mature neuronal circuits of the cortex (reviewed in [1]). Not surprisingly, perturbation of the cortical GABAergic system has been observed in several neurodevelopmental disorders, including Down Syndrome[2, 3], Fragile X syndrome[4, 5], and autism spectrum disorder (ASD)[6, 7], and pharmacological modulation of GABA receptors has been therapeutic in some contexts[8, 9]. Recently, the transplantation of immature interneurons into the postnatal cortex has been explored as an alternative to pharmacological therapy in mouse models of epilepsy[10, 11, 12]. The laminar position and marker expression of cortical interneurons depend more on intrinsic factors than extrinsic, and transplanted cortical GABAergic interneurons have the potential to integrate into existing circuits. Understanding the developmental steps and regulatory events governing cortical interneuron development is thus essential to generate interneurons for successful therapeutic transplants.

In mice, the majority of cortical interneurons are mainly produced in the ventral telencephalon in transient structures called the medial ganglionic eminence (MGE) and the caudal ganglionic eminence (CGE). MGE- and CGE-derived interneurons migrate tangentially into the developing cortical marginal and intermediate zones before radially invading the cortical plate and forming connections with the cortical pyramidal neurons[13]. Transcriptional cascades in the MGE result in a peak of neurogenesis between embryonic (E) days 12-14 that generates the future Somatostatin (SST) and Parvalbumin (PV)-expressing GABAergic interneuron subtypes[14,15]. MGE secondary progenitors (in the subventricular zone) and a subset of post-mitotic neurons express both LHX6 and LHX8, two LIM homeobox factors with partially overlapping function[16,17]. The cells destined to become cortical interneurons express only LHX6, while the neurons that express LHX8 (some in combination with LHX6) are fated to become cholinergic interneurons or pallidal GABAergic projection neurons[16,18]. *Lhx6*-null interneurons resemble CGE-derived neurogliaform interneurons with regard to marker expression, laminar position and electrophysiology[19], indicating that LHX6 can specify the fate of MGE-derived interneurons.

CTCF is a ubiquitously expressed protein that orchestrates loop formation in chromatin by binding to a consensus sequence and simultaneously dimerizing or partnering with other chromatin-associated proteins like the cohesin complex (reviewed in[20]). These loops can bring distant genomic elements into close proximity, such as promoters and enhancers, or act as a barrier, such as when CTCF functions as an insulator protein. In parallel, emerging evidence suggests that CTCF is required for normal development and functioning of the central nervous system. *De novo* mutations in one copy of the human *CTCF* gene were recently identified in five patients with microcephaly, intellectual disability (ID), and short stature[21,22]. Two individuals with ID screened as part of a cohort selected for ASD were also identified as having mutations in one allele of *CTCF*[23]. Polymorphisms in and around the *CTCF* gene have also been associated with schizophrenia in two different patient-control cohorts[24]. Moreover, CTCF has been shown to regulate the expression of the protocadherin membrane adhesion proteins for which the combinatorial expression in neurons is thought to underlie the specificity of neuronal connectivity[25]. The analysis of dorsal projection neurons in *Ctcf*-deficient mice revealed defects in dendritic arborisation and reduced spine density[25]. Viral-mediated knockdown of *Ctcf* in hippocampal cells also results in reduced spine density and leads to impaired learning[26].

In this study we present our findings from *Ctcf* gene inactivation in the developing mouse ventral telencephalon. We show that CTCF expression is required for the normal development and fate specification of MGE-derived cortical GABAergic interneurons. *Ctcf* deletion results in reduced expression of *Lhx6*, and an up-regulation of *Lhx8*, resulting in aberrant fate specification and reduced number of cortical PV+ and SST+ interneuron subtypes. Re-introduction of Lhx6 in CTCF-null MGE progenitors is sufficient to re-establish the normal number of SST-positive interneurons and lamination pattern in transplantation experiments. These findings suggest that disturbing chromatin organization during embryonic ventral telencephalon development can affect postnatal cortical inhibitory activity, perhaps contributing to cognitive abnormalities.

ults

A-seq of CTCF-null telencephalon identifies clustered protocadherins and genes involved ABAergic neuron differentiation

We previously reported dorsal telencephalon defects upon conditional inactivation of *Ctcf* in the embryonic brain using the *NestinCre* driver line of mice[27], which deleted *Ctcf* in early neural progenitors (radial glia). Analysis of the dorsal forebrain of E16.5 *Ctcf*$^{Nes\text{-}Cre}$

revealed extensive TP53 and PUMA-dependent cell death as well as premature differentiation of neural precursor cells, leading to depletion of the progenitor pool[27].

Taking advantage of the short period of time preceding apoptosis induction, we proceeded to identify differences in the E14 telencephalon transcriptomes of *Ctcf*$^{Nes\text{-}Cre}$ and littermate control embryos. Using a criterion of i) a minimum expression of 2% of the average reads, and ii) a minimum average fold-change of 1.5, we generated a list of genes (n= 2024) with altered expression in the *Ctcf*$^{Nes\text{-}Cre}$ E14 forebrain (Fig. 1A). Of this list, about half (n=1050) exhibited decreased expression in the *Ctcf*$^{Nes\text{-}Cre}$ E14 telencephalon. A large number of the down-regulated genes belonged to the clustered Ca^{2+}binding protocadherin (*Pcdh*) genes, with a more pronounced effect on Pcdh-β genes (Fig. 1A,B). We confirmed the effects of *Ctcf* inactivation on the *Pcdh* genes by quantitative RT-PCR (Fig. S1). These results expand on previous reports by demonstrating embryonic regulation of the *Pcdh* cluster genes by CTCF prior to neuronal network establishment.

The list of down-regulated genes was analyzed for GO term enrichment using PANTHER version 11.1 (Pantherdb.org). The significantly enriched GO Biological Processes with >2.0 fold enrichment included several terms related to synaptic transmission, which might be expected in light of recent studies implicating CTCF in learning and memory[26]. Of note was the unexpected enrichment for genes involved in GABAergic neuron differentiation, suggesting a potential novel role of CTCF in the embryonic production of inhibitory interneurons.

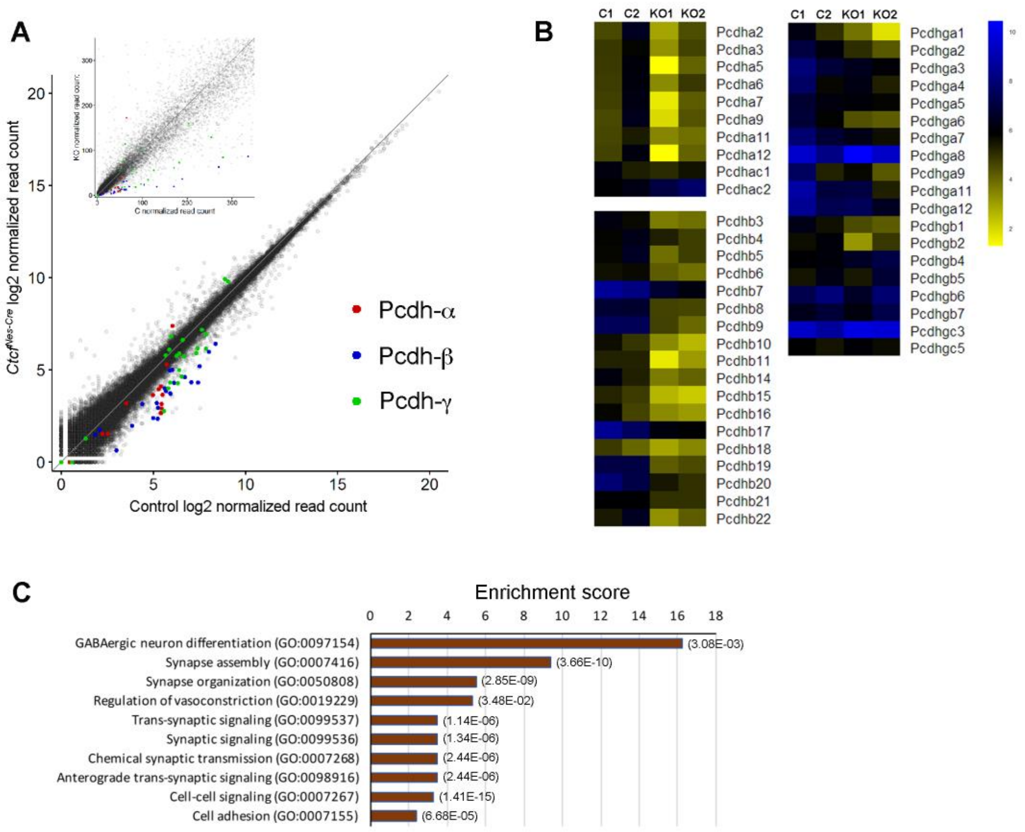

Figure 1: Transcriptional profiling of *Ctcf*-null E14 telencephalon. (A) Log$_2$ of normalized read counts of control and *Ctcf$^{Nes\text{-}Cre}$* E14 telencephalon RNA sequencing. *Pcdh* cluster genes are highlighted in colour. Inset provides a view of low-expressing genes using a linear scale. (B) Heatmaps of *Pcdh* gene expression across the a, b and g clusters. (C) List of top ten Gene Ontology terms for biological processes showing enrichment in the list of genes downregulated in *Ctcf$^{Nes\text{-}Cre}$* E14 telencephalon. The list was generated using the PANTHER over-representation test. P-values with a Bonferroni correction are shown on the right for each category.

regulates the expression of Lhx6 and Lhx8 in the MGE

The list of down-regulated genes in the *Ctcf$^{Nes\text{-}Cre}$* E14 telencephalon included *Lhx6*, which encodes a master transcription factor critical for the development of cortical GABAergic interneurons^{28}. LHX6 is required for the production of PV+ and SST+

interneuron subtypes derived from the MGE that eventually populate multiple areas of the forebrain, including the striatum and cortex. RT-qPCR confirmed a ~2.5-fold decrease in *Lhx6* transcript levels (P=0.028). Similarly, the expression of *Sst*, a known downstream target of LHX6, exhibited a ~10-fold decrease in expression (P=0.0001) (Fig. 2A). *In situ* hybridization (ISH) of E13.5 embryonic sections confirmed decreased *Lhx6* mRNA in the $Ctcf^{Nes\text{-}Cre}$ MGE (Fig. 2B) and we observed that in a subset of embryos, reduction in *Lhx6* expression was restricted to the caudal MGE (data not shown). ISH of *Sst* transcripts identified fewer *Sst+* cells migrating tangentially from the MGE towards the cortex in the $Ctcf^{Nes\text{-}Cre}$ compared to control embryos (Fig. 2C). Given that CTCF protein expression is no longer detectable in the MGE of the $Ctcf^{Nes\text{-}Cre}$ embryos by E12.5[27] (Fig. S2A), we examined *Lhx6* expression at this time point by ISH, and observed only a subtle decrease in the $Ctcf^{Nes\text{-}Cre}$ MGE compared to control (Fig. S2B). Together, these data suggest that *Lhx6* expression is affected in the $Ctcf^{Nes\text{-}Cre}$ MGE mostly after E12.5, and this reduction either begins with, or is most pronounced in cells of the posterior MGE.

We considered the possibility that the reduction in *Lhx6* transcripts reflected a loss of cells due to apoptosis of *Ctcf*-null neuroprogenitor cells. We previously reported that apoptosis in the $Ctcf^{Nes\text{-}Cre}$ embryonic brain can be prevented by concomitant deletion of the *Bbc3* gene, which encodes the TP53 apoptotic effector PUMA[27]. We thus repeated ISH for *Lhx6* and *Sst* in $Ctcf^{Nes\text{-}Cre}$ embryos in a PUMA-null background. We find that preventing apoptosis of cells in the $Ctcf^{Nes\text{-}Cre}$ telencephalon via removal of PUMA fails to rescue the level of *Lhx6* or *Sst* (Fig. 2D,E). To determine whether the reduction of *Lhx6* and *Sst* transcript levels in *Ctcf* mutant embryos results from decreased cell proliferation, we performed acute BrdU incorporation assays to calculate the percentage of proliferating cells in the ventricular zone of the MGE at E12.5, during the peak of neurogenesis. There was no significant difference in the proliferative capacity of the *Ctcf*-null MGE compared to control (Fig. S2C). Together these results indicate that the reduction of *Lhx6* and *Sst* transcripts is not caused by altered survival or proliferative capacity of *Ctcf*-deficient MGE cells.

Beginning at E9.75, MGE cells are specified in the ventricular zone by NKX2.1, a transcription factor necessary for the expression of *Lhx6* and *Lhx8*. Through unknown mechanisms, a subset of the cells that co-express these genes become either LHX6 or LHX8 positive[16]. LHX8 promotes a genetic program specifying telencephalic cholinergic interneurons that remain in the basal ganglia as striatal interneurons, or projection neurons in the septum and pallidum and *Lhx8*-deficient mice have a reduced number of these cell types[29]. We therefore also examined the effect of CTCF loss on *Lhx8* expression by ISH and RT-qPCR of RNA isolated from the MGE. In contrast to *Lhx6*, the expression of *Lhx8* was significantly increased compared to control (P=0.0058), suggesting that a greater number of MGE cells retain *Lhx8* at the expense of cells retaining *Lhx6* expression (Fig. 2F,G,I). Increased expression of *Gbx2*, a downstream target of LHX8[29], indeed supports a scenario where *Ctcf*-null MGE cells might implement different fate pathways due to the reduced *Lhx6* expression and the increased *Lhx8* expression (Fig. 2F,H,J).

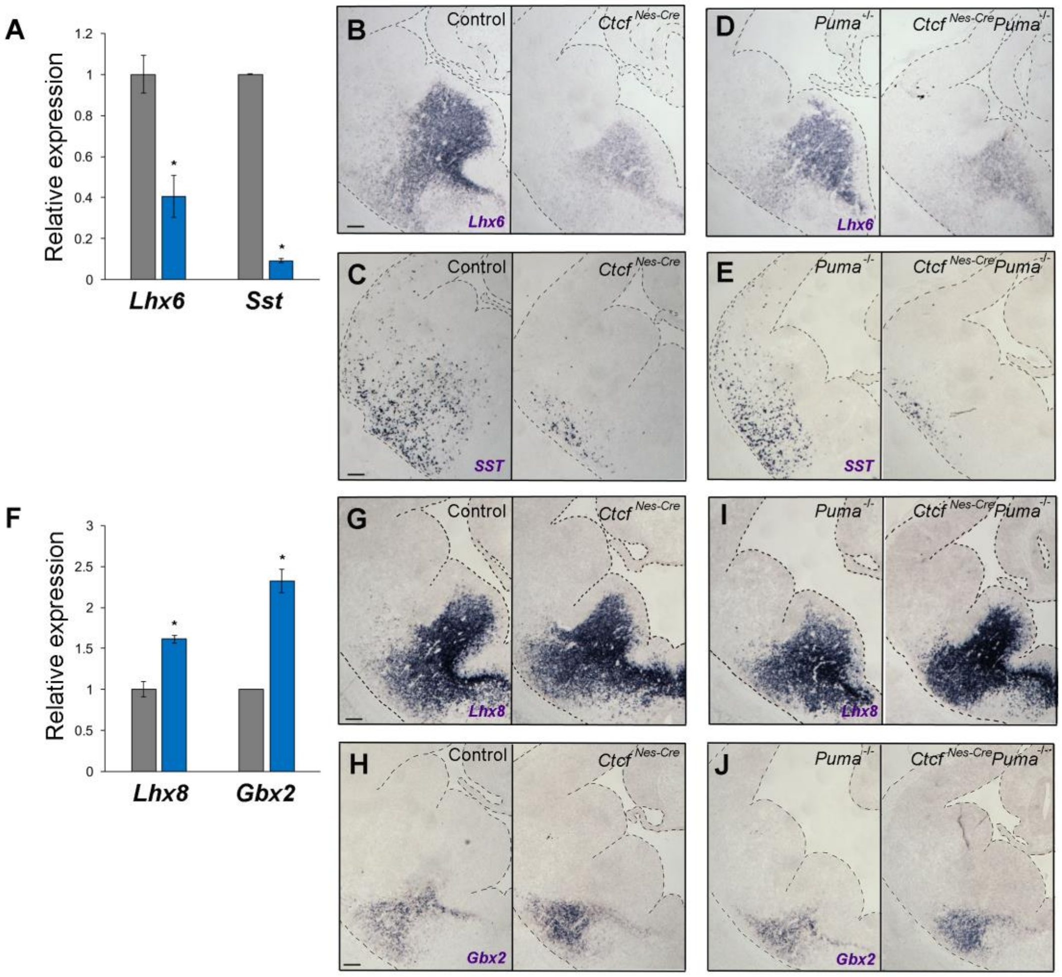

Figure 2: The *Ctcf*-null embryonic MGE exhibits altered expression of genes implicated in fate specification. (A,D) RT-qPCR of E14 telencephalon (or MGE for *Lhx8*) isolated from control (grey) or *Ctcf*$^{Nes\text{-}Cre}$ (blue) embryos (n= 3 pairs). Data was normalized to β-actin expression. Asterisks demark P <0.05, Student's t-test. Error bars represent SEM. (B-J) ISH of the indicated transcripts on E13.5 coronal brain sections of control and *Ctcf*$^{Nes\text{-}Cre}$ embryos (B, C, E, F) or PUMA-/- and *Ctcf*$^{Nes\text{-}Cre}$; PUMA-/- embryos (G-J). Scale bars represent 100 µm. Tissue edges are outlined for ease of visualization.

CF acts in parallel to, or downstream of NKX2.1 to regulate Lhx6 and Lhx8 expression

Since NKX2.1 induces the expression of *Lhx6* and *Lhx8*, we wondered whether CTCF acts upstream or in parallel with this transcription factor in the embryonic MGE. Western blot analysis demonstrates that NKX2.1 protein level is not altered in E13.5 *Ctcf*$^{Nes\text{-}Cre}$ compared to littermate-control forebrain tissue (Fig. 3A). We also stained coronal slices of E13.5 *Ctcf*$^{Nes\text{-}Cre}$ and littermate-control embryos with an anti-NKX2.1 antibody which showed no obvious change in NKX2.1 levels or localization (Fig. 3B). We next tested whether CTCF interacts with NKX2.1 to regulate *Lhx6* and *Lhx8* by co-immunoprecipitation of CTCF and NKX2.1 in pooled MGE tissue dissected from wildtype E13.5 embryos, but found no evidence for an interaction between these two proteins (Fig. 3C). In addition, we compared the chromatin occupancy of these two factors by ChIP-seq analysis. ChIP-seq for CTCF was performed on pooled wildtype E13.5 MGE tissue and the data obtained was compared to previously published NKX2.1 ChIP-seq data[30]. We find that only a small percentage of CTCF peaks (6.5%) overlap with NKX2.1 binding sites ($P<0.01$, Fig. 3D). Regulatory elements previously identified in the promoter and in the first intron of *Lhx6*[31,32] do not exhibit CTCF binding (Fig. 3E). We also examined CTCF binding to several enhancers that have activity in the MGE[32]: enhancer 422 (chr2:71,373,435–71,374,614 [mm9]), *DlxI12b* (chr2:71,374,047–71,374,552 [mm9]), the murine sequence corresponding to enhancer 692 near the human *SOX6* gene (chr7:122,275,029-122,275,957 [mm9]), the murine sequence corresponding to the human enhancer 1056 (chr18:81,349,730-81,351,184 [mm9]), and the murine sequence corresponding to the human enhancer 1538 (chr2:71,373,514-71,374,608 [mm9]). No peaks corresponding to CTCF binding are found at any of these sites (data not shown). On the other hand, we observed CTCF-binding sites that flank a large genomic region surrounding *Lhx6*, suggesting that CTCF may promote long-range loop formation perhaps required for proper regulation of *Lhx6* by NKX2.1. We also examined the pattern of CTCF binding at the *Lhx8* locus, and identified a peak in intron 6 and another ~30kb upstream of the gene (Fig.3E). This pattern of CTCF binding has been observed at other loci that exhibit negative transcriptional regulation by CTCF, including the *Bbc3*/PUMA gene[33]. Altogether, these data suggest that CTCF could act either in parallel or downstream of NKX2.1 to control *Lhx6* and *Lhx8* expression.

CF regulates MGE development cell-autonomously

While useful for the investigation of early forebrain development, the $Ctcf^{Nes\text{-}Cre}$ mice present some drawbacks: extensive cell death ensues beyond E15.5 in the telencephalon and the mice die in the perinatal period, preventing any postnatal analysis of cortical GABAergic interneurons. To circumvent these difficulties, we deleted *Ctcf* using the *Nkx2.1Cre* driver line, hereon referred to as $Ctcf^{Nkx\text{-}Cre}$ mice, which is expressed in progenitors of the MGE and the preoptic area (POA). In this model, *Ctcf* deletion occurs in the MGE before E12.5. CTCF absence from the MGE was confirmed by immunofluorescence staining of brain sections at E13.5. Loss of CTCF expression is seen in most of the MGE, except for a small dorso-medial region in some embryos, as reported previously by others[19] (Fig. 4A). Importantly, *Ctcf* deletion in the E13.5 MGE recapitulates differences in *Lhx6*, *Sst*, and *Lhx8* transcripts detected in $Ctcf^{Nes\text{-}Cre}$ embryos, establishing that these transcriptional effects are cell autonomous (Fig. 4B-D). $Ctcf^{Nkx\text{-}Cre}$ mice are smaller than controls and exhibit failure to thrive postnatally (Fig. 4E-G). While this could be caused by loss of CTCF in the MGE, NKX2.1-driven Cre expression can sometimes occur in the lung and the thyroid[34], and reduced survival of *Ctcf*$^{Nkx\text{-}Cre}$ could be caused by Cre-mediated deletion of *Ctcf* in these tissues. In support of this, we found that circulating thyroxine (T4) levels were reduced in *Ctcf*$^{Nkx\text{-}Cre}$ mice aged P20-22 (Fig. S3).

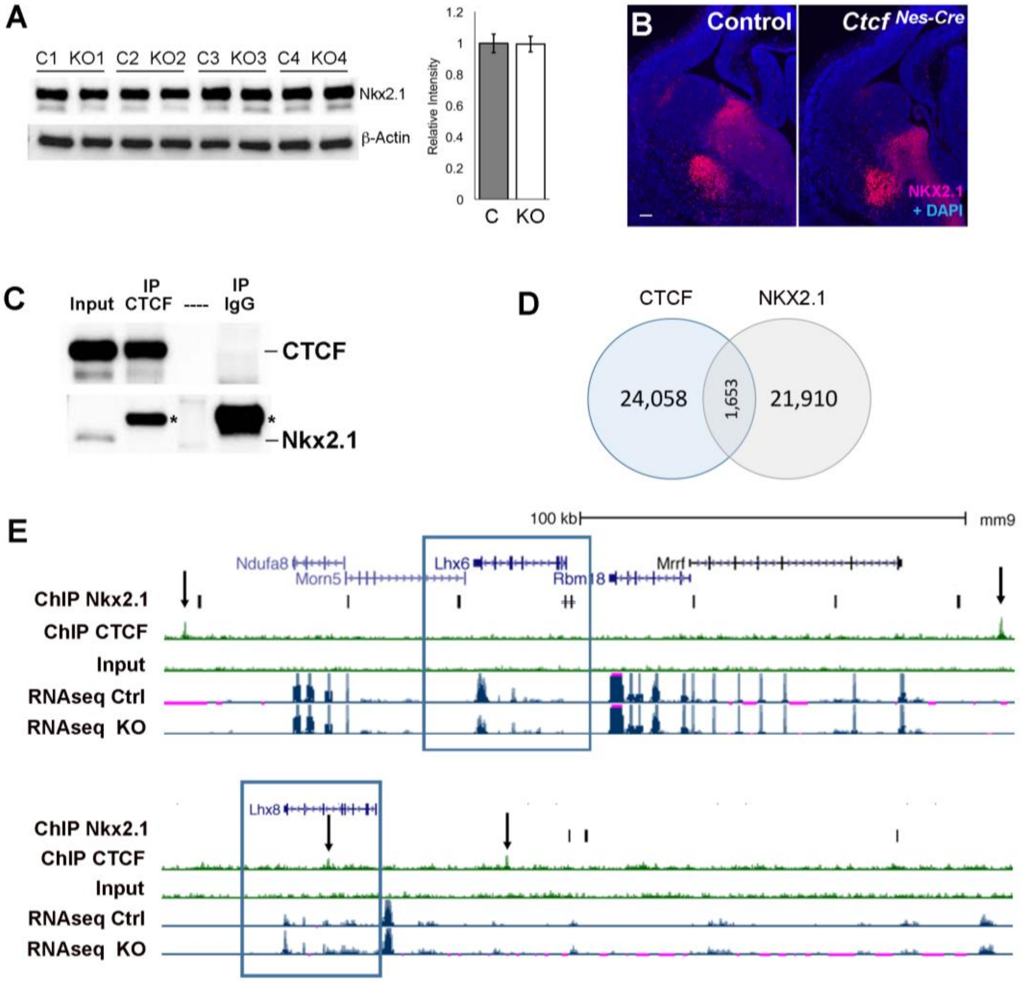

Figure 3: CTCF functions in parallel or downstream of Nkx2.1 to regulate *Lhx6* and *Lhx8.* (A) Western blot of NKX2.1 in four control (C) and *Ctcf*$^{Nes\text{-}Cre}$ (KO) E13.5 telencephalons. β-actin was used as a loading control for normalization. Quantification is shown graphically on the right. Error bars represent SEM. P=0.968, Student's t-test.(B) NKX2.1 immuno-fluorescence staining (red) in E13.5 coronal sections. Nuclei were counterstained with DAPI (blue). Scale bar represents 100 µm. (C) Co-IP of CTCF and NKX2.1 using pooled wildtype MGE tissue. Asterisks indicate non-specific IgG band. (D) Venn diagram showing the overlap of CTCF and NKX2.1 ChIP-seq peaks in the

MGE ($p<0.01$) (E) Diagram depicting UCSC genome browser views of the *Lhx6* and *Lhx8* loci (boxed), ChIP-seq peaks for NKX2.1, CTCF and input as well as the RNA-seq tracks of control and *Ctcf*$^{Nes\text{-}Cre}$ E14 telencephalon. Relevant CTCF binding sites are indicated by arrows.

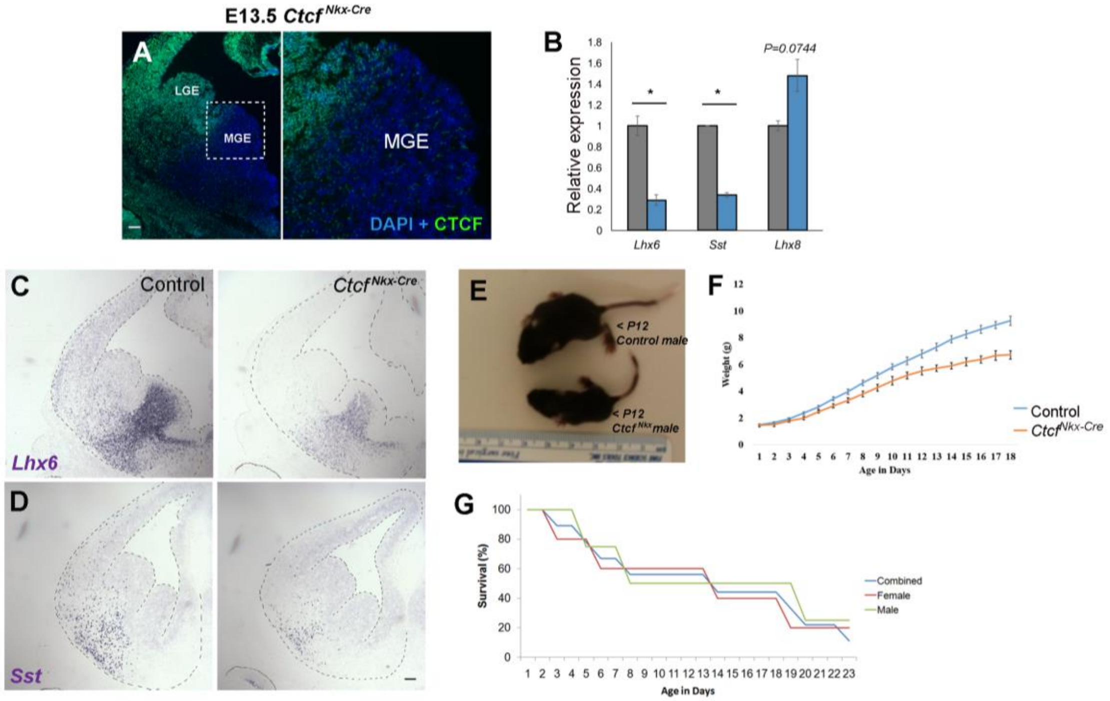
E13.5 Ctcf Nkx-Cre
A
LGE
MGE
MGE
DAPI + CTCF
B
Relative expression
P=0.0744
*
*
Lhx6
Sst
Lhx8
C
Control
Ctcf Nkx-Cre
Lhx6
D
Sst
E
< P12 Control male
< P12 Ctcf Nkx male
F
Weight (g)
Age in Days
Control
Ctcf Nkx-Cre
G
Survival (%)
Age in Days
Combined
Female
Male

Figure 4: MGE-specific inactivation of Ctcf replicates gene expression changes and extends postnatal survival. (A) CTCF immunofluorescence staining (green) of E13.5 *Ctcf*$^{Nkx\text{-}Cre}$ coronal brain sections. Nuclei are counterstained with DAPI. Higher magnification view of the MGE is shown on the right. Scalebar, 100 µm. (B) RT-qPCR of *Lhx6*, *Sst* and *Lhx8* in E14 telencephalon normalized to β-actin (n=3). Error bars represent SEM and asterisks denote $P< 0.05$ by Student's t-test. (C-D) ISH of *Lhx6* and *Sst* in E13.5 coronal sections. Scalebar, 100 µm. Tissue is outlined for ease of visualization. (E) Representative image of a 12 day-old *Ctcf*$^{Nkx\text{-}Cre}$ male mouse and littermate control. (F) Plot of weights of *Ctcf*$^{Nkx\text{-}Cre}$ (n=4) and littermate controls (n=12) over time. Error bars represent SEM. (G) Survival curve of *Ctcf*$^{Nkx\text{-}Cre}$ mice (males=4; females=5). Five animals were sacrificed due to severe distress or imminent death.

E-specific deletion of Ctcf leads to a reduction of cortical interneurons expressing Pv and

Tangential migration of MGE interneurons into the developing dorsal pallium is mediated by several molecular signals downstream of LHX6, including the interaction of chemoreceptors CXCR4 and CXCR7, present on the interneuron cell surface, with stromal cell-derived factor 1 (SDF1), which is present in the marginal and intermediate zones of the neocortex[35]. To test for defects in MGE-derived interneuron migration in the *Ctcf*$^{Nkx\text{-}Cre}$ embryos, we introduced the Cre-responsive *Rosa-mTmG* reporter gene that results in *GFP* expression upon Cre-mediated recombination (Fig. 5A). The number of GFP+ (*Ctcf*-null) MGE-derived cells were identified and counted in the E16.5 cortex of *Ctcf*$^{Nkx\text{-}Cre}$ and littermate controls. We found a significant decrease in the number of GFP+ cells in the *Ctcf*$^{Nkx\text{-}Cre}$ neocortex, consistent with either a defect in production by the MGE, survival and/or with a defect in tangential migration to the cortex (Fig. 5B,C). In support of a migration defect, the expression of *Cxcr4* was significantly decreased in the *Ctcf*$^{Nkx\text{-}Cre}$ and *Ctcf*$^{Nes\text{-}Cre}$ E14 embryos, compared to controls (Fig. S4).

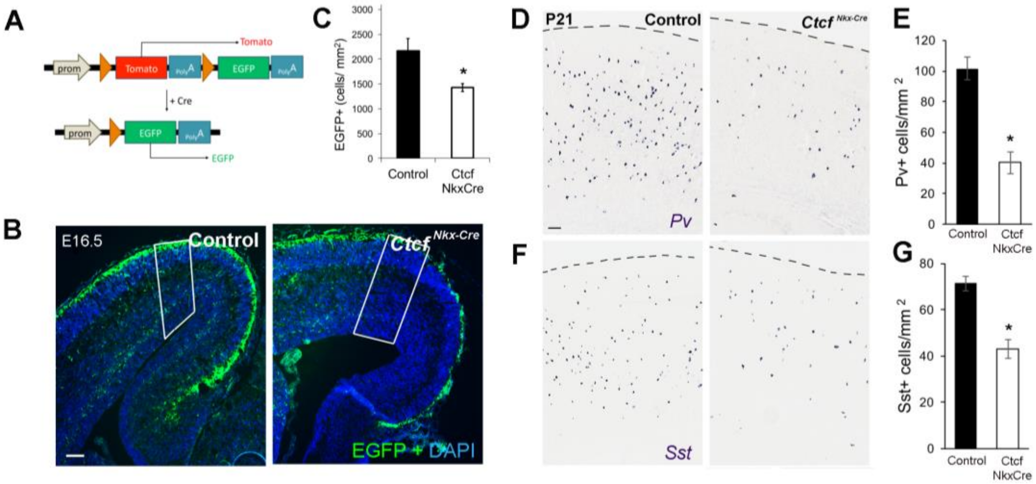
A
prom
Tomato
PolyA
EGFP
PolyA
Tomato
+ Cre
prom
EGFP
PolyA
EGFP
C
EGFP+ (cells/ mm²)
3000
2500
2000
1500
1000
500
0
*
Control
Ctcf NkxCre
B
E16.5
Control
Ctcf Nkx-Cre
EGFP + DAPI
D
P21
Control
Ctcf Nkx-Cre
Pv
E
Pv+ cells/mm 2
120
100
80
60
40
20
0
*
Control
Ctcf NkxCre
F
Sst
G
Sst+ cells/mm 2
80
60
40
20
0
*
Control
Ctcf NkxCre

Figure 5: Fewer CTCF-null MGE-derived cells reach their destination in the cortex. (A) Diagram depicting the Rosa-mTmG allele and the Cre-dependent recombination that results in a switch from red to green fluorescence. Orange arrows represent loxP sites.(B) Fluorescence microscopy of E16.5 cortical sections of the indicated genotypes after DAPI counterstaining (blue). Green fluorescence is evident in Cre+ cells originating from the MGE that are migrating tangentially in the cortex. Note that the red fluorescence channel is not shown. Scalebar,100 µm. *Nkx-Cre* control animals were used for this experiment (C) Quantification of the density of GFP+ cells (outlined in white in B), n=5 controls, n=6 *Ctcf*$^{Nkx\text{-}Cre}$. (D,F) *Pv* and *Sst* ISH in the cortex of P21 *Ctcf*$^{Nkx\text{-}Cre}$ mice and littermate controls (E, G). Quantification of the density of *Pv*+ cells (n=4 pairs) or *Sst*+ cells (n=3 pairs). Error bars represent SEM and asterisks indicate P<0.05, Student's t-test.

The extended survival of these mice compared to the *Ctcf*$^{Nes\text{-}Cre}$ allowed us to investigate the outcome of embryonic MGE abnormalities on cortical GABAergic interneurons at P21, a time at which cortical interneuron number and laminar position have attained adult patterns[36]. ISH of brain sections from control and mutant P21 mice revealed that the number of *Pv*+ and *Sst*+ interneurons in the *Ctcf*$^{Nkx\text{-}Cre}$ cortex is significantly reduced compared to controls, (Fig. 5D-G). We also examined the outcome of CTCF loss on laminar positioning of interneurons, by dividing a sampled cortical area into ten equal bins, with bin 1 corresponding to the most superficial of these (ie cortical layer I). This analysis showed that *Sst*+ and *Pv*+ cells in *Ctcf*$^{Nkx\text{-}Cre}$ cortices were reduced equally among lamina (data not shown). As MGE-derived interneurons occupy laminar layers based on developmental time, these findings suggest that *Ctcf* deletion affects MGE interneuron production equally over time.

tion of Ctcf results in altered fate and distribution of MGE-derived cells

To further evaluate the postnatal consequences of the transcriptional alterations of *Lhx6* and *Lhx8* in the embryonic CTCF-null MGE, we investigated the relative proportion of interneuron subtypes as well as their respective cortical position at P21. Despite the observed reduction of *Pv*+ and *Sst*+ cells in the cortex, *Gad1* ISH shows that the total number of cortical GABAergic interneurons was not different (Fig. 6A,B). Moreover, we observed no difference in the number of *Reelin*+ interneurons, a gene expressed in a portion of interneurons originating from the MGE and the CGE (Fig. 6D,E). However, we find that *Gad1*+ interneurons in the *Ctcf*$^{Nkx\text{-}Cre}$ cortex tend to occupy upper cortical layers at the expense of deeper ones when compared to controls (Fig. 6C). This change in laminar distribution was also observed with *Reelin*+ interneurons (Fig. 6F).

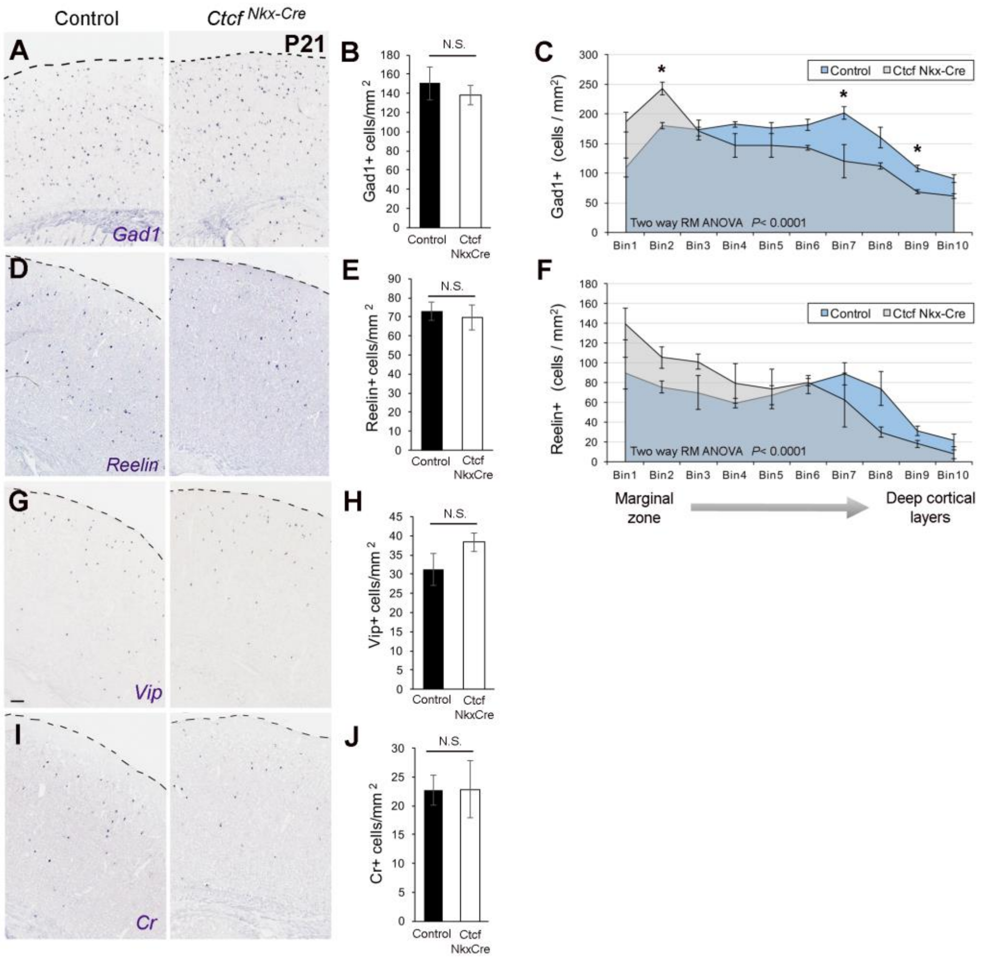

Figure 6: CTCF is required for final cortical lamination of interneurons. ISH of P21 cortices (A , D, G, I). *Gad1* marks all cortical interneurons; *Reelin* marks a subset of MGE and CGE-derived interneurons; *Vip* and *Calretinin* (*Cr*) are markers of CGE-derived interneurons. Quantification of cortical cell densities. Error bars represent SEM.

(C, F) Cell densities by cortical bin. Cortex was divided into ten horizontal bins, where bin 1 represents the most superficial and approximates the marginal zone. Two-way repeated measures ANOVA was significant for both *Gad1* and *Reelin*. Student's t-test was performed for each bin, and significantly different bins ($P<0.05$) are marked by asterisks (not corrected for multiple testing).

As CGE-derived interneurons tend to occupy superficial layers, we hypothesized that there was aberrant specification of the MGE-derived cells into CGE-like cells. The latter scenario is supported by previous work showing that *Lhx6* deletion in MGE-derived cells cause a fate switch to more CGE-like subtypes as determined by laminar distribution and marker expression[19]. To test whether *Ctcf*-null MGE-derived cells adopt a CGE-like fate, we examined known markers of CGE-derived cortical interneurons (*Vip, Cr* and SP8) in P21 cortex of control and $Ctcf^{Nkx\text{-}Cre}$ animals. No significant difference in either total number (Fig. 6G-J, S5) or laminar position (data not shown) was observed, indicating that *Ctcf*-null MGE cells, despite expressing lower levels of *Lhx6*, do not ectopically express CGE markers. Taken together these data indicate that the *Ctcf*-null MGE cells that migrate tangentially into the cortex likely fail to laminate normally because of a radial migration defect.

ed Lhx6 expression in CTCF-null MGE-derived cells restores SST-expressing rneurons upon transplantation in the cortex of wildtype mice.

The fate and migration defects of *Ctcf*-null MGE interneurons was further evaluated by viral-mediated labeling and transplantation of *Ctcf*-null or control MGE cells into wildtype host cortex, as previously described[19,37]. Briefly, the MGE was dissected from E13.5 $Ctcf^{Nkx\text{-}Cre}$ embryos or heterozygous littermate embryos (acting as controls). The MGE was dissociated and either transplanted directly into hosts or transduced with lentiviral constructs before transplantation (Fig. 7A). For phenotyping experiments, the MGE was dissected from $Ctcf^{Nkx\text{-}Cre}$ embryos carrying the Cre-sensitive *Rosa-mTmG* reporter allele to label cells with GFP. The GFP-labelled MGE cells were then transplanted into wildtype host pups (P1). The brains were removed from transplant-host pups at P35 and cortical sections were examined by immunofluorescence microscopy. Immunofluorescence staining for SST revealed a marked reduction (~50%) in the number of transplanted $Ctcf^{Nkx\text{-}Cre}$ GFP+ cells expressing SST compared to control (Fig. 7B-E, R). Conversely, no changes were observed in PV-expressing cells (Fig. 7N-Q, T). We detected a significantly higher number of GFP+ transplanted cells in layer I ($p < 0.0001$), and a reduction in cortical layer V, similar to the laminar defects observed in the $Ctcf^{Nkx\text{-}Cre}$ mice at P21 (Fig. 7U). Importantly, a striking increase in the number of transplanted $Ctcf^{Nkx\text{-}Cre}$ GFP+ cells that co-express LHX8 was detected (Fig. H-K, S). These GFP+/ LHX8+ cells remained close to the injection site (Fig. 8A,B), indicating that their migratory capacity was defective in the cortical environment, as opposed to GFP+/ LHX8- cells.

We then asked whether the reduction of *Lhx6* in CTCF-null MGE cells is the cause of the observed phenotypes. To test this, we re-expressed *Lhx6* in the MGE transplants by transducing $Ctcf^{Nkx\text{-}Cre}$ MGE cells (not expressing the *Rosa-mTmG* reporter) with the lentiviral construct *(Dlx)I12b–GFP–T2A–Lhx6*, as previously described[19] (refer to Fig. 7A for schema). At P35, twice as many GFP+ transplanted cells that had been transduced with *Lhx6* co-expressed SST (back to normal levels) compared to those transduced with a control vector lacking *Lhx6* (Fig. 7R). The lamination defect of $Ctcf^{Nkx\text{-}Cre}$ transplanted cells was also rescued upon re-expression of *Lhx6* (Fig. 7U). However, the proportion of GFP+/LHX8+ cells remained high upon forced expression of *Lhx6*, indicating that *Lhx8* upregulation is probably not a compensatory response to reduced *Lhx6* levels, but is more likely caused by a failure to repress gene expression in the absence of CTCF. Finally, we wanted to assess whether the number of transplanted cells was similar between genotypes. Thus, we counted the number of GFP+ cells observed for each group and normalized this number to the number of tissue sections used for analysis (Table S1). While the numbers varied between groups, there were trends towards less cells being detected in the *CTCF* cKO and *Lhx6* rescued cells compared to controls, suggesting that some cells might be compromised in the CTCF cKO.

CF-null MGE cells acquire a GABAergic projection neuron fate

Many of the transplanted CTCF-null MGE cells that express LHX8 did not migrate into the cortex and remained close to the injection site (Fig. 8A,B). Since many LHX8+ cells are fated to become cholinergic striatal neurons, we examined whether they had gained expression of choline acetyltransferase (ChAT), a marker of cholinergic fate. Only a small proportion of the transplanted GFP+ cells co-expressed ChAT (~10.5%), most of which were located near or within the injection site (Fig. 8C,D,G,H). Fate mapping studies also indicate that approximately 60-70% of LHX8+ cells in the basal forebrain become GABAergic, instead of cholinergic[18], prompting us to examine transplanted cells for co-expression of GABA. The results indicate that the majority of CTCF-null LHX8+ transplanted cells are GABAergic (Fig 8E,F).

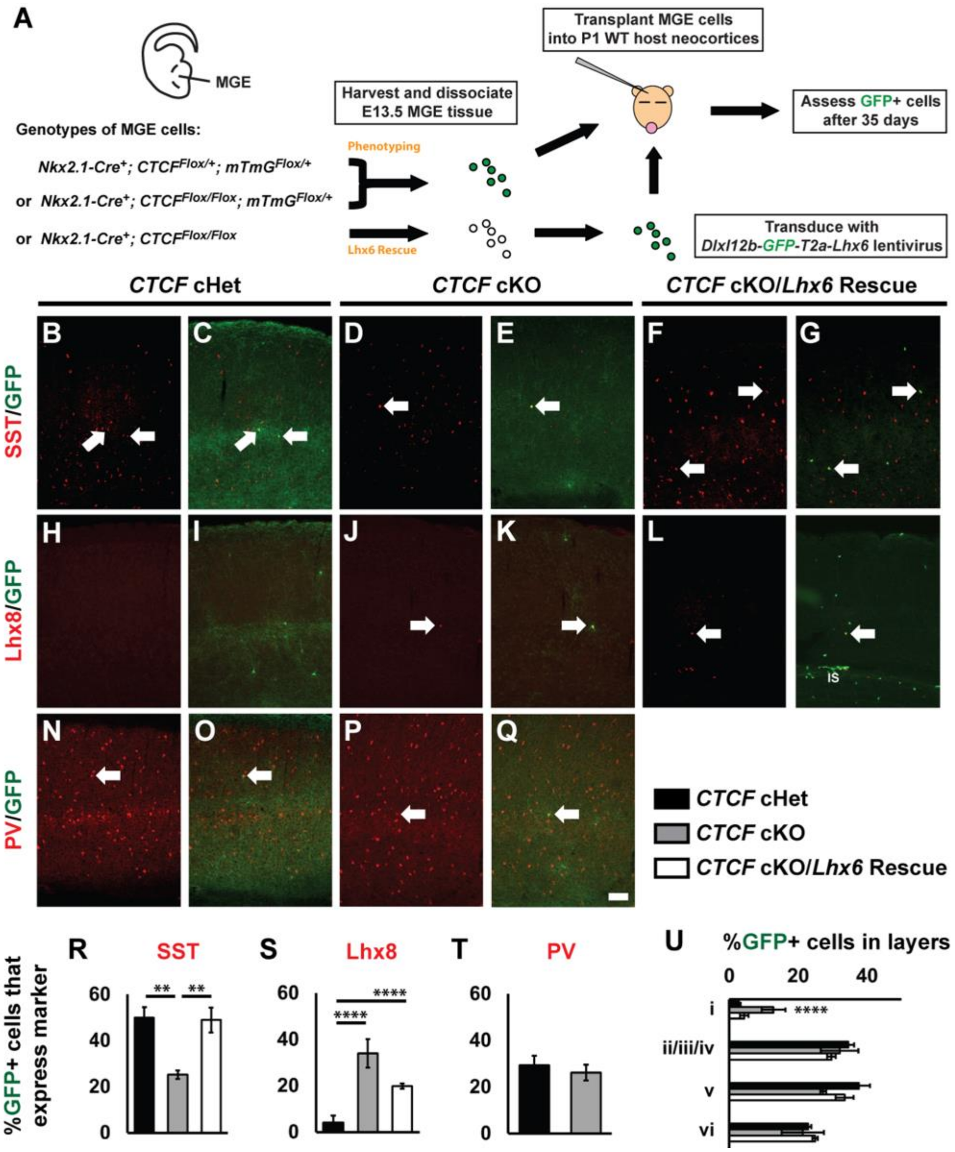
A
MGE
Genotypes of MGE cells:
$Nkx2.1$-Cre^{+}; $CTCF^{Flox/+}$; $mTmG^{Flox/+}$
or $Nkx2.1$-Cre^{+}; $CTCF^{Flox/Flox}$; $mTmG^{Flox/+}$
or $Nkx2.1$-Cre^{+}; $CTCF^{Flox/Flox}$
Harvest and dissociate E13.5 MGE tissue
Phenotyping
Lhx6 Rescue
Transplant MGE cells into P1 WT host neocortices
Assess GFP+ cells after 35 days
Transduce with Dlxl12b-GFP-T2a-Lhx6 lentivirus
CTCF cHet
CTCF cKO
CTCF cKO/Lhx6 Rescue
SST/GFP
Lhx8/GFP
PV/GFP
B
C
D
E
F
G
H
I
J
K
L
IS
N
O
P
Q
CTCF cHet
CTCF cKO
CTCF cKO/Lhx6 Rescue
R
SST
S
Lhx8
T
PV
%GFP+ cells that express marker
0
20
40
60
**
****
U
%GFP+ cells in layers
0
20
40
i
ii/iii/iv
v
vi
****

Figure 7: Analysis of transplanted CTCF-null MGE cells and rescue by ectopic *Lhx6* expression. (A) Schema depicting the MGE transplantation and rescue strategy. Briefly, $Ctcf^{Nkx\text{-}Cre}$ heterozygotes (cHets) or knockouts (cKO) were transplanted into P1 WT neocortices and then assessed for cortical interneuron markers and laminar distribution. In addition, CTCF cKOs were transduced with a lentivirus expressing Lhx6 and GFP, transplanted, and then assessed in the same manner. After 35 days, transplanted cells were assessed for GFP and SST (B-G), LHX8 (L-M) or PV (N-Q). Arrows denote co-labelled cells. Quantification of the proportion of GFP+ cells that co-express either SST (R), LHX8 (S), or PV (T). (U) Quantification of the proportion of GFP+ cells that occupy different cortical lamina. (IS) injection site. Data are expressed as the mean ± SEM. n= 3, all groups. $**p < 0.01$, $****p < 0.0001$. Scale bar in (Q) represents 100 µm.

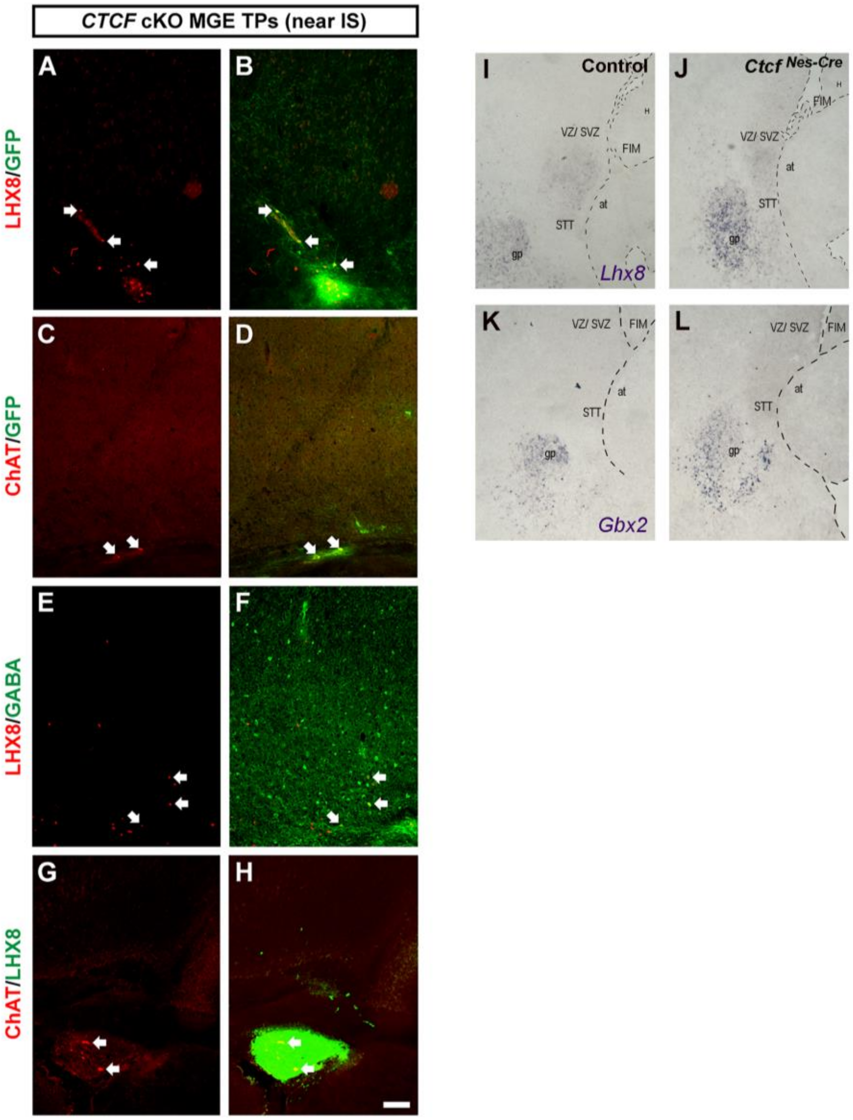
CTCF cKO MGE TPs (near IS)
A
B
LHX8/GFP
C
D
ChAT/GFP
E
F
LHX8/GABA
G
H
ChAT/LHX8
I
Control
J
Ctcf Nes-Cre
VZ/ SVZ
FIM
H
at
STT
gp
Lhx8
K
L
Gbx2

Figure 8: Specification of CTCF-null MGE cells to Lhx8+Gbx2+ GABAergic projection neurons of the globus pallidus. Transplanted CTCF-null MGE-derived cells that fail to migrate away from the injection site (IS) express LHX8 and ChAT (A-D) and LHX8+ cells co-express ChAT and GABA (E-H). An increased number of *Lhx8*+ and *Gbx2*+ cells migrate from the MGE to the globus pallidus in the $Ctcf^{Nes\text{-}Cre}$ E15.5 embryonic brain (I-L). VZ/SVZ: ventricular and subventricular, FIM: fimbria, H: hippocampus, at: anterior thalamic nucleus, STT: stria terminalis, gp: globus pallidus.

GBX2 is a downstream effector of LHX8, and its expression marks either striatal cholinergic neurons (LHX8+, GBX2+, ChAT+) or GABAergic projection neurons of the basal forebrain (LHX8+, GBX2+, ChAT-)[38]. Indeed, upon further examination of the $Ctcf^{Nes\text{-}Cre}$ embryos at E15.5 by ISH, we observed more *Gbx2+* and *Lhx8*+ cells that migrate radially from the MGE to the globus pallidus (Fig. 8E-H). Collectively, these results suggest that loss of *Ctcf* in MGE cells likely re-specifies a portion of LHX6+ GABAergic cells destined for the cortex to LHX8+ GABAergic projection neurons that migrate radially into the basal forebrain.

ussion

The MGE generates a variety of different cell types including GABAergic cortical and striatal interneurons, GABAergic projection neurons (e.g. globus pallidus), cholinergic striatal interneurons, and cholinergic projection neurons[16,39–41]. The mechanism of genetic programming in the MGE that allows for this cellular diversity is the subject of intense research. The present study advances knowledge of these events by demonstrating that CTCF, a factor involved in higher order organization of chromatin structure, is required for fate specification of interneurons born in the MGE. Loss of CTCF alters the balance between GABAergic cells fated to become cortical interneurons versus basal forebrain projection neurons, through the regulation of LHX6 and LHX8 LIM homeodomain factors.

Expression of *Lhx6* and *Lhx8* was altered upon *Ctcf* inactivation, while NKX2.1 remained unaffected, indicating that CTCF either acts downstream or in parallel with this factor. We found no evidence that CTCF interacts with NKX2.1 or co-occupies binding sites in E13.5 MGE chromatin around *Lhx6* and *Lhx8* gene loci. Alternate possibilities for regulation must therefore be considered, such as loss of another NKX2.1 binding partner upon *Ctcf* deletion, or that CTCF is required to set up specific chromatin architecture permissive for NKX2.1 binding, without direct protein-protein interaction.

Deletion of another genome organizer, Special AT-rich DNA Binding Protein 1 (*Satb1*), also impairs differentiation of SST+ interneurons[43], confirming that chromatin organization is a key regulatory mechanism of cell fate specification and differentiation of MGE-derived cells. CTCF has been shown in other models to influence gene expression by modulating looping, topological chromatin domains, and enhancer-binding[44]. Additional studies will be required to precisely uncover how CTCF affects chromatin structure and gene expression in the MGE.

Decreased expression of *Lhx6* upon loss of *Ctcf* is associated with reduced number of SST+ and PV+ interneurons in the cortex. The effect on SST+ interneurons is directly caused by the reduced *Lhx6* expression, since lentiviral transduction of *Lhx6* in *Ctcf*-null MGE cells fully re-instated normal number of SST+ cells in transplantation experiments. Our transplantation studies failed to replicate a loss of PV+ interneurons seen in the $Ctcf^{Nkx\text{-}Cre}$ model. One possible explanation is a variable necessity for LHX6 expression in different mouse strains/ genetic backgrounds. For the transplantation experiments, *Ctcf* deletion was performed in a CD1 background to maximize litter size, whereas our P20-22 $Ctcf^{Nkx\text{-}Cre}$ mice were generated in the C57BL/6 strain. Another possibility is that the PV+ interneurons that are lost in the genetic mouse model described herein are either born at a different age or may fail to migrate into the neocortex. Notably, we only transplanted E13.5 MGE cells, however, multiple PV+ subgroups are born over a long period of time. Moreover, while transplanted MGE cells can still migrate in the neocortex where they are placed, they do not experience the same obstacles that endogenous MGE would while tangentially migrating into the neocortex. It is possible that the cells fated to become PV+ may be more affected by migration than by fate, although this remains to be determined. Additionally, a similar phenomenon has previously been described in SST cell fate by Neves et al (2013)[45] using a hypomorphic allele of *Lhx6*, which resulted only in loss of SST but not PV interneuron subtypes, in a C57BL/6 background. Together, with the work presented here, these data suggest that the role of LHX6 is stricter for SST+ subtype specification, and that its role in PV+ subtype specification may be compensated for in different genetic backgrounds.

Lhx6-null MGE cells were previously found to undergo a partial fate switch to CGE-like cells[19] but we failed to observe this in the CTCF-null MGE cells, indicating that only complete loss of *Lhx6* expression leads to this switch to CGE-like fate. *Lhx6* deletion models show defective tangential migration of interneurons into the cortex, which we also observed with deletion of *Ctcf* in the MGE. Reduced expression of the CXCR4 chemoreceptor, whose expression is promoted by *Lhx6*[46], could contribute to this phenotype. By weaning age however, the mutants had the same number of cortical GABAergic interneurons, albeit with defective lamination. Since there was no difference in lamination of interneurons expressing CGE markers, this suggests the lamination defects of the GABAergic interneurons is a result of cell-autonomous effects of *Ctcf* loss in MGE-derived interneurons. This also appears to be a defect related to reduced *Lhx6*, as re-expression of *Lhx6* in transplanted *Ctcf*-null cells corrected laminar positioning.

Ctcf loss from MGE cells also causes increased expression of *Lhx8*, which provides a possible explanation for the increased number of GBX2+ cells in the basal forebrain in the *Ctcf*$^{Nes\text{-}Cre}$ embryos. These cells likely represent basal forebrain GABAergic neurons that project to the cortex, as transplanted *Ctcf*-null cells co-expressed LHX8 and GABA, but few expressed ChAT or Nkx2.1. Re-expression of *Lhx6* was not sufficient to reduce the number of LHX8+ cells to normal levels in transplants. However, this could also be explained by reduced functionality of the *DlxI12b* enhancer to re-express *Lhx6* in LHX8+ *Ctcf*-null cells.

Understanding the molecular control switches in cell fate specification of MGE cells is relevant to the *in vitro* differentiation of these progenitors to specific neuron types and in the treatment of human neurological disorders[12,47,48]. The genetic pathways in MGE differentiation and specification are highly conserved between mouse and human[49–51], therefore the molecular understanding of MGE development has direct influence on our ability to effectively generate MGE-derived cell subtypes from human stem cells. In addition, understanding the role of CTCF in the developing brain could impact our ability to treat human disorders caused by *CTCF* dysregulation, as here we provide evidence that CTCF loss decreases *Lhx6* expression and cortical GABAergic neurons. Mutation of one copy of *CTCF* in humans can result in intellectual disability[21], ASD[52] and conditions with altered GABAergic neuron function[6,53]. In addition, CTCF has been associated with schizophrenia[24], which has also been linked with defects in *LHX6*[54]. Our study implicates CTCF in fate specification of MGE progenitors and complements current efforts to understand MGE development from the perspective of chromatin regulators.

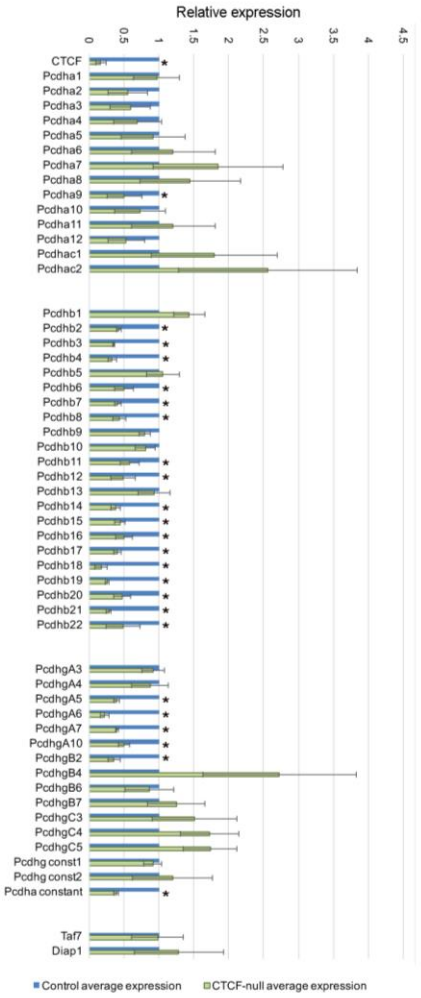

Figure S1 (Related to Figure 1): Early deletion of *Ctcf* from neuroprogenitors results in dysregulated expression of Protocadherin (*Pcdh*) clusters. (A) Relative expression by RT-qPCR of *Pcdh* genes from clusters a, b, and g in *Ctcf*$^{Nes\text{-}Cre}$, normalized to littermate-control set to 1, and to *Gapdh*. N=3, error bars represente mean +/- SEM. Asterisks indicate $P< 0.05$ using Student's t-test. Not corrrected for multiple testing. *Taf7* and *Diap1* are genes located between the *Pcdh-b* and *Pcdh-g* clusters.

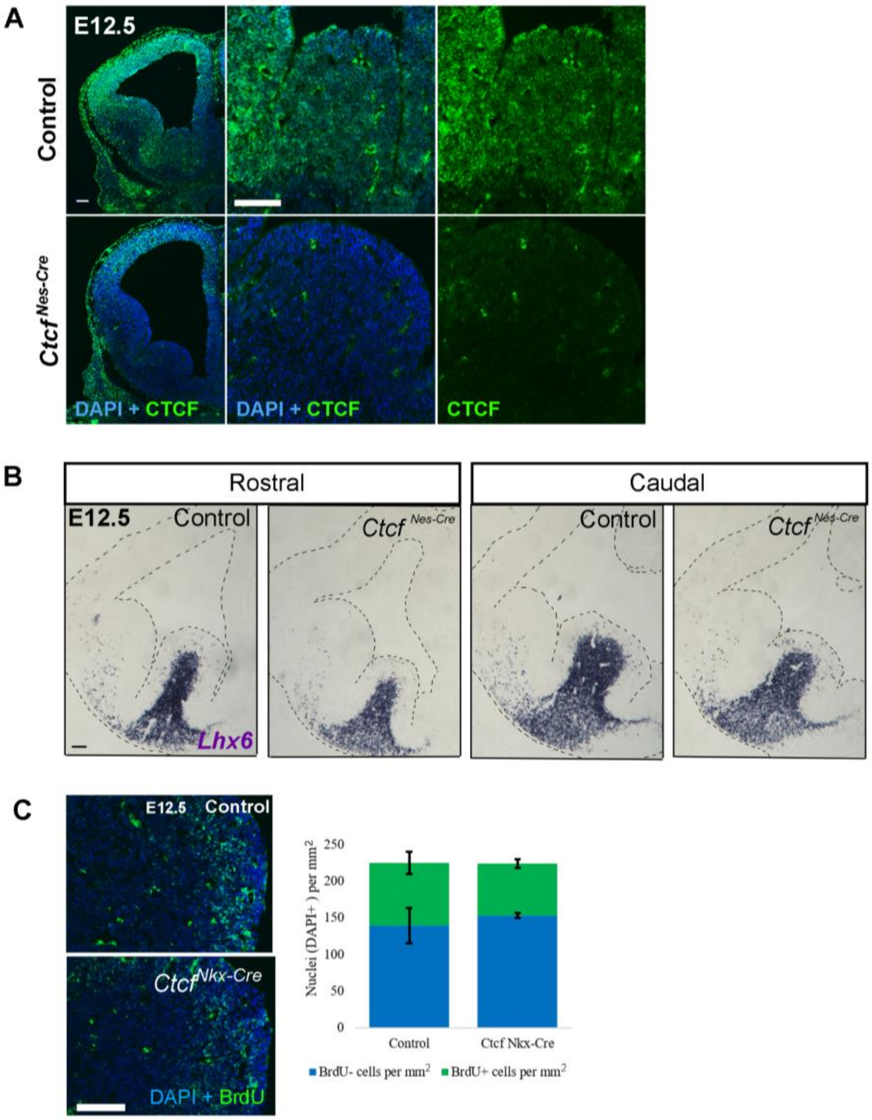
A
E12.5
Control
Ctcf Nes-Cre
DAPI + CTCF
DAPI + CTCF
CTCF
B
Rostral
Caudal
E12.5
Control
Ctcf Nes-Cre
Control
Ctcf Nes-Cre
Lhx6
C
E12.5
Control
Ctcf Nkx-Cre
DAPI + BrdU
Nuclei (DAPI+) per mm2
250
200
150
100
50
0
Control
Ctcf Nkx-Cre
BrdU- cells per mm2
BrdU+ cells per mm2

Figure S2 (Related to Figure 2): CTCF expression is lost early in conditional knockouts but does not impact number of proliferative cells at peak interneuron-genesis. (A) Immunofluorescence staining for CTCF (green) at E12.5 in *Ctcf*$^{Nes\text{-}Cre}$ coronal brain sections (Watson et al. 2014). Nuclei are counterstained with DAPI. Adjacent insets show CTCF is expressed in the MGE of control, but absent from the *Ctcf*$^{Nes\text{-}Cre}$ MGE by E12.5. (B) *Lhx6* ISH in E12.5 rostral and caudal coronal sections. Tissue is outlined for ease of visualization. (C) Immunofluorescence staining for BrdU, marker of S-phase cells, one hour after BrdU injection of pregnant dam. Quantification of density of BrdU+ nuclei in E12.5 MGE VZ of control and *Ctcf*$^{Nkx\text{-}Cre}$ embryos (n=3). Error bars represent mean +/-SEM. In all panels, scalebar represents 100 µm.

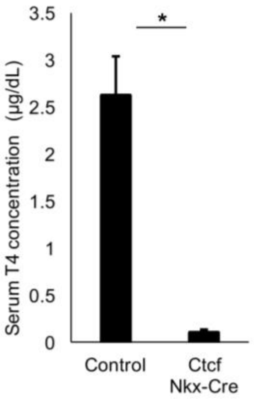

Figure S3 (Related to Figure 4*) Ctcf*$^{Nkx\text{-}Cre}$ mice have low serum T4 levels. (A) Quantification of serum T4 from P20-22 *Ctcf*$^{Nkx\text{-}Cre}$ mice and control siblings by ELISA. Error bars represent mean +/-SEM, (n= 6 pairs). Asterisk indicates P<0.05 by Student's t-test.

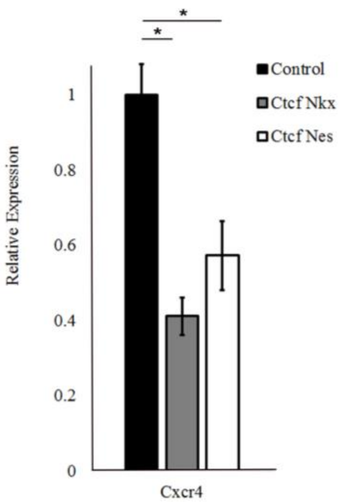

Figure S4 (Related to Figure 5): Reduced expression of the *Lhx6* downstream effector *Cxcr4* in the CTCF-null E14 telencephalon. Quantitative RT-PCR was performed using *Cxcr4* primers using RNA isolated from E14 telencephalon of *Ctcf*$^{Nes\text{-}Cre}$ or *Ctcf*$^{Nkx\text{-}Cre}$ embryos. Data was normalized to β-actin expression. Error bars represent mean +/-S.E.M. Asterisks indicate P<0.05, Student t-test.

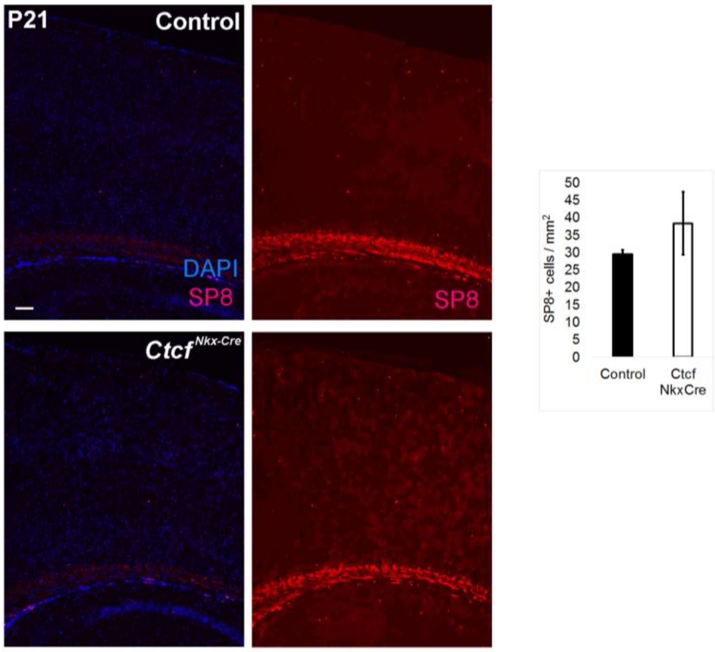
P21
Control
DAPI
SP8
SP8
Ctcf^Nkx-Cre
SP8+ cells / mm²
50
45
40
35
30
25
20
15
10
5
0
Control
Ctcf NkxCre

Figure S5: Deletion of *Ctcf* does not promote fate switch to SP8+ interneuron subtype. (A) Immunofluorescence staining for SP8 (red) in P21 cortex, counter-stained with DAPI. Merged blue and red channels, and red channel alone are shown. Scalebar represents 100 µm. (B) Quantification of SP8+ cell density. Error bars represent mean +/- SEM, n=6 pairs. P=0.383, Student's t-test.

Table S1: Number of GFP+ cells observed 35 days after MGE cell transplantation for each genotype

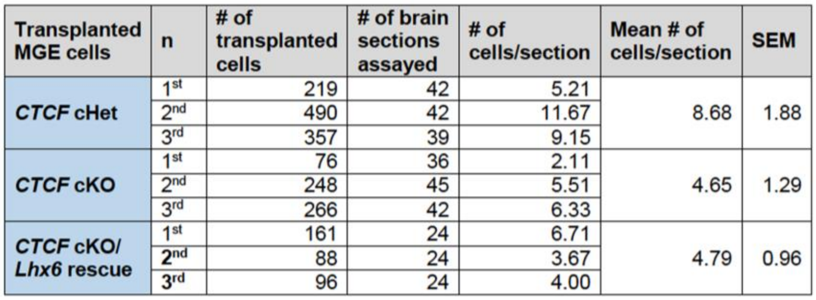

Transplanted MGE cells	n	# of transplanted cells	# of brain sections assayed	# of cells/section	Mean # of cells/section	SEM
***CTCF* cHet**	1st	219	42	5.21	8.68	1.88
	2nd	490	42	11.67		
	3rd	357	39	9.15		
***CTCF* cKO**	1st	76	36	2.11	4.65	1.29
	2nd	248	45	5.51		
	3rd	266	42	6.33		
***CTCF* cKO/ *Lhx6* rescue**	1st	161	24	6.71	4.79	0.96
	2nd	88	24	3.67		
	3rd	96	24	4.00		

Table S2: Primer sequences used for genotyping, RT-qPCR, and ISH probe synthesis

Gene (purpose)	Forward Sequence	Reverse Sequence
Ctcf (genotype)	CTAGGAGTGTAGTTCAGTGAGGCC	GCTCTAAAGAAGGTTGTGAGTTC
Sry (genotype)	GCAGGTGGAAAAGCCTTACA	AAGCTTTGCTGGTTTTTGGA
Cre (genotype)	TGACCAGAGTCATCCTTAGCG	AATGCTTCTGTCCGTTTGCC
Puma (genotype)	AGGCTGTCCCTGCGGTCATCC	WT: GGACTGTCGCGGGCTAGACCCTCTA MUT: ACCGCGGGCTCCGAGTAGC
Rosa mTmG (genotype)	CTCTGCTGCCTCCTGGCTTCT	WT: CGAGGCGGATCACAAGCAATA MUT: TCAATGGGCGGGGGTCGTT
Ctcf (qPCR)	CGATATGCTCTCATCCAGCA	TCCCACACTTGGAACAGACA
Lhx6 (qPCR)	CTTGGGCTGACTGTCCTGTT	GGTGCGGCAGACAAATCTAT
B actin (qPCR)	CTGTCGAGTCGCGTCCACCC	ACATGCCGGAGCCGTTGTCG
Lhx8 (qPCR)	CCACCCATGTTGGAAGAAAT	CATTGGATGGGGTAACAAGG
Cxcr4 (qPCR)	GAAGTAGATGGTGGGCAGGA	ACGGCTGTAGAGCGAGTGTT
Sst (qPCR)	GGGCATCATTCTCTGTCTGG	GAGGCAAGGAAGATGCTGTC
Lhx8 (probe)	GAAGAGCGATCAGATGTTTGTG	TAATACGACTCACTATAGGGCACCTGTATGACACGTCTGCTT
Pvalb (probe)	GGATGTCGATGACAGACGTG	TAATACGACTCACTATAGGGACTCAACCCCTTCCCTTCC
Sst (probe)	TGAAGGAGACGCTACCGAAG	TAATACGACTCACTATAGGGAGGGTCAAGTTGAGCATCG
Gbx2 (probe)	GATGAAGAGAAGCTAGAGCCCC	TAATACGACTCACTATAGGGAGGTTCAGATCCTGTGACTTCC
Gad1 (probe)	GGGACCCTTGAACCGTAGAG	TAATACGACTCACTATAGGGCCCGTACTTCAGGGTGTCTC
Cr (probe)	GATGCTGACGGAAATGGG	TAATACGACTCACTATAGGGCCCTACCAGCCACCCTCT
VIP (probe)	CCTGGCATTCCTGATACTCTTC	TAATACGACTCACTATAGGGATTCTCTGATTTCAGCTCTGCC

erials and methods

Mice and Genotyping

Animal studies were approved by the University of Western Ontario Animal Care Committee according to guidelines established by the Canadian Council on Animal Care. Mice were housed in the London Regional Cancer Program vivarium (12 h light/dark cycle) and were provided with regular chow and water *ad libitum*. The *Ctcf*$^{\text{flox/flox}}$ mice were generated by Heath et al. (2008)[55] on a C57BL/6 background. The *NestinCre* mice

(C57BL/6 background) were previously described[56]. *Bbc3*/*Puma*$^{-/-}$ (stock #011067), *Nkx2.1Cre* (stock #008661) and *Rosa*^{mTmG} (stock #007576) mice were purchased from the Jackson Laboratory. Mice carrying *Rosa*^{mTmG} are of a mixed background and were bred to *Ctcf*$^{\text{flox/flox}}$ mice to homozygosity.

Ctcf$^{\text{flox/flox}}$ and *NestinCre* were mated and the *NestinCre*$^{+}$ offspring were time-mated with *Ctcf*$^{\text{flox/flox}}$ to generate *Ctcf*$^{Nes\text{-}Cre}$ conditional knockout embryos (*Ctcf*$^{Nes\text{-}Cre}$), as done previously[27]. *Ctcf*$^{Nes\text{-}Cre}$ embryos exhibit efficient Cre-mediated recombination at *loxP* sites flanking exons 3 to 12 of the *Ctcf* locus in neuroprogenitors beginning at about E11[27]. Embryos without the *NestinCre* transgene and wildtype *Ctcf* expression were used as controls.

Ctcf$^{Nkx\text{-}Cre}$ mice were generated in the same fashion as *Ctcf*$^{Nes\text{-}Cre}$ animals. *Nkx2.1Cre+* mice were maintained on a C57BL/6 background, with the exception of the transplant experiments which were performed using *Nkx2.1Cre*$^{+}$ mice maintained on a CD1 background. For these mice, care and procedures were performed according to the University of California at San Francisco Laboratory Animal Research Center guidelines. For timed matings, time of conception was arbitrarily designated as the midnight before vaginal plug discovery. To label proliferative cells, pregnant dams were injected intraperitoneally with BrdU labelling agent (GE Healthcare Life Sciences) at 1 mL/ 100g body weight, as previously described, 1 h prior to sacrifice[27].

P20 mouse brains were harvested after transcardial perfusion with 20 mL PBS (DEPC-treated) followed by perfusion with 20 mL 4% paraformaldehyde (PFA)/PBS (DEPC-treated) before brain dissection.

RNA-sequencing analysis

Telencephalons of two E14 *Ctcf*$^{Nes\text{-}Cre}$ embryos and littermate controls (*Ctcf* $^{flox/flox}$) were processed for RNA-seq at Otogenetics. Raw reads were aligned to mouse genome mm10 using STAR[57] version 2.5.3a with GENCODE M11 primary annotations. Count matrices were generated using the R GenomicAlignments package[58] and normalized using DeSeq2[59]. Low expressing genes (counts less than 2% of the average of all samples) were removed and genes with an average fold change of 1.5 fold or greater were used for downstream analysis by *The Protein ANalysis THrough Evolutionary Relationships* (PANTHER) (http://pantherdb.org/).

Quantitative RT-PCR analysis

For RT-qPCR, total RNA was extracted using an RNeasy Mini kit (Qiagen) and cDNA was synthesized using SuperScript™ II Reverse Transcriptase (Invitrogen), as previously described[27]. Primer sequences used for qPCR are listed in Table S2. All primers in this study were designed using Primer3 software (http://bioinfo.ut.ee/primer3-0.4.0/primer3/). PCR amplification was performed using iQ SYBR Green supermix (Bio-Rad) under the following conditions: 95˚C for 3 mins, [95˚C for 10 s, 58˚C for 20 s, 72˚C for 30 s]x35, 72˚C for 5 mins. A melting curve for each sample was generated from 55°C to 95°C in increments of 1°C and PCR products were run on agarose gel to verify band size. β-actin was quantified and used for normalization of the data.

Immunofluorescence (IF) and in situ hybridization (ISH) staining

Dissected samples were incubated in 4% PFA/PBS (DEPC-treated) overnight, then dehydrated in 30% sucrose until samples sank to the bottom, before being frozen in cryomatrix (OCT) and sectioned at 8 µm thickness. IF and BrdU labelling was performed as previously described[27]. For IF, slides with sections were re-hydrated in PBS then incubated overnight (8-16 h) with the primary antibody at 4°C in 0.3% Triton X-100 in PBS at the following dilutions: rabbit anti-CTCF (1:400; Cell Signaling Technology), mouse anti-BrdU (1:50; BD Biosciences), rabbit anti-NKX2.1 (1:100; Santa Cruz) and goat anti-SP8 (1:100; Santa Cruz). For BrdU, tissue sections were treated with 2N HCl, then 0.1 M $Na_2B_4O_7$, pH8.5, before primary antibody incubation. For anti-SP8 staining, slides were heated in 10 mM sodium citrate, then blocked with 10% NGS/ 0.3% Triton X-100 in PBS for 1 hour before incubation with the primary antibody. The following morning, sections were washed with 0.3% Triton X-100 in PBS and incubated with the corresponding secondary antibody (1:800 Alexa 594 or 488; Invitrogen) for 1 h. Sections were then washed again and stained with DAPI (Sigma-Aldrich).

ISH riboprobes were synthesized as follows, with the exception of the *Reelin* ISH probe, which was a kind gift from the Rubenstein lab; Template DNA was PCR amplified using primers, where the reverse primer was labelled with the T7 recognition sequence at the 5' end (Table S1). Digoxigenin-labelled riboprobes were then synthesized from the gel purified template DNA using T7 (antisense probe) polymerase (Roche) according to the manufacturer's instructions. For ISH, sections were incubated overnight (12-18 h) with antisense digoxigenin-labelled riboprobes at 65°C in a humidified chamber. Riboprobes were diluted in formamide-based hybridization buffer at 1:1000 from stock. The following morning, sections were washed in formamide-based ISH wash buffer, then maleic acid buffer containing Tween 20 (MABT) before incubation with alkaline phosphatase conjugated anti-Digoxigenin Fab fragments (Roche) overnight. Excess antibody was removed with a series of MABT and prestaining-buffer washes, before riboprobe detection using the NBT/BCIP system (Roche) in a polyvinyl alcohol-based solution. After staining, the reaction was ended with vigorous PBS washing. Sections were cleared by dehydration in serial ethanol dilutions (70%, 90%, 100%) and xylene, then mounted.

Microscopy and imaging

Fluorescence and light microscopy was performed using an inverted (DMI 6000b) Leica microscope. Light microscopy was also performed with the Aperio CS2 digital pathology scanner (Scanscope; Leica). For transplant experiments, fluorescent images were taken using a Coolsnap camera (Photometrics) mounted on a Nikon Eclipse 80i microscope using NIS Elements acquisition software (Nikon). Images were processed with Volocity (PerkinElmer), Imagescope (Leica), ImageJ and Adobe Photoshop.

Co-immunoprecipitation and Western blot analysis

Total protein was extracted from embryonic telencephalon or MGE, using standard protocol with RIPA buffer, and quantified with the Bradford assay. For immunoprecipitation, E13.5 MGE were pooled from wildtype embryos, the protein was incubated overnight with either anti-CTCF, anti-NKX2.1 or IgG antibody (mock IP). Antibody-protein complexes were incubated with protein-G Dynabeads and isolated by centrifugation. After washing, interactions were disrupted and proteins were detected by Western blotting as below.

Protein lysates were resolved on an 8% SDS-polyacrylamide gel and transferred to a nitrocellulose membrane. Anti-CTCF (1:1000; Cell signalling), anti-NKX2.1 (1:2000;

Santa Cruz) and anti-β-ACTIN (1:7000; Sigma Alderich) were used to probe the membrane, followed by secondary detection with the corresponding horseradish peroxidase-conjugated antibodies (1:4000; GE Healthcare Life Sciences). Protein was quantified using ImageJ software (version 1.47).

ChIP sequencing

ChIP in MGE was performed as previously described for mouse forebrain[27]. E13.5 MGE was dissected and pipetted up and down in DMEM to create a single cell suspension. Cells were fixed in 1% formaldehyde, then lysed in SDS buffer. Chromatin was sonicated to an average size of 500 bp, then 1/25 of total chromatin was set aside (input). The rest of the chromatin was incubated overnight with rabbit anti-CTCF antibody (Cell Signaling Technology) or rabbit IgG, as a control. CTCF-bound chromatin fragments were then purified using magnetic Dynabeads (Invitrogen), and crosslinking was reversed. ChIP-seq reads were aligned to mouse genome mm9 or mm10 using Bowtie2[60] version 2.3.2 using default settings. Peaks were called using MACS2[61] version 2.1.1.20160309 with P=0.001. Wig files were generated using deepTools[62] and overlapping peaks were identified using Bedtools[63].

T4 ELISA

Blood was collected from P20 mice by trans-cardiac puncture using an EDTA-coated syringe (pH 7.0). Blood was centrifuged for 10 minutes (14,000 RPM) at 4˚C, then the plasma collected and stored at -20˚C. Plasma was loaded onto the T4 ELISA kit (Calbiotech, T4044T-100) according to manufacturer protocols.

Cell Counts

To determine the density of marker-positive cells, 5 to 10 serial cryosections (8 µm thickness) were evaluated in a blinded manner. Areas within the indicated brain regions were calculated (mm^2) from microscope images in Volocity or Imagescope softwares and counts were performed in a blinded manner. For counts performed in P20-22 cortex, the cortex was divided into 10 equal-sized horizontal bins to simultaneously determine laminar changes. The first cortical bin location and size corresponds approximately to the marginal zone.

Cloning

The *DlxI12b-GFP-T2a-Lhx6* vector[19] was modified to remove *loxP* sites that flanked the expression cassettes. PCR was used to generate a *DlxI12b-GFP* fragment that harbored a 5’ XbaI restriction enzyme site, but excluded the loxP site from the original vector, and a 3’ primer against *GFP* that included a BsrGI site. This product was then ligated into the same backbone in the 5’ XbaI and 3’ BsrGI sites. The resulting vector lacked a flanking loxP site and could be expressed in cells expressing Cre recombinase. Vectors were verified by restriction digest and sequencing.

Lentiviral generation

HEK293T cells grown in DMEM H21 with 10% FBS were transfected using Lipofectamine2000 (Thermo Fisher) with the lentiviral expression vector and three helper plasmids (*pVSV-g*, *pRSVr* and *pMDLg-pRRE*) to generate lentivirus particles as previously described[19]. Media containing lentiviruses was collected after four days and filtered through a 0.45 low protein binding membrane to remove cells and large debris. The filtered media was pooled and ultracentrifuged at 100,000 x g for 2.5 hours at 4°C. The supernatant was removed and the pellet was resuspended overnight at 4°C in sterile PBS then stored at -80°C until use.

MGE transplantation

MGE transplantation and rescue assays have been previously described[19]. Briefly, E13.5 MGE tissue from either *Ctcf*$^{flox/wt}$*:NestinCre* (controls) or *Ctcf*$^{flox/flox}$*:NestinCre* (KO) embryos were harvested and dissociated into a single cell suspension before injection into a WT P1 host. For rescue experiments, MGE cells from *Ctcf*$^{flox/flox}$*:NestinCre* (KO) embryos were collected in the same manner and then incubated with lentiviruses that expressed Lhx6 and GFP for 30 minutes at 37°C in media at physiological pH before transplantation. Transplanted cells were allowed to develop *in vivo* for 35 days before analysis. Immunofluorescence staining of sections at day 35 were performed with the following antibodies: rabbit anti-GFP (Clontech, 1:2000), or chicken anti-GFP (Aves, 1:2000), rabbit anti-PV (Swant, 1:500), or mouse anti-PV (Millipore, 1:500), rat anti-SST (Millipore, 1:200), guinea pig anti-Lhx8 (generous gift from Aleksandar Rajkovic, University of Pittsburgh).

rences

1. Tremblay, R., Lee, S. & Rudy, B. GABAergic Interneurons in the Neocortex: From Cellular Properties to Circuits. *Neuron* **91,** 260–292 (2016).

2. Pérez-Cremades, D. *et al.* Alteration of inhibitory circuits in the somatosensory cortex of Ts65Dn mice, a model for Down's syndrome. *J. Neural Transm. Vienna Austria 1996* **117,** 445–455 (2010).
3. Ruiz-Mejias, M. *et al.* Overexpression of Dyrk1A, a Down Syndrome Candidate, Decreases Excitability and Impairs Gamma Oscillations in the Prefrontal Cortex. *J. Neurosci. Off. J. Soc. Neurosci.* **36,** 3648–3659 (2016).
4. Gibson, J. R., Bartley, A. F., Hays, S. A. & Huber, K. M. Imbalance of neocortical excitation and inhibition and altered UP states reflect network hyperexcitability in the mouse model of fragile X syndrome. *J. Neurophysiol.* **100,** 2615–2626 (2008).
5. Paluszkiewicz, S. M., Olmos-Serrano, J. L., Corbin, J. G. & Huntsman, M. M. Impaired inhibitory control of cortical synchronization in fragile X syndrome. *J. Neurophysiol.* **106,** 2264–2272 (2011).
6. Blatt, G. J. & Fatemi, S. H. Alterations in GABAergic biomarkers in the autism brain: research findings and clinical implications. *Anat. Rec. Hoboken NJ 2007* **294,** 1646–1652 (2011).
7. Hashemi, E., Ariza, J., Rogers, H., Noctor, S. C. & Martínez-Cerdeño, V. The Number of Parvalbumin-Expressing Interneurons Is Decreased in the Medial Prefrontal Cortex in Autism. *Cereb. Cortex* bhw021 (2016). doi:10.1093/cercor/bhw021
8. Lozano, R., Martinez-Cerdeno, V. & Hagerman, R. J. Advances in the Understanding of the Gabaergic Neurobiology of FMR1 Expanded Alleles Leading to Targeted Treatments for Fragile X Spectrum Disorder. *Curr. Pharm. Des.* **21,** 4972–4979 (2015).

9. Potier, M.-C., Braudeau, J., Dauphinot, L. & Delatour, B. Reducing GABAergic inhibition restores cognitive functions in a mouse model of Down syndrome. *CNS Neurol. Disord. Drug Targets* **13,** 8–15 (2014).
10. Southwell, D. G. *et al.* Interneurons from Embryonic Development to Cell-Based Therapy. *Science* **344,** 1240622 (2014).
11. Hammad, M. *et al.* Transplantation of GABAergic Interneurons into the Neonatal Primary Visual Cortex Reduces Absence Seizures in Stargazer Mice. *Cereb. Cortex N. Y. N 1991* **25,** 2970–2979 (2015).
12. Chohan, M. O. & Moore, H. Interneuron Progenitor Transplantation to Treat CNS Dysfunction. *Front. Neural Circuits* 64 (2016). doi:10.3389/fncir.2016.00064
13. Marín, O. Cellular and molecular mechanisms controlling the migration of neocortical interneurons. *Eur. J. Neurosci.* **38,** 2019–2029 (2013).
14. Xu, Q., Cobos, I., De La Cruz, E., Rubenstein, J. L. & Anderson, S. A. Origins of cortical interneuron subtypes. *J. Neurosci. Off. J. Soc. Neurosci.* **24,** 2612–2622 (2004).
15. Miyoshi, G. & Fishell, G. GABAergic interneuron lineages selectively sort into specific cortical layers during early postnatal development. *Cereb. Cortex N. Y. N 1991* **21,** 845–852 (2011).
16. Fragkouli, A., van Wijk, N. V., Lopes, R., Kessaris, N. & Pachnis, V. LIM homeodomain transcription factor-dependent specification of bipotential MGE progenitors into cholinergic and GABAergic striatal interneurons. *Dev. Camb. Engl.* **136,** 3841–3851 (2009).

17. Marin, O., Anderson, S. A. & Rubenstein, J. L. Origin and molecular specification of striatal interneurons. *J. Neurosci. Off. J. Soc. Neurosci.* **20,** 6063–6076 (2000).
18. Fragkouli, A. *et al.* Loss of forebrain cholinergic neurons and impairment in spatial learning and memory in LHX7-deficient mice. *Eur. J. Neurosci.* **21,** 2923–2938 (2005).
19. Vogt, D. *et al.* Lhx6 Directly Regulates Arx and CXCR7 to Determine Cortical Interneuron Fate and Laminar Position. *Neuron* **82,** 350–364 (2014).
20. Merkenschlager, M. & Nora, E. P. CTCF and Cohesin in Genome Folding and Transcriptional Gene Regulation. *Annu. Rev. Genomics Hum. Genet.* **17,** null (2016).
21. Gregor, A. *et al.* De novo mutations in the genome organizer CTCF cause intellectual disability. *Am. J. Hum. Genet.* **93,** 124–131 (2013).
22. Bastaki, F. *et al.* Identification of a novel CTCF mutation responsible for syndromic intellectual disability – a case report. *BMC Med. Genet.* **18,** 68 (2017).
23. Iossifov, I. *et al.* The contribution of de novo coding mutations to autism spectrum disorder. *Nature* **515,** 216–221 (2014).
24. Juraeva, D. *et al.* Integrated pathway-based approach identifies association between genomic regions at CTCF and CACNB2 and schizophrenia. *PLoS Genet.* **10,** e1004345 (2014).
25. Hirayama, T., Tarusawa, E., Yoshimura, Y., Galjart, N. & Yagi, T. CTCF is required for neural development and stochastic expression of clustered Pcdh genes in neurons. *Cell Rep.* **2,** 345–357 (2012).

26. Sams, D. S. *et al.* Neuronal CTCF Is Necessary for Basal and Experience-Dependent Gene Regulation, Memory Formation, and Genomic Structure of BDNF and Arc. *Cell Rep.* **17,** 2418–2430 (2016).
27. Watson, L. A. *et al.* Dual Effect of CTCF Loss on Neuroprogenitor Differentiation and Survival. *J. Neurosci.* **34,** 2860–2870 (2014).
28. Liodis, P. *et al.* Lhx6 Activity Is Required for the Normal Migration and Specification of Cortical Interneuron Subtypes. *J. Neurosci.* **27,** 3078–3089 (2007).
29. Zhao, Y. *et al.* The LIM-homeobox gene Lhx8 is required for the development of many cholinergic neurons in the mouse forebrain. *Proc. Natl. Acad. Sci. U. S. A.* **100,** 9005–9010 (2003).
30. Sandberg, M. *et al.* Transcriptional Networks Controlled by NKX2-1 in the Development of Forebrain GABAergic Neurons. *Neuron* **91,** 1260–1275 (2016).
31. Du, T., Xu, Q., Ocbina, P. J. & Anderson, S. A. NKX2.1 specifies cortical interneuron fate by activating Lhx6. *Development* **135,** 1559–1567 (2008).
32. Chen, Y.-J. J. *et al.* Use of 'MGE Enhancers' for Labeling and Selection of Embryonic Stem Cell-Derived Medial Ganglionic Eminence (MGE) Progenitors and Neurons. *PLoS ONE* **8,** (2013).
33. Gomes, N. P. & Espinosa, J. M. Gene-specific repression of the p53 target gene PUMA via intragenic CTCF–Cohesin binding. *Genes Dev.* **24,** 1022–1034 (2010).
34. Minoo, P., Su, G., Drum, H., Bringas, P. & Kimura, S. Defects in tracheoesophageal and lung morphogenesis in Nkx2.1(-/-) mouse embryos. *Dev. Biol.* **209,** 60–71 (1999).

35. Abe, P. *et al.* Intermediate Progenitors Facilitate Intracortical Progression of Thalamocortical Axons and Interneurons through CXCL12 Chemokine Signaling. *J. Neurosci.* **35,** 13053–13063 (2015).
36. Del Rio, J. A., Soriano, E. & Ferrer, I. Development of GABA-immunoreactivity in the neocortex of the mouse. *J. Comp. Neurol.* **326,** 501–526 (1992).
37. Vogt, D. *et al.* Viral-mediated Labeling and Transplantation of Medial Ganglionic Eminence (MGE) Cells for In Vivo Studies. *J. Vis. Exp. JoVE* (2015). doi:10.3791/52740
38. Chen, L., Chatterjee, M. & Li, J. Y. H. The Mouse Homeobox Gene Gbx2 Is Required for the Development of Cholinergic Interneurons in the Striatum. *J. Neurosci.* **30,** 14824–14834 (2010).
39. Flandin, P., Kimura, S. & Rubenstein, J. L. R. The Progenitor Zone of the Ventral Medial Ganglionic Eminence Requires Nkx2-1 to Generate Most of the Globus Pallidus But Few Neocortical Interneurons. *J. Neurosci.* **30,** 2812–2823 (2010).
40. Zechel, S., Zajac, P., Lönnerberg, P., Ibáñez, C. F. & Linnarsson, S. Topographical transcriptome mapping of the mouse medial ganglionic eminence by spatially resolved RNA-seq. *Genome Biol.* **15,** (2014).
41. Xu, Q., Tam, M. & Anderson, S. A. Fate mapping Nkx2.1-lineage cells in the mouse telencephalon. *J. Comp. Neurol.* **506,** 16–29 (2008).
42. Flandin, P. *et al.* Lhx6 and Lhx8 Coordinately Induce Neuronal Expression of Shh that Controls the Generation of Interneuron Progenitors. *Neuron* **70,** 939–950 (2011).
43. Denaxa, M. *et al.* Maturation-Promoting Activity of SATB1 in MGE-Derived Cortical Interneurons. *Cell Rep.* **2,** 1351–1362 (2012).

44. Oti, M., Falck, J., Huynen, M. A. & Zhou, H. CTCF-mediated chromatin loops enclose inducible gene regulatory domains. *BMC Genomics* **17,** 252 (2016).
45. Neves, G. *et al.* The LIM Homeodomain Protein Lhx6 Regulates Maturation of Interneurons and Network Excitability in the Mammalian Cortex. *Cereb. Cortex* **23,** 1811–1823 (2013).
46. Zhao, Y. *et al.* Distinct Molecular Pathways for Development of Telencephalic Interneuron Subtypes Revealed Through Analysis of Lhx6 Mutants. *J. Comp. Neurol.* **510,** 79–99 (2008).
47. Danjo, T. *et al.* Subregional Specification of Embryonic Stem Cell-Derived Ventral Telencephalic Tissues by Timed and Combinatory Treatment with Extrinsic Signals. *J. Neurosci.* **31,** 1919–1933 (2011).
48. Chen, C. Y. *et al.* Transcriptome and in Vitro Differentiation Profile of Human Embryonic Stem Cell Derived NKX2.1-Positive Neural Progenitors. *Stem Cell Rev. Rep.* 1–13 (2016). doi:10.1007/s12015-016-9676-2
49. Ahn, S., Kim, T.-G., Kim, K.-S. & Chung, S. Differentiation of human pluripotent stem cells into Medial Ganglionic Eminence vs. Caudal Ganglionic Eminence cells. *Methods* **101,** 103–112 (2016).
50. Hansen, D. V. *et al.* Non-epithelial stem cells and cortical interneuron production in the human ganglionic eminences. *Nat. Neurosci.* **16,** 1576–1587 (2013).
51. Wang, C. *et al.* Human and monkey striatal interneurons are derived from the medial ganglionic eminence but not from the adult subventricular zone. *J. Neurosci. Off. J. Soc. Neurosci.* **34,** 10906–10923 (2014).

52. Chang, J., Gilman, S. R., Chiang, A. H., Sanders, S. J. & Vitkup, D. Genotype to phenotype relationships in autism spectrum disorders. *Nat. Neurosci.* **18,** 191–198 (2015).

53. Smith-Hicks, C. L. GABAergic dysfunction in pediatric neuro-developmental disorders. *Front. Cell. Neurosci.* **7,** 269 (2013).

54. Volk, D. W., Edelson, J. R. & Lewis, D. A. Cortical Inhibitory Neuron Disturbances in Schizophrenia: Role of the Ontogenetic Transcription Factor Lhx6.

Schizophr. Bull. **40,** 1053–1061 (2014).

55. Heath, H. *et al.* CTCF regulates cell cycle progression of αβ T cells in the thymus. *EMBO J.* **27,** 2839–2850 (2008).

56. Hébert, J. M. & McConnell, S. K. Targeting of cre to the Foxg1 (BF-1) locus mediates loxP recombination in the telencephalon and other developing head structures. *Dev. Biol.* **222,** 296–306 (2000).

57. Dobin, A. *et al.* STAR: ultrafast universal RNA-seq aligner. *Bioinformatics* **29,** 15–21 (2013).

58. Lawrence, M. *et al.* Software for Computing and Annotating Genomic Ranges. *PLOS Comput. Biol.* **9,** e1003118 (2013).

59. Love, M. I., Huber, W. & Anders, S. Moderated estimation of fold change and dispersion for RNA-seq data with DESeq2. *Genome Biol.* **15,** 550 (2014).

60. Langmead, B. & Salzberg, S. L. Fast gapped-read alignment with Bowtie 2. *Nat. Methods* **9,** 357–359 (2012).

61. Zhang, Y. *et al.* Model-based analysis of ChIP-Seq (MACS). *Genome Biol.* **9,** R137 (2008).

62. Ramírez, F., Dündar, F., Diehl, S., Grüning, B. A. & Manke, T. deepTools: a flexible platform for exploring deep-sequencing data. *Nucleic Acids Res.* **42,** W187-191 (2014).
63. Quinlan, A. R. & Hall, I. M. BEDTools: a flexible suite of utilities for comparing genomic features. *Bioinforma. Oxf. Engl.* **26,** 841–842 (2010).

Chapter 3

in dysmorphology and sexually dimorphic behaviour impairments uced by embryonic CTCF haploinsufficiency

Elbert, A.[1,2], Levy, M.[1,2], Watson, L.A. [1,2], Schmid, S.[3], Lerch, J.[4], Bérubé, N.G.[1,2,*]

Affiliations: [1]Children’s Health Research Institute, London, Ontario, Canada. [2]Department of Paediatrics, Schulich School of Medicine and Dentistry, the University of Western Ontario, Victoria Research Laboratories, London, Ontario, Canada. [3]Department of Anatomy and Cell Biology, [4]Department of Medical Biophysics, University of Toronto, Mouse Imaging Centre, Hospital for Sick Children, Toronto, ON, Canada.

tract

Genetic variation in *CTCF*, a ubiquitous chromatin organizer, is associated with increased risk for schizophrenia, while *de novo* mutation or deletion of one allele results in a dominantly-inherited intellectual disability syndrome with autistic features (OMIM #615502). To model human *CTCF* haploinsufficiency, we generated mice with *Cre*-mediated deletion of a single copy of *Ctcf* in the embryonic brain. An early and progressive transcriptional compensation by the wildtype allele was observed in the brain of these mice, with CTCF levels reaching near control levels in adulthood. Despite nominal CTCF reduction, Magnetic Resonance Imaging (MRI) revealed changes in adult brain volume of limbic system structures and cerebellum. $\mathit{Ctcf}^{\mathrm{Nestinhet}}$ mice exhibited delayed spatial learning and hyperactivity. Male, but not female $\mathit{Ctcf}^{\mathrm{Nestinhet}}$ mice had differences in anxiety and social behaviours, compared with controls. These findings suggest that a minor decrease in CTCF protein levels in the developing brain can lead to important morphological and behavioural defects in adulthood, in a sex-specific manner.

oduction

CTCF encodes an 11 zinc-finger DNA-binding protein that functions in chromatin higher order organization, often with the cohesin complex[1]. The interaction of CTCF with itself and its protein partners mediates chromatin loop formation, which creates topologically distinct regions in the genome. This epigenetic process regulates the level and timing of gene expression across development[2].

Deletion of both copies of *Ctcf* is believed to cause embryonic lethality in humans[3], but mutation or deletion of a single copy of *CTCF* leads to intellectual disability (ID), microcephaly, and growth retardation (MIM #615502). Gregor and colleagues identified four children with varying levels of ID carrying *de novo* changes to one copy of the *CTCF* locus[4]. A recent report described an ID patient with a previously uncharacterized frameshift mutation in *CTCF*[5].

CTCF has also been linked to schizophrenia[6] and autism spectrum disorder (ASD)[7], which have overlapping clinical features and may have shared etiological pathways that are neurodevelopmental in origin[8–10]. Features of schizophrenia include hallucinations, delusions, social impairments, alogia, abnormal motor behaviour and disorganized thinking[11]. A large body of evidence supports a pathophysiological model for schizophrenia in which developmental and genetic vulnerabilities interact with secondary environmental insults during critical periods of brain development[12]. Schizophrenia mouse models are reported to model the disorder in three areas: i) positive symptoms (eg spontaneous hyperactivity), ii) cognitive impairment (eg impaired re-learning), and iii) negative symptoms (eg social impairments)[13]. These mice often have altered behaviour in open field, MWM with reversal, Y-maze, prepulse inhibition and acoustic startle, and social investigations[13,14].

ASD is characterized by deficits in social-emotional reciprocity, communication and adaptive behaviours, and an increase in restricted, repetitive patterns of behaviour, which may or may not be accompanied by intellectual impairment[11]. ASD mouse models often show increased digging, which manifests in marble burying assays, as well as reduced sociability and vocalization, among other features[15].

Given the growing evidence for a role for CTCF in neurodevelopmental disorders, mouse models of CTCF loss were generated to investigate its function in the brain. Our group has shown that deletion of *Ctcf* in embryonic neuroprogenitors results in microcephaly, caused by aberrant proliferation resulting in premature depletion of the neuroprogenitor pool[16]. Hirayama and colleagues have shown that deletion of *Ctcf* in neurons causes altered dendritic arborisation, reduced spine density and disorganized barrel cortices, indicative of impaired somatosensory mapping[17]. Another group created mice with conditional inactivation of *Ctcf* in excitatory neurons[18]. Mutant mice exhibited impaired learning and memory in the MWM paradigm and these findings were replicated by viral-mediated depletion of *Ctcf* in the hippocampus. These conditional knockout mice had normal sociability but had no preference for a novel versus familiar mouse.

Notwithstanding these recent contributions, the effect of haploinsufficiency for CTCF on the brain has not been addressed in a model system. In this study, we characterized mice with deletion of one copy of *Ctcf* in the developing brain. Despite the heterozygosity at the locus, we observed near control levels of CTCF protein in the adult brain, due to compensation from the remaining allele. We find that the brain structure in these $Ctcf^{\mathrm{Nestinhet}}$ mice is grossly altered and that these mice display abnormal behaviours that are more severe in, or unique to, the male mutant mice.

lts

lence of allelic compensation in the brain of $Ctcf^{Nestinhet}$ mice.

We generated mice that model CTCF haploinsufficiency in the developing brain through crossing *Ctcf flox/ flox* animals to the NestinCre driver line. Both male and female $Ctcf^{Nestinhet}$ mice are viable and fertile (data not shown). To verify that the level of CTCF expression was halved in the mutant mice, we performed RT-qPCR and Western blot analysis of embryonic and adult brain tissue. However, we observed levels exceeding 50% in E14.5 and E16.5 forebrain samples. The reduction in *Ctcf* expression only reached statistical significance in E13.5 wholebrain (Fig. 1C). Levels of *Ctcf* mRNA and protein were also not significantly altered in adult cortex (Fig. 1A, C). Hippocampal tissue from the adult $Ctcf^{Nestinhet}$ mice showed an average CTCF protein level that was 82% of control (P=0.343). Adult male cerebellum and cortical samples had, on average, comparable CTCF levels to those of control (94%), indicating substantial compensation from the wildtype locus.

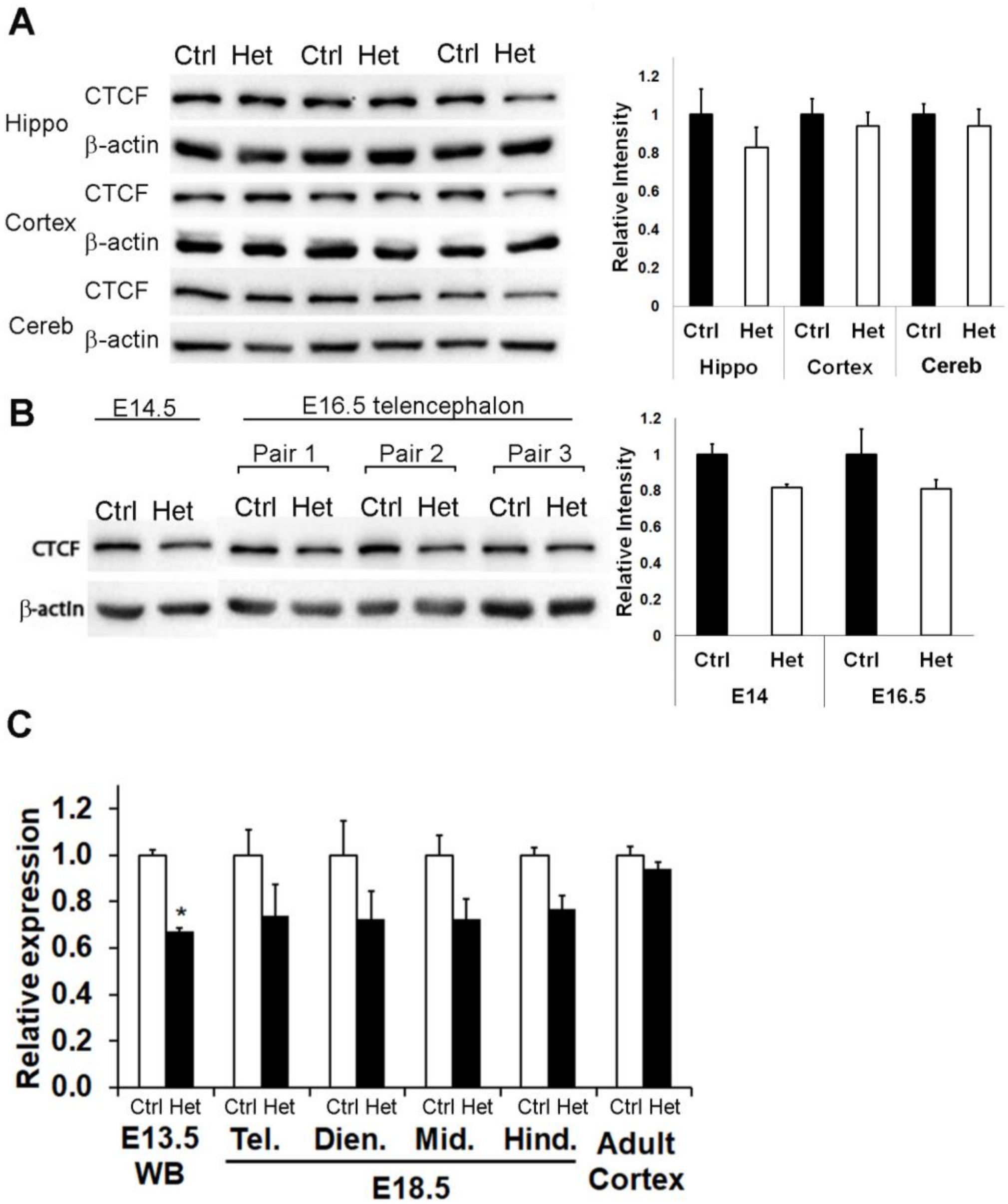

Figure 1: CTCF expression in *Ctcf*^{NestinCre} brain suggests significant compensation from the wildtype allele. (A) Representative western blot of CTCF in three control (Ctrl) and *Ctcf*^{NestinCre} (Het) adult sibling pairs from hippocampus (hippo), cortex, and cerebellum (cereb) to show inter-individual variability. β-ACTIN was used as a loading control for quantification in n=6 pairs, on the right. (B) Representative western blot of CTCF in E14.5 and E16.5 telencephalon, with quantification on the right, normalized to β-ACTIN (E14.5 n=2 pairs; E16.5 n=3 pairs). (C) RT-qPCR of *Ctcf* in E13.5 whole brain; E18.5 telencephalon, diencephalon, midbrain, and hindbrain; and adult cortex, normalized to *β-actin.* For all graphs, error bars represent SEM.

^{Nestinhet} and NestinCre control mice are smaller and display hind-limb clasping compared to negative controls

We measured the weight of control and mutant mice from weaning until 10 weeks of age. We found that at 3 weeks of age, there was already a significant difference in weights between genotypes (Fig. 2B; *P*= 0.0046 by ANOVA); *Ctcf*^{Nestinhet} male mice and *NestinCre* controls weighed less than *Cre*-negative control counterparts, and this discrepancy increased across the 7 week period. Females showed a similar trend, but the effect of carrying the *NestinCre* gene was less pronounced. The size difference between *NestinCre* controls and *Ctcf*^{Nestinhet} mice across 3 to 10 weeks of age was negligible, indicating that the reduced size of *Ctcf*^{Nestinhet} mice is a consequence of *NestinCre* expression and not a reduction in CTCF levels.

Paw-clasping, typically in the hind-limbs, is associated with abnormal neurological function, in particular due to cerebellar lesions, but also due to defects in the basal ganglia and cortex[19].As a crude measure of neurological function, we tested *Ctcf*^{Nestinhet} and control siblings for hind-limb clasping. An increased proportion of *Ctcf*^{Nestinhet} and *NestinCre* mice exhibit hind-limb clasping compared to the others (Fig. 2A), suggesting again that this effect was mediated by the NestinCre transgene.

uced brain volume in adult *Ctcf*^{Nestinhet} mice

We next examined whether we could detect morphological defects in the brain using high-resolution ex-vivo MRI combined with automated image analysis. These analyses revealed widespread reductions in brain volumes of both male and female *Ctcf*^{Nestinhet} mice compared to controls, at 5-6 months of age (*Ctcf*^{Nestinhet}, n=27, sibling controls, n=30; Fig. 3A-B).These reductions in volume appear to be consistent with what others report with the *NestinCre* transgene. Therefore we analyzed brain volumes as relative volumes to *Cre*-negative controls. Genotype by sex interactions did not survive multiple testing, therefore genotypes are sub-grouped by sex only for total brain volume.

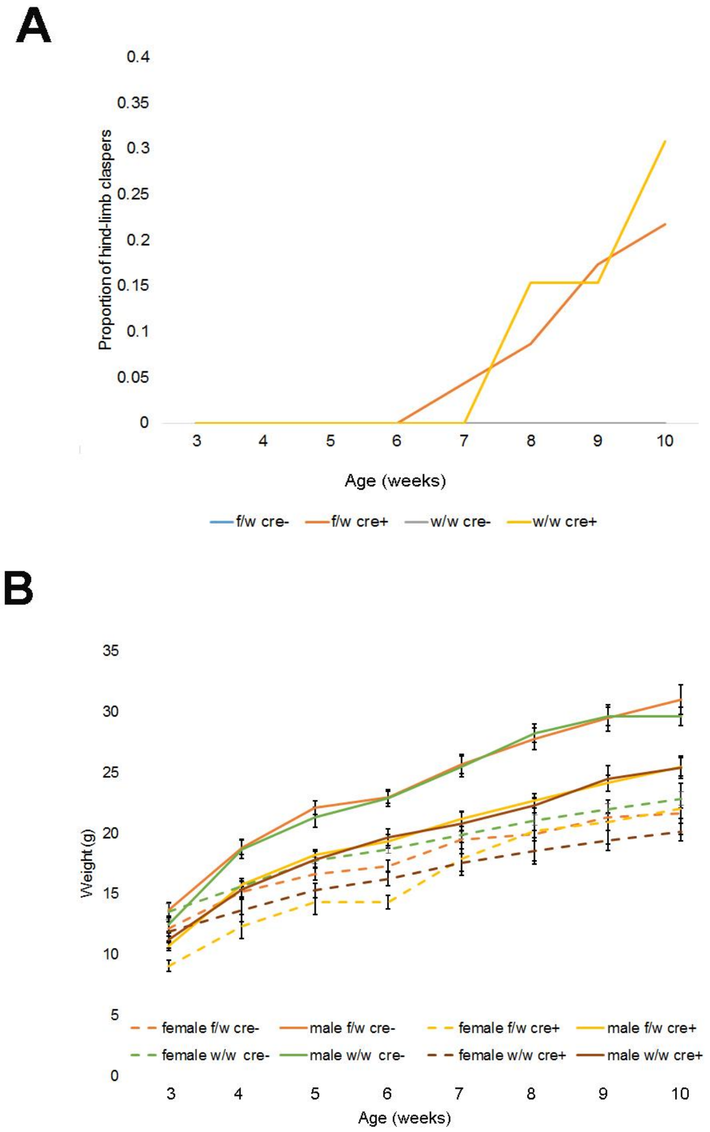

Figure 2: *Ctcf*^{NestinCre} and *NestinCre* control mice are smaller and develop hind-limb clasping. (A) Proportion of *Ctcf*^{NestinCre} mice (orange line; n= 16 males, n= 7 females), *NestinCre+* siblings (gold line; n= 4 males, n= 2 females), *Ctcf*$^{f/w}$ siblings (blue line; n= 14 males, n= 4 females), and wildtype siblings (silver line; n= 7 males, n= 14 females) that show hind-limb clasping on at least three occasions, over 7 weeks. (B) Weight of *Ctcf*^{NestinCre} mice (n= 20 males, n= 8 females), *NestinCre+* siblings (n= 12 males, n= 7

females), *Ctcf*$^{f/w}$ siblings (n= 17 males, n= 9 females), and wildtype siblings (n= 12 males, n= 15 females) over 7 weeks. Error bars represent SEM.

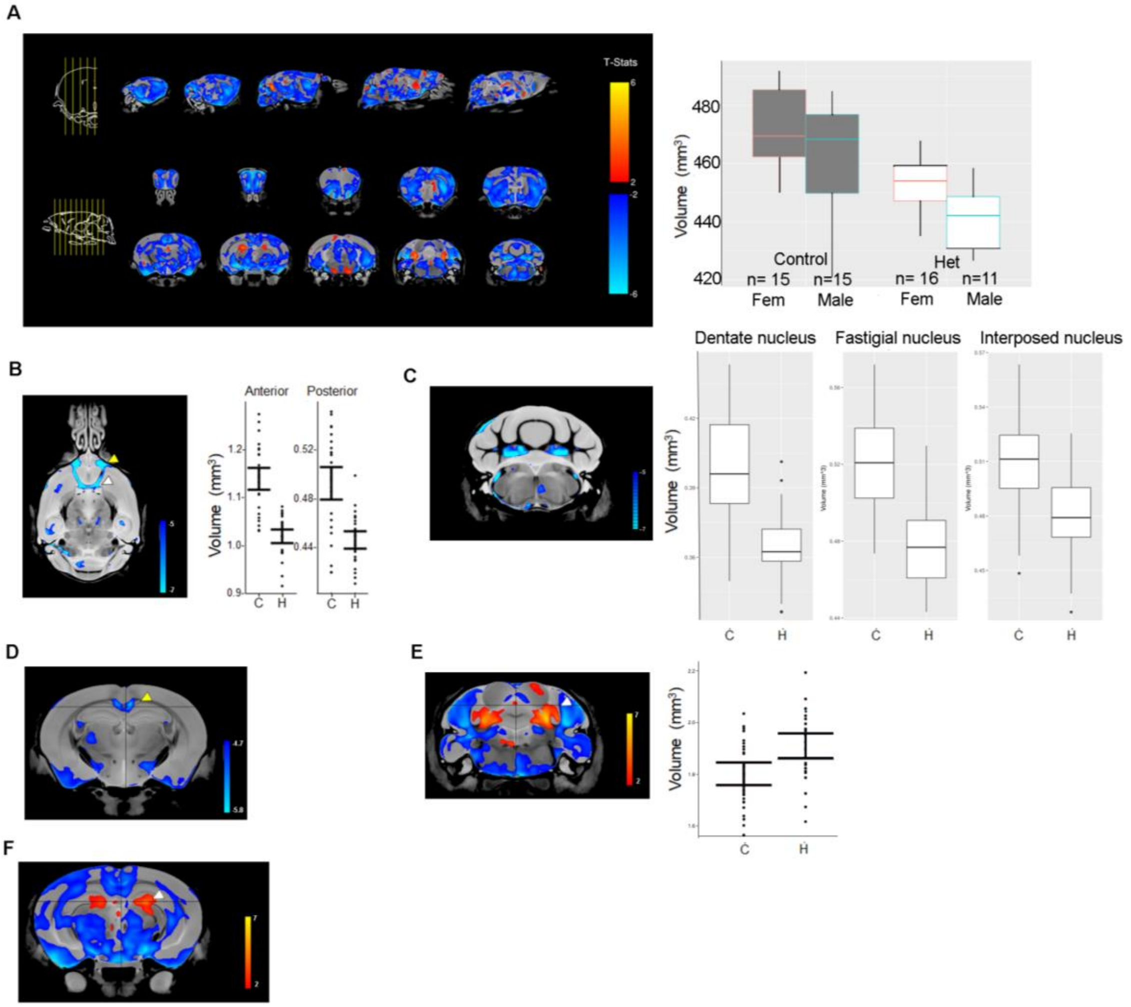
A
T-Stats
Volume (mm³)
480
460
440
420
Control
Het
n= 15
n=15
n= 16
n=11
Fem
Male
Fem
Male
B
Anterior
Posterior
Volume (mm³)
1.2
1.1
1.0
0.9
0.52
0.48
0.44
C
H
C
H
C
Dentate nucleus
Fastigial nucleus
Interposed nucleus
Volume (mm³)
C
H
C
H
C
H
D
E
Volume (mm³)
C
H
F

Figure 3. *Ctcf*^{NestinCre} mice have altered brain anatomy on MRI. For all image panels, blue depicts relative decreases, and red represents relative increases, from averaged MRI data acquired in *Ctcf*^{NestinCre} (n= 11 males, n= 16 females) compared with control siblings (n= 15 males, n= 15 females). For all graphs, the *Ctcf*^{NestinCre} genotype is denoted by "H" and control by "C". (A) Representative sagittal (rows 1) and coronal (rows 2-3) slices, and adjacent quantification of total brain volume by genotype and sex. (B) Representative axial slice at the level of the anterior commissure (relative brain volume) with quantification of the pars anterior (yellow arrow) and posterior (white arrow) of the anterior commissure volume by genotype (normalized). (C) Deep cerebellar nuclei (relative brain volume) with adjacent quantification (D) Representative coronal slice at the level of the corpus callosum (relative brain volume). Quantification for relative brain volume was not available. (E) Representative coronal slice showing relative increase in volume at the level of the anterior lobules of cerebellum (absolute brain volume) in the

Ctcf^{NestinCre}, with adjacent quantification (normalized). (F) Representative coronal slice (absolute brain volume) showing relative increase in volume of the hippocampal dentate gyri in the *Ctcf*^{NestinCre}. Quantification was not available.

We measured a marked reduction in the normalized volume of the anterior commissure (q-value$_{\text{F-statistic}}$= 7.4 x 10^{-9}, Fig. 3B), the white matter tract connecting the two temporal lobes and orbitofrontal areas, which also contain decussating fibres from the olfactory tracts[20]. Defects in the anterior commissure are consistent with reduced inter-hemispheric connectivity.

There are three sets of deep cerebellar nuclei in mice: the dentate, the fastigial and the interposed nuclei. When examining for focal changes in volume, there was a striking decrease in size of the dentate and fastigial deep cerebellar nuclei, when normalized to total brain volume (Fig. 3C). In addition, there were focal volume increases of the anterior lobes (lobules 4-5) of the cerebellum (Fig. 3E) and in the dentate gyrus of the hippocampus (Fig 3F) in the *Ctcf*^{Nestinhet} brain.

ormal behaviours are observed in *Ctcf*^{Nestinhet} mice

Human cases with mutations in one allele of the *CTCF* locus have intellectual disability, and some develop features of ASD. To evaluate how having a single copy of *Ctcf* affects adult mouse behaviour, 12 week-old male and female *Ctcf*^{Nestinhet} mice were subjected to a battery of behavioural tests over a 5-week period and compared with *Ctcf flox/ wildtype* sibling controls. The open field test was used to detect abnormalities in exploration behaviour and activity over a two-hour period in low light conditions. When male and female *Ctcf*^{Nestinhet} mice were analyzed together, this genotype was significantly associated with hyperactivity, with the *Ctcf*^{Nestinhet} mice showing a lot more variability than sibling controls (P=0.0345, Fig. 4A). When analyzed by sex, the hyperactivity was more pronounced in males than females, but was not statistically significant (*P*=0.0711 males only, Fig. S1A; *P*=0.2665 females only Fig. S1B).

In the MWM, a test of spatial learning and memory, there was a significant delay of *Ctcf*^{Nestinhet} mice to get to the platform (ANOVA *P*= 0.0077; Fig. 5A). When post-hoc per-day analysis was performed, this effect was driven by the delay to platform on Day 2 of training (*P*= 0.0009). There was no defect in MWM reversal, suggesting that *Ctcf*^{Nestinhet} mice do not have altered cognitive flexibility or re-learning deficit (Fig. S2B-C). Both short-term memory (Day 5) and long-term memory (Day 12) were intact, with no significant difference between *Ctcf*^{Nestinhet} mice and controls (Fig. 5B-E). We also tested motor learning using the rotarod (Fig. S2D-E) and working memory in the Y maze but found no significant difference between *Ctcf*^{Nestinhet} and control mice (Fig. 5F-G).

Deficits in sensory gating, measured by prepulse inhibition in mice, are frequently observed in schizophrenia[21] and relevant mouse models[13]. Due to the association between *CTCF* and schizophrenia[6], we began by testing the startle reflex to an acoustic stimulus of 105-115 db. This reflex involves the anterior cingulate cortex, the amygdala, the hippocampus, and the bed nucleus of the stria terminalis[22]. The strength of the startle was larger in *Ctcf*^{Nestinhet} mice, although it did not reach statistical significance (male and female combined, *P*=0.0550; Fig. 6A). We observed prepulse inhibitions of 48-75% of the startle response, which is typical for these settings, and there was no statistically significant difference between the *Ctcf*^{Nestinhet} and control mice (Fig. 6B-C). These results indicate that *Ctcf*^{Nestinhet} do not have any abnormalities in the filtering and processing of sensory information.

Since *CTCF* mutations can cause ASD[7], we tested for stereotyped and repetitive behaviours. There were no significant differences in the number of marbles buried between the $Ctcf^{Nestinhet}$ and controls (*P*-value= 0.355, Fig. 8A). There was also no significant difference in the time spent digging or grooming, during the social approach test (Fig. 8B).

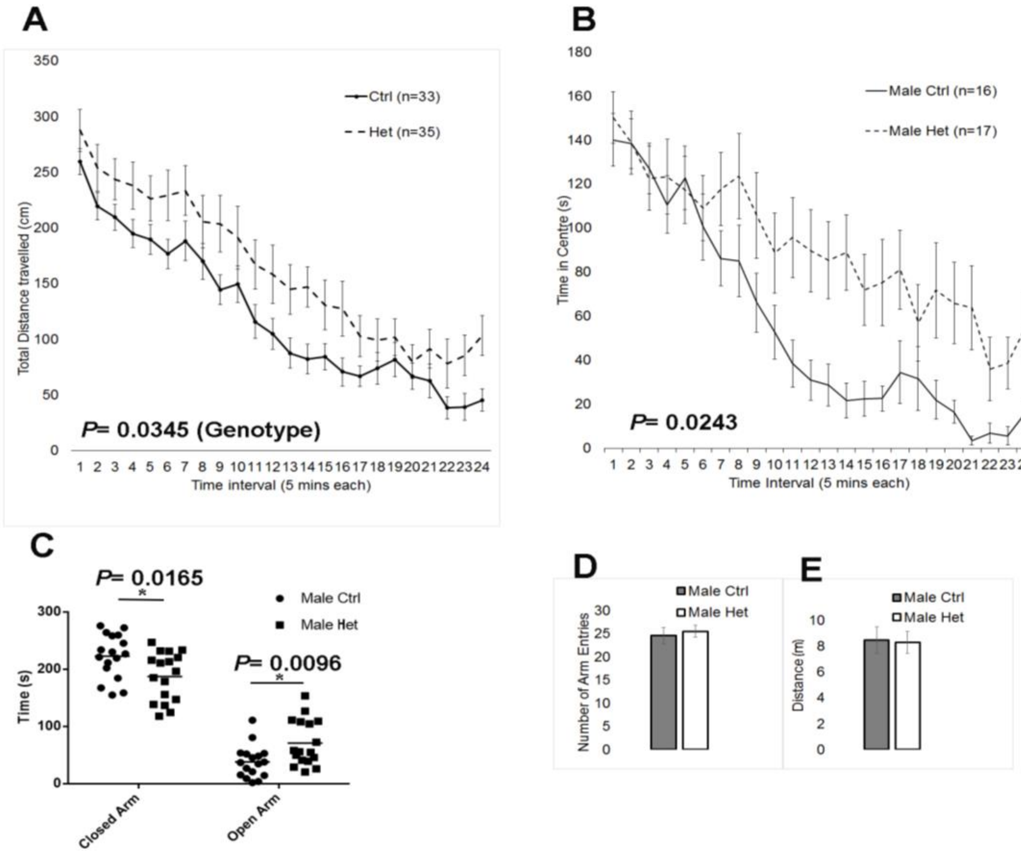

Figure 4: $Ctcf^{NestinCre}$ mice are hyperactive, and male $Ctcf^{NestinCre}$ mice have reduced anxiety, compared to control siblings. For all graphs, error bars represented SEM and horizontal bar represents the mean. (A) Distance travelled by $Ctcf^{NestinCre}$ (het; n= 18 females, n= 17 males) and controls (ctrl; n= 17 females, n= 16 males) in the open field test, totalled across 24 five-minute intervals, analyzed by repeated-measures ANOVA. (B) Time spent in the centre of open field enclosure by male $Ctcf^{NestinCre}$ (het) and controls (ctrl), totalled across the same 24 five-minute intervals, analyzed by repeated-measures ANOVA. (C) Time spent in closed and open arms of the elevated plus maze, analyzed by Student's *t-test*. (D) Average number of arm entries in the elevated plus maze. (E) Average distance travelled in the elevated plus maze.

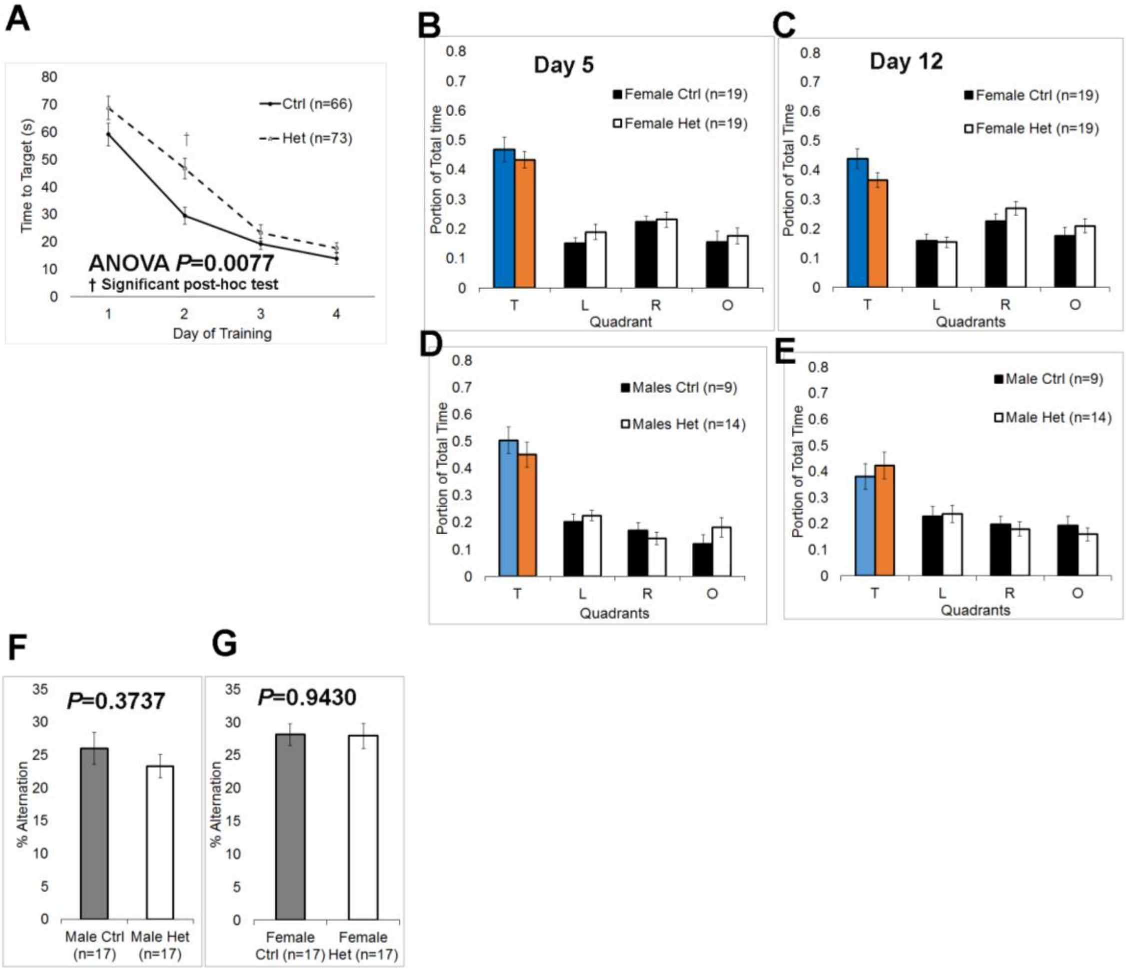

Figure 5. *Ctcf*^{NestinCre} mice have delays in spatial learning but no impairments in short and long-term memory. For all graphs, error bars represent SEM. (A) Latency to target platform in MWM of *Ctcf*^{NestinCre} (het) and controls (ctrl) over four training days. Repeated-measures ANOVA across training days was significantly different between genotypes. Post-hoc per-day Student's *t-test* was significant for day 2, as denoted by †. (B-E) Proportion of time spent in each quadrant (target= T, opposite=O, left= L, right= R) on day 5 (short-term memory test) and day 12 (long-term memory test) of MWM. (F-G) Percentage of spontaneous alternations in the Y-maze, where one alternation consists of consecutive entry into the three different arms, analyzed by Student's *t-test*.

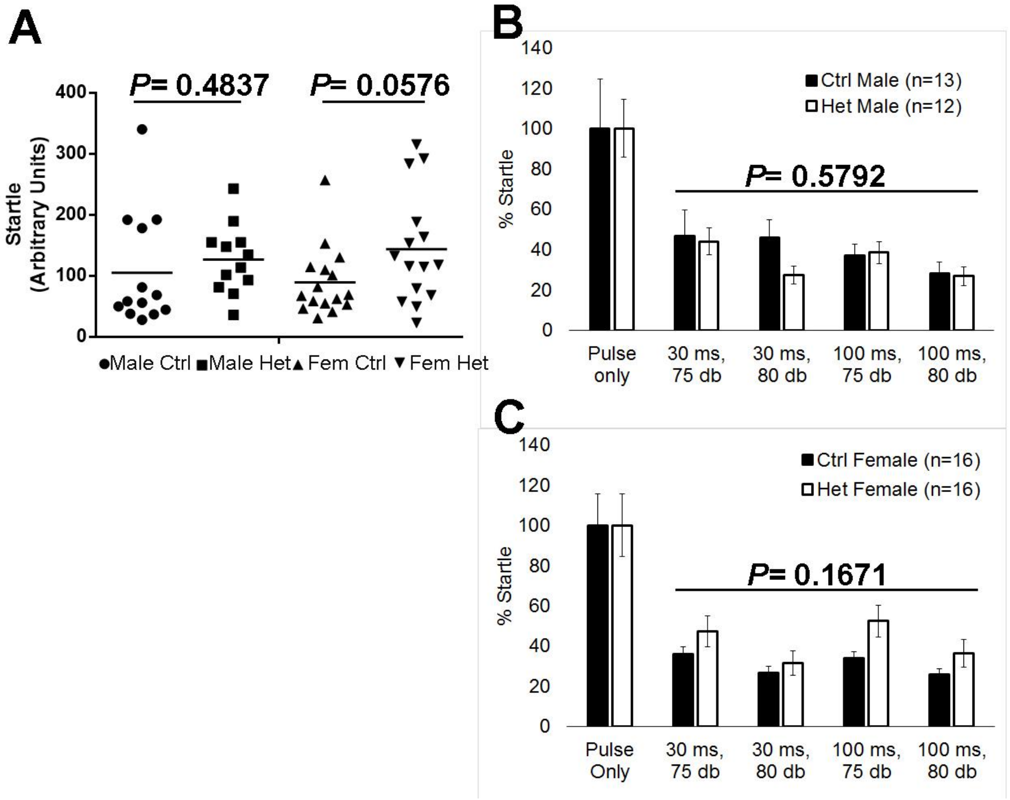

Figure 6. *Ctcf*^{NestinCre} mice have normal sensory gating. The *Ctcf*^{NestinCre} genotype is denoted by "het", and control by "ctrl". For all graphs, error bars represent SEM and horizontal bar represents the mean. (A) Quantification of the acoustic startle response by genotype and sex, analyzed by Student's *t-test*. (B-C) Averaged prepulse inhibition for four conditions generated by varied interstimulus intervals (30 ms or 100 ms) and prepulse intensity (75 db or 80 db). Startle response for trials types is expressed as a percentage of the normalized "pulse only" trial in (B) males and (C) females. Results were analyzed by ANOVA.

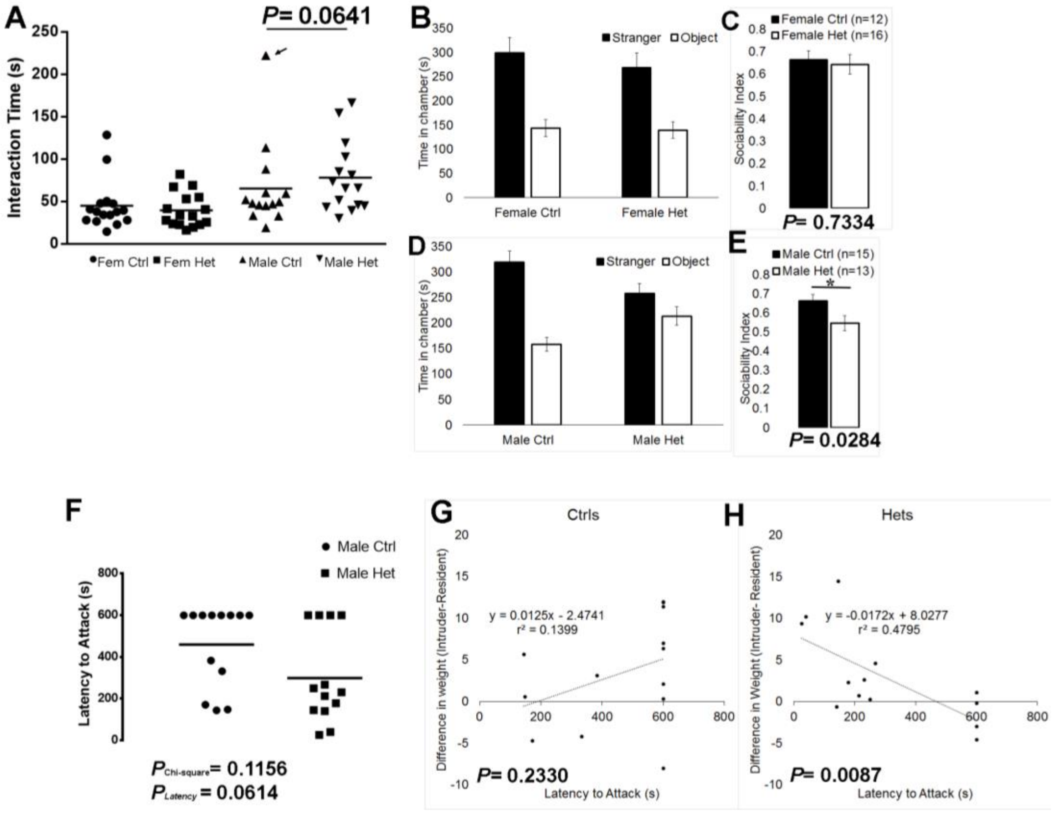

Figure 7: Male *Ctcf*^{NestinCre} have decreased sociability and altered aggression behaviour. The *Ctcf*^{NestinCre} genotype is denoted by "het", and control by "ctrl". For all graphs, error bars represent SEM and horizontal bar represents the mean. (A) Interaction time of mice conspecific for genotype and sex in the social approach test, analyzed by Student's *t-test*. The arrow indicates a significant outlier, which was not included in the analysis. (B-E) Time spent in chambers with stranger mouse or novel object by genotype in females (B) or males (D) in the social choice paradigm. The sociability index for each mouse was calculated as the time spent in the stranger mouse chamber, divided by the total time in the stranger mouse and novel object chambers. The average sociability index by genotype is shown for females (C) and males (E), and compared by Student's *t-test*. (F) Latency to attack in the resident-intruder paradigm. Resident mice that did not attack in the assay have a default latency of 600 s, the total length of the interaction. Latency to attack was compared between genotypes by Student's *t-test.* The number of attackers and non-attackers between genotypes was compared by Fisher's exact test. (G-H) Correlation between difference in intruder mouse weight and resident mouse weight of controls (G) and *Ctcf*^{NestinCre} (H) and latency to attack. Regression lines are plotted with corresponding equations and correlation coefficients (r^2).

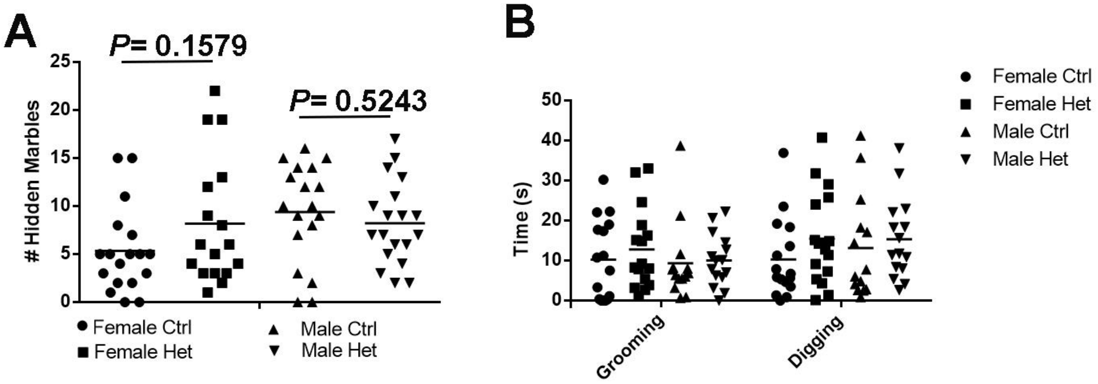

Figure 8: *Ctcf*^{NestinCre} do not have stereotyped or repetitive behaviours. The *Ctcf*^{NestinCre} genotype is denoted by "het", and control by "ctrl". For all graphs, the horizontal bar represents the mean. (A) Number of marbles hidden in the marble bury assay, grouped by genotype and sex, and analyzed by Student's *t-test* (B) Time spent grooming or digging during the social approach assay, grouped by genotype and sex, and analyzed by Student's *t-test*.

iety, sociability and aggressive behaviour were observed in male *Ctcf*^{NestinCre} mice.

We found that male mutant mice, but not the females, showed defects in a subset of behaviours. For example, male *Ctcf*^{Nestinhet} mice spent more time in the centre of the enclosure in the open field, a measure that is associated with decreased anxiety (*P*=0.0243, Fig. 4B). Consistent with this, male *Ctcf*^{Nestinhet} mice also spent significantly more time in the open arms of the elevated plus maze, another finding suggestive of decreased anxiety (*P*= 0.0096, Fig. 4C). These measures of anxiety were not significantly different between female *Ctcf*^{Nestinhet} mice and sibling controls (Fig. S1C-D).

In the social approach test, pairs of unfamiliar mice with the same genotype (conspecific) are placed in a neutral cage and their interactions are observed. This test allows for the quantification of high quality social interactions. There was no statistically significant difference in quality of social interactions between *Ctcf*^{Nestinhet} mice and controls, although male *Ctcf*^{Nestinhet} tended to spend more time sniffing (*P*= 0.0641; Fig. 7A). In the social choice paradigm, male *Ctcf*^{Nestinhet} mice spent only marginally more time with the stranger mouse than with the object, as indicated by a significantly lower sociability index compared to control male siblings (P= 0.0284; Fig. 7D-E), Conversely, female *Ctcf*^{Nestinhet} mice displayed comparable sociability to their control counterparts, indicating that loss of one copy of *Ctcf* in the brain causes a sex-specific defect in social behaviour. Male mice were then subjected to the resident-intruder assay. There was a number of mice of both genotypes that did not attack the intruder by the end of the allotted ten minutes (Fig. 7F). We observed aggression in nearly double the number of *Ctcf*^{Nestinhet} mice compared with controls, however this was not statistically significant by Fisher's exact test (P= 0.1156). We also compared the latency to attack, by Student's *t-test*. We found no significant difference in latency to attack by genotype when including the non-attackers (P= 0.0614), and when comparing only the aggressive mice (P= 0.2712), although the latter comparison was under-powered. The relative body weight of the resident mouse compared to the intruder can influence the resident-intruder assay, in that smaller size dampens aggressive behaviour[23]. Since the *Ctcf*^{Nestinhet} mice are significantly smaller than control mice, we wanted to control for the weight difference between intruder and resident mice, denoted hereon as Δ_{size}. On average, there was no difference in weight between any groups (Fig. S3A), and the Δ_{size} for controls was not correlated with aggression (r^2= 0.1399; P= 0.2330, Fig. 7G). However we found there was a significant association between the Δ_{size} of *Ctcf*^{Nestinhet} and aggressive behaviour (P= 0.0087), and this effect was in the opposite direction than expected; smaller *Ctcf*^{Nestinhet} mice were more likely to be aggressive with larger intruders (Fig. 7H). The interaction between Δ_{size} and genotype was significantly associated with aggression (P=0.004).

Importantly, the weight of $Ctcf^{Nestinhet}$ mice was not correlated with aggression (P= 0.8937; Fig. S3B), suggesting the observed effect is not due to smaller $Ctcf^{Nestinhet}$ mice being more aggressive but instead due to their relative weight to the intruder.

ussion

Here we explore the role of CTCF in brain development and function using mice. The *NestinCre* driver of deletion targets *Ctcf* in neuroprogenitors at one allele, complementing previous work by others[16–18]. In summary, $Ctcf^{Nestinhet}$ mice had altered volumes in the limbic system and cerebellum, and were hyperactive with delayed spatial learning. *NestinCre* mice, tested by others[24], had no difference from control with regards to spatial learning and memory in multiple maze paradigms, locomotor activity in the open field, and acoustic startle response. This suggests our findings can be attributed to loss of a single copy of *Ctcf* in neuroprogenitors. In addition to these altered behaviours, male $Ctcf^{Nestinhet}$ have reduced anxiety, altered sociability, and are more aggressive than control siblings when presented with a larger opponent. This is in contrast to *NestinCre* male mice, which were reported to have increased anxiety, compared with controls[24].

The reduction of CTCF protein by only 25-30% embryonically in $Ctcf^{Nestinhet}$ mice is suggestive of a compensation mechanism through up-regulation of expression from the remaining allele. This suggests that CTCF levels are tightly regulated in the brain. This phenomenon has been observed in other mouse models, such as the $Nipbl^{+/-}$ mouse, a model of CdLS[25,26]. Approximately 40% of reported CdLS cases are attributed to heterozygous mutations in the *NIPBL* gene, which encodes the protein that loads the cohesin complex onto DNA[27]. The transcript level of *Nipbl* in $Nipbl^{+/-}$ mice was only reduced by 25-30% in embryonic brain and liver, however these mice still had multiple severe organ and growth defects. Similar allelic compensation was observed in patients with CdLS, with levels depending on the type of mutation in *NIPBL*[25,28,29]. These studies of *NIPBL*, along with our findings, suggest that even small changes in the dose of chromatin organizer proteins are likely to affect chromatin looping and gene expression, and that if these occur during development, they can have drastic consequences in the adult.

MRI of the *Ctcf*^{Nestinhet} mouse brain revealed changes in total volume, as well as specialized regions including the anterior commissure, deep cerebellar nuclei, and the dentate gyrus of the hippocampus. These defects could explain many of the behaviours observed in our mice, or in human patients with *CTCF* mutations. Volumetric MRI performed by another group on *NestinCre* (Tubb5E401K/+; *NestinCre*+) mouse brains compared to control (Tubb5E401K/+) showed similar total reduced brain volume, suggesting that the microcephaly of *Ctcf*^{Nestinhet} mice is due to *NestinCre* expression[30].

Although the cerebellum has been traditionally associated with balance, motor control and motor learning, it now has well-established roles in higher cognitive functions and has been implicated in cognitive dysmetria (difficulty in processing, prioritizing and responding to information) observed in schizophrenia[31–34]. In addition, functional MRI has demonstrated cerebellar activity during the processing of emotional facial expressions[35,36], which has implications to both ASD and schizophrenia. Theory-of-mind tasks have also noted functional hypoconnectivity in ASD between medial cortex and cerebellum[37]. We did not see any aberrant murine behaviours traditionally associated with the cerebellum, such as impairment on the rotarod[38,39]. Typically, although motor learning is affected, motor training is possible on the rotarod even in cerebellum-lesioned mice where there is massive degeneration of cerebellar Purkinje cells and 20% reduction of deep nuclei cell numbers[39]. Therefore, it is likely that the cerebellum changes in *Ctcf*^{Nestinhet} mice, which consist predominantly of deep nuclei volume loss, are not sufficient to cause detectable deficits in this task.

The *Ctcf*^{Nestinhet} mice had evidence of impaired hippocampal function, including defects in traditional hippocampal-dependent tasks such as impaired learning in the Morris Water Maze[38,40–42], and hyperactivity in the open field paradigm, which has been observed in hippocampus-lesioned mice[38,41–43]. This suggests a role for CTCF in the hippocampus and corroborates previous report from others which find down-regulation of CTCF in the hippocampus impairs acquisition and retention in the MWM[18]. Further, our data suggests that even small reductions in CTCF protein can impact spatial learning. Of interest, damage to the dentate nuclei bilaterally in rats impairs spatial learning in the MWM, without causing defect in probe trials[44], which is consistent with what is observed in *Ctcf*^{Nestinhet} mice in terms of behaviour. The increase in volume of the hippocampal dentate gyri in *Ctcf*^{Nestinhet} mice is interesting, and further study of the role of CTCF in this region is warranted.

Findings in the *Ctcf*^{Nestinhet} mice are also suggestive of hypoconnectivity, as we observed reductions in volume of multiple white matter tracts including the anterior and posterior commissures, and the corpus callosum. There is evidence from mouse models implicating corpus callosum defects in ASD-like behaviour[45]. There is evidence for both under and over connectivity in ASD, particularly in regards to cortico-cortical regions and interhemispheric connections[46,47]. In addition, reduced functional connectivity in the cortex has also been correlated with auditory hallucinations and impaired cognition in schizophrenia[48,49].

Social behaviour has not been previously compared between *NestinCre* transgene-carrying mice and controls. We found male *Ctcf*$^{\mathit{Nestinhet}}$ mice to have decreased sociability in the three-chamber social choice paradigm, which is found in mouse models of ASD[50–55]. We did not find any evidence of increased repetitive behaviour in male *Ctcf*$^{\mathit{Nestinhet}}$ mice, another ASD-associated behaviour. We did find that there was an effect of size difference of *Ctcf*$^{\mathit{Nestinhet}}$ males and intruders with aggression, such that when the *Ctcf*$^{\mathit{Nestinhet}}$ mouse was smaller than the intruder, there was a decreased latency to attack. To our knowledge, such a phenomenon has not been previously reported in the literature. In fact, based on another study[23], we had expected the smaller size of *Ctcf*$^{\mathit{Nestinhet}}$ mice to dampen aggression. We interpret this effect on aggression as an altered perception of danger or altered salience. In schizophrenia, altered catecholamine signaling results in impaired salience and responsiveness to environmental danger cues, resulting in hyper-arousability[56–59]. In support of this, we observed increased startle reflex in both sexes, albeit this was not statistically significant. Changes in habituation and startle reflex are often attributed to aberrant salience[58,59], however, we did not observe any difference in habituation in the open field test. Therefore, further testing and replication are required before interpretation of this finding.

Sex-specific behavioural differences were found in *Ctcf*$^{\mathit{Nestinhet}}$ mice. Namely, males had decreased anxiety and sociability compared with littermate controls. We also note that the traits of locomotor hyperactivity and spatial learning delay in MWM appear more pronounced in males, although sex was not a statistically significant co-variable. Our findings are consistent with others who have found that male mice tend to be more sensitive to neurological perturbation and have more robust impairments[60,61], which is a reason why female mice are often neglected from behavioural and neurobiological studies (reviewed in [62]). Both schizophrenia and ASD have higher incidence in males[63,64]. Estrogen has been suggested as having protective effects on the brain[65], particularly from neurodevelopmental insults, through its influence on gene expression and cell excitability (the protective effects of estrogen with regards to schizophrenia and ASD are reviewed in [66]). As it relates to CTCF, males and females with syndrome-causing mutations in the CTCF gene have been identified at similar rates[4,5,7]. As for the association of *CTCF* with schizophrenia, it remains unclear how the gene levels or function may be affected, and whether the association was stronger in males than females[6]. *Ctcf*^{Nestinhet} mice share behavioural deficits with mice heterozygous for *Bcl11a*, which functions in the Baf swi/snf chromatin-remodelling complex, suggesting there may be shared gene expression changes[67].

In summary we present a model of CTCF loss in which one copy of the gene is deleted in neuroprogenitors, providing insight into the human syndrome resulting from *CTCF* haploinsufficiency. We present evidence for anatomical changes in the brain of *Ctcf*^{Nestinhet}, specifically loss of volume in deep cerebellar nuclei, increased volume of the anterior cerebellar lobules, and limbic structure changes. Finally, we describe the behavioural changes in *Ctcf*^{Nestinhet} mice, which include some sex-specific findings. Future studies will attempt to identify the molecular underpinnings of these anatomical and behavioural changes with CTCF loss.

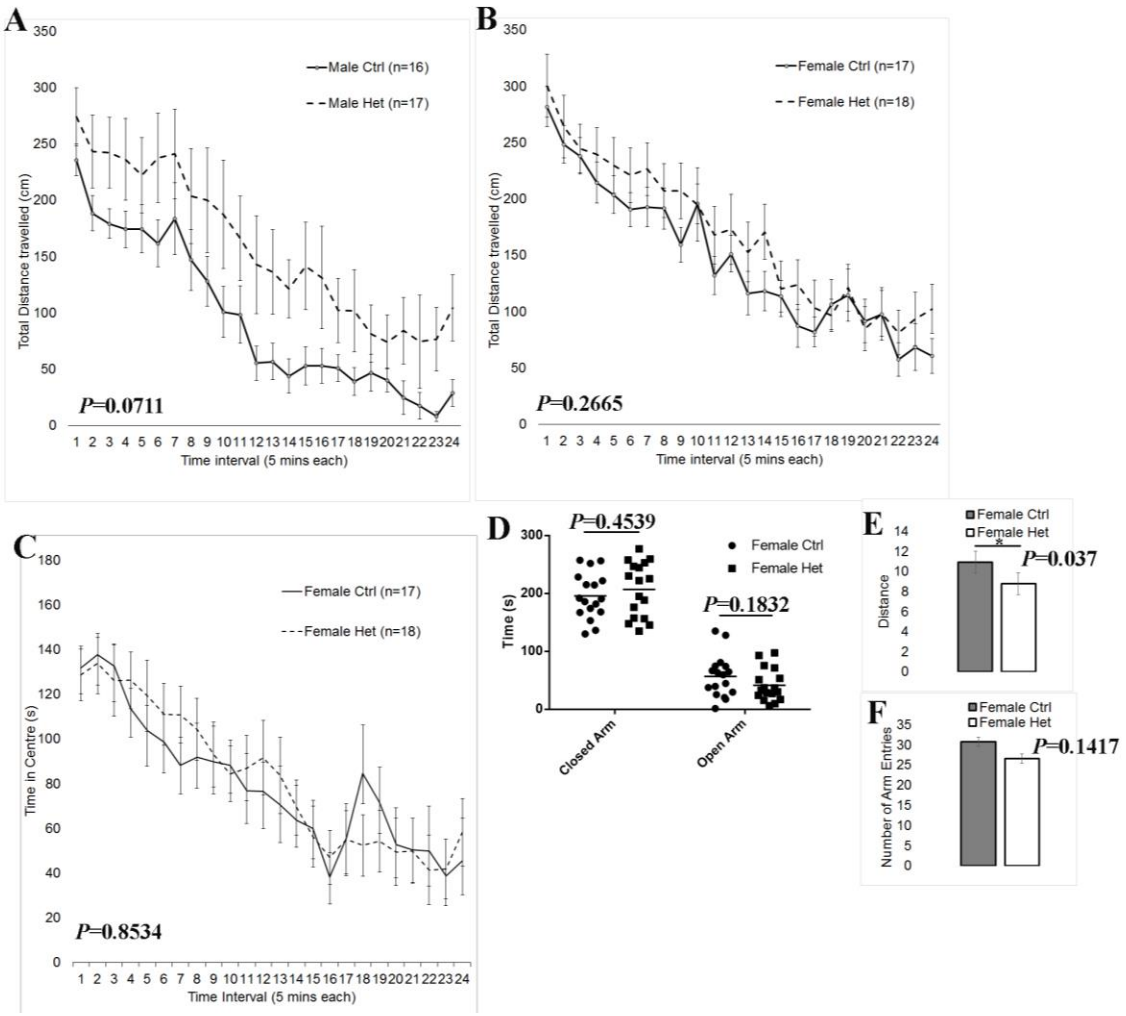

Figure S1. ***Ctcf*^{NestinCre} mice display sex differences in hyperactivity and anxiety.** For all graphs, error bars represented SEM and horizontal bar represents the mean. Distance travelled by (A) male and (B) female *Ctcf*^{NestinCre} (het) and sibling controls (ctrl) in the open field test, totalled across 24 five-minute intervals, analyzed by repeated-measures ANOVA. (C) Time spent in the centre of open field enclosure by female *Ctcf*^{NestinCre} (het) and controls (ctrl), totalled across the same 24 five-minute intervals, analyzed by repeated-measures ANOVA. (D) Time spent in closed and open arms of the elevated plus maze, analyzed by Student's *t-test*. (D) Average number of arm entries in the elevated plus maze. (E) Average distance travelled in the elevated plus maze.

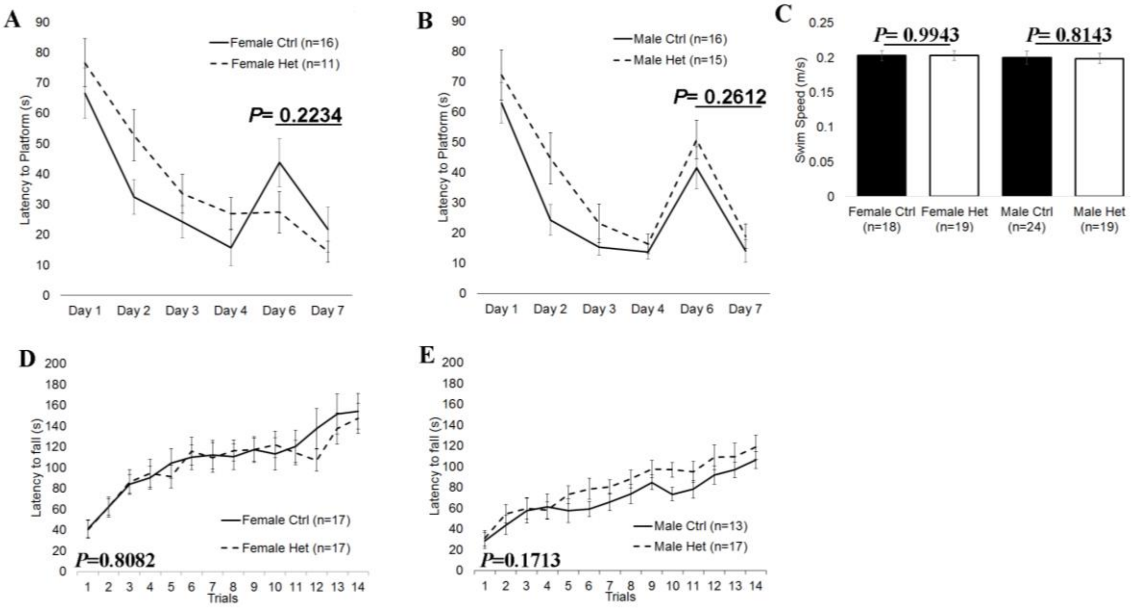

Figure S2. ***Ctcf^{NestinCre}*** **mice have normal reversal and motor learning.** For all graphs, error bars represent SEM. (A-B) Latency to target platform in MWM of *Ctcf^{NestinCre}* (het) and controls (ctrl) over four training days, then two additional training days with a new platform location (reversal). Comparison of first four training days is shown elsewhere (Fig. 5). Repeated-measures ANOVA across reversal training days was not significantly different between genotypes for females (A), or for males (B). (C) Average swimming speed from MWM day 2, grouped by sex. Genotypes were compared with Student's *t-test.* (D-E) Latency to fall from accelerating rotating rod, across 10 trials on day 1, and 4 additional trials on day 2 for females (D), and males (E). Repeated-measures ANOVA was used to compare latencies across trials, a measure of motor learning, between genotypes.

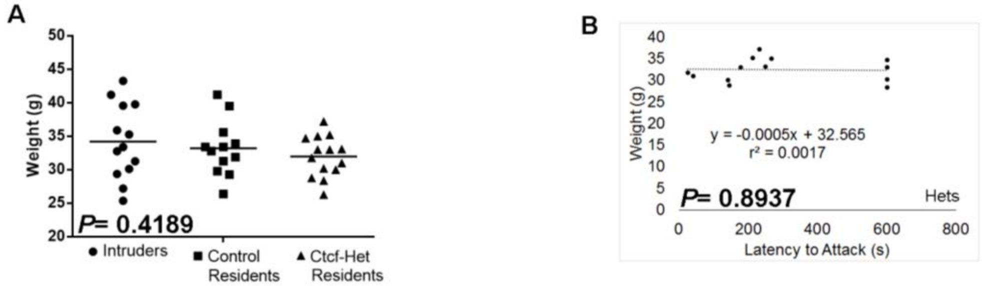

Figure S3. Smaller size of ***Ctcf^{NestinCre}*** **is not correlated with aggression.** (A) Weight of animals participating in the resident-intruder paradigm. The horizontal bar represents the mean of each group, which was compared by ANOVA. (B) Correlation between weight of resident- *Ctcf^{NestinCre}* and latency to attack. Regression line is plotted with corresponding equation and correlation coefficient (r^2).

hods

Mouse husbandry and breeding

Mice were maintained on a 12 hour light/ dark cycle with water and chow *ad libitum*. Behaviours were tested during the light cycle, when mice reached 3 months of age. Mice were group-housed with littermates, 2-5 animals per cage, and tester was blinded to genotype. Cages were changed once every 1-2 weeks depending on the number of mice per cage, and not disturbed prior to behavioural testing. Animals were handled according to protocols in accordance with the regulations of the Animals for Research Act of the province of Ontario, and approved by the University of Western Ontario Animal Care and Use Committee (2008-041-02).

All mice tested were from the C57BL/6J strain. The *NestinCre* driver line has been described previously[68]; as have been *Ctcf*^{loxP} mice[69]. Briefly, the *Nestin* regulatory element drives CRE-recombinase expression in neuroprogenitors, beginning at approximately E11. Homozygous *Ctcf*^{loxP} mice were mated with mice carrying the *NestinCre* gene to generate male and female *Ctcf*^{Nestinhet} mice and littermate controls. Embryos for brain dissection were generated in the same way by timed mating, described in[16]. To generate the four genotypes for weighing and examination of hind-limb clasping, *Ctcf*^{Nestinhet} mice were mated with mice heterozygous for *Ctcf*^{loxP}.

Brain dissection

Embryos from time-mated dams were dissected at E14.5 or E16.5 on ice, and brains removed. Telencephalon, midbrain and hindbrain were separated then frozen on dry ice and stored at -80˚C for later mRNA and protein extraction. For adult tissue, mice were killed after behavioural testing by CO_2 asphyxiation and brain harvested on ice. The cortices, hippocampi and cerebellum were dissected and frozen to be used later for mRNA or protein extraction.

RT-qPCR

Total RNA was extracted with Qiagen RNeasy Mini kit and cDNA synthesis was performed as previously described[16] using SuperScript™ II Reverse Transcriptase from Invitrogen. PCR was amplified with iQ SYBR Green supermix (Bio-Rad) using previously described protocols and primers[16].

Western blot analysis

Total protein was extracted from fresh frozen tissue, using standard protocol with RIPA buffer. After quantification by Bradford assay, protein lysates were resolved on an 8% SDS-polyacrylamide gel and transferred to a nitrocellulose membrane. Anti-CTCF (1:1000; Cell signalling) and anti-β-ACTIN (1:7000; Sigma Alderich) were used for primary detection, followed by the appropriate horseradish peroxidase-conjugated secondary antibodies (1:4000; GE Healthcare Life Sciences). Protein was quantified using ImageJ software (version 1.47).

Brain perfusion for MRI and imaging

Mice were killed by CO_2 asphyxiation then perfused through the left ventricle of the heart with 30 mL of PBS (containing 1 µL/ mL heparin and 2mM ProHance) at a rate of 1.0 mL/ min. Then 30 mL of 4% PFA + 2 mM ProHance fixation was passed at same rate. After perfusion, the brain was left in the skull, but the zygomatic bones, eyes, and lower jaw were removed. The specimen was then placed in 20 mL of 4% PFA + 2 mM

ProHance overnight at 4˚C. The next day, the specimen was transferred into PBS + 0.02% sodium azide + 2 mM ProHance for storage.

Behavioural testing

From weaning age (21 days), mice were weighed and hind-limb clasping was measured on a weekly basis by a scorer who was blinded to genotype. Briefly, mice were suspended by the tail and lowered gently toward a solid flat surface. Wildtype mice, when suspended by the tail and descended towards a surface, will splay their limbs in anticipation of making contact, and this response was scored as non-clasping/ normal (0). Intermittent flexion in one or both limbs upon lowering was scored as 1, and frank clasping of hindlimb paws was scored as 2. Mice were considered as positive for clasping (score of 1 or 2) once the mouse showed clasping on at least three occasions.

Mouse cages were randomized to cohorts, and were tested in progressively demanding behavioural paradigms. Mice were tested in only one paradigm per day. Cohorts were assigned to one of two behavioural routines A) open-field, elevated plus maze, Y-maze, rotating rod, and MWM with probe trials, resident-intruder, and B) marble dig, social approach, social choice, MWM with reversal, and acoustic startle/ prepulse inhibition.

Open field was tested in low light conditions in a chamber 20 cm by 20 cm in size. Prior to starting, mice were acclimated to the room for 10 minutes. Mice were tracked using the AccuScan Instrument, and locomotor measures calculated over 5 minute intervals for two hours. To measure height-induced anxiety, we used the elevated plus maze in high light conditions. The total time spent in the open and closed arms was recorded over 5 minutes by the AnyMaze software. Spontaneous alteration was measured in the threearmed Y-maze. Mice were tracked using the AnyMaze software and an alternation was recorded when a mouse entered the three different arms without re-visiting a previous one.

To test motor learning, mice were placed on a rotating rod (Rotarod, San Diego Instruments), which was accelerated from a minimum speed of 5 to a maximum speed of 35 rpm, by 7.0 rpm per minute. Latency to fall was measured for 14 trials, 10 performed on the first day, and 4 performed on the 2nd day. Inter-trial duration on the same day was approximately 10 minutes, during which mice were placed in their home cage.

The MWM is a test of spatial learning and memory (reviewed in[70]). The MWM test was conducted in a 1.5 m diameter pool with 25˚C water, in dim lighting. Black and white shapes were placed on the walls of the room as spatial cues to find the platform which was submerged 0.5 cm beneath the water surface. Mice underwent 4 training sessions per day, each from different release points, for 4 days. The trial ended when the mouse found the platform. The maximum length per trial was 90 seconds, after which the mouse was gently guided to the platform and immobilized there for 10 seconds. The length of the four sessions was averaged per day and termed ‘latency to platform’. On the fifth day, mice underwent one probe trial lasting 60 seconds, in which the platform had been removed from the water. The total time spent in each quadrant was recorded using the AnyMaze software. Then, mice undergoing long-term spatial memory testing were housed for days 6-11 and underwent another probe trial on day 12. For mice undergoing the MWM-reversal paradigm, the platform was repositioned to the opposite quadrant and mice underwent four sessions per day on day 6 and 7.

Acoustic startle was measured as previously described[71]. Mice were placed in the chamber with background noise (65 db) for five minutes on days 1 and 2, to acclimatize the mice to the apparatus (SR-LAB, San Diego Instruments). On day 3, mice again were acclimated for 10 minutes with background noise and then underwent a habituation block, consisting of fifty acoustic startle trials, with 20 ms stimulus of 115 db, and intertrial interval of 20 seconds. After the habituation block, the mice underwent a prepulse-inhibition block consisting of ten sets of five types of trials randomly ordered with variable intertrial intervals of 10, 15, or 20 seconds. Four of the five trial types consisted of prepulses (intensity of 75 or 80 db, length of 20 ms), separated from the startle stimulus (intensity of 115 db, length of 40 ms) by an interstimulus interval of either 30 ms or 100 ms. The fifth trial type was a startle pulse alone. The startle response was measured by the mouse's movement on the platform, which generates a transient force analyzed by the software. The startle magnitude was an average for the ten trials of each trial type.

Marble burying was tested as previously described by others[74]. The marble burying assay was conducted under dim lighting conditions in a 32 x 43 cm cage was filled with 4 cm of corncob bedding with 25 evenly-spaced marbles. Mice were left in the cage for 30 minutes, after which the total number of buried marbles ($\geq$3/4 surface covered) were recorded.

For the social approach paradigm, mice underwent 2 days of habituation to a neutral cage, before being placed with a stranger conspecific, same-genotype mouse on the third day for 10 minutes. Among the male mice, we found there was one outlier among the controls which we excluded from the analysis. Time spent interacting (sniffing the other mouse), as well as time spent grooming and digging, was recorded for the test mouse by an observer blinded to genotype.

The three chamber social choice test was set up as follows: two chambers containing a cylindrical enclosure, separated by a middle neutral chamber. The test mouse was allowed to move freely between the three chambers during a 10 minute habituation phase, after which a conspecific wildtype stranger mouse was placed in one of the cylindrical enclosures, and a novel object was placed in the other. The test mouse was again allowed to explore the apparatus for 10 minutes, during which the time spent in the “novel object” and “stranger mouse” chambers were measured. To calculate sociability index, the time spent with the stranger mouse was divided by the sum of time spent with stranger mouse and novel object.

Aggression was tested using the resident-intruder paradigm[60] in male mice (typically female mice are insufficiently aggressive for testing). Male mice were housed alone for 21 days and then a group-housed, same age (4-month), wildtype male (intruder) was placed in the test mouse’s cage (resident). Mice were observed closely for up to 10 minutes in order to stop the test if the resident mouse attacked. Attack latency was recorded. There was no instance of an intruder mouse attacking the resident mouse.

rences:

1. Ghirlando, R. & Felsenfeld, G. CTCF: making the right connections. *Genes Dev.* **30,** 881–891 (2016).
2. Zuin, J. *et al.* Cohesin and CTCF differentially affect chromatin architecture and gene expression in human cells. *Proc. Natl. Acad. Sci.* **111,** 996–1001 (2014).

3. Moore, J. M. *et al.* Loss of maternal CTCF is associated with peri-implantation lethality of Ctcf null embryos. *PloS One* **7,** e34915 (2012).
4. Gregor, A. *et al.* De novo mutations in the genome organizer CTCF cause intellectual disability. *Am. J. Hum. Genet.* **93,** 124–131 (2013).
5. Bastaki, F. *et al.* Identification of a novel CTCF mutation responsible for syndromic intellectual disability – a case report. *BMC Med. Genet.* **18,** 68 (2017).
6. Juraeva, D. *et al.* Integrated Pathway-Based Approach Identifies Association between Genomic Regions at CTCF and CACNB2 and Schizophrenia. *PLOS Genet* **10,** e1004345 (2014).
7. Iossifov, I. *et al.* The contribution of de novo coding mutations to autism spectrum disorder. *Nature* **515,** 216–221 (2014).
8. Chisholm, K., Lin, A., Abu-Akel, A. & Wood, S. J. The association between autism and schizophrenia spectrum disorders: A review of eight alternate models of co-occurrence. *Neurosci. Biobehav. Rev.* **55,** 173–183 (2015).
9. McCarthy, S. E. *et al.* De novo mutations in schizophrenia implicate chromatin remodeling and support a genetic overlap with autism and intellectual disability. *Mol. Psychiatry* **19,** 652–658 (2014).
10. St Pourcain, B. *et al.* ASD and schizophrenia show distinct developmental profiles in common genetic overlap with population-based social communication difficulties. *Mol. Psychiatry* (2017). doi:10.1038/mp.2016.198
11. Diagnostic and statistical manual of mental disorders : DSM-5. - NLM Catalog - NCBI. Available at: https://www-ncbi-nlm-nih-gov.proxy1.lib.uwo.ca/nlmcatalog/101604226. (Accessed: 6th March 2017)

12. Davis, J. *et al.* A review of vulnerability and risks for schizophrenia: Beyond the two hit hypothesis. *Neurosci. Biobehav. Rev.* **65,** 185–194 (2016).
13. Jones, C., Watson, D. & Fone, K. Animal models of schizophrenia. *Br. J. Pharmacol.* **164,** 1162–1194 (2011).
14. Powell, C. M. & Miyakawa, T. Schizophrenia-Relevant Behavioral Testing in Rodent Models: A Uniquely Human Disorder? *Biol. Psychiatry* **59,** 1198–1207 (2006).
15. Silverman, J. L., Yang, M., Lord, C. & Crawley, J. N. Behavioural phenotyping assays for mouse models of autism. *Nat. Rev. Neurosci.* **11,** 490–502 (2010).
16. Watson, L. A. *et al.* Dual Effect of CTCF Loss on Neuroprogenitor Differentiation and Survival. *J. Neurosci.* **34,** 2860–2870 (2014).
17. Hirayama, T., Tarusawa, E., Yoshimura, Y., Galjart, N. & Yagi, T. CTCF is required for neural development and stochastic expression of clustered Pcdh genes in neurons. *Cell Rep.* **2,** 345–357 (2012).
18. Sams, D. S. *et al.* Neuronal CTCF Is Necessary for Basal and Experience-Dependent Gene Regulation, Memory Formation, and Genomic Structure of BDNF and Arc. *Cell Rep.* **17,** 2418–2430 (2016).
19. Lalonde, R. & Strazielle, C. Brain regions and genes affecting limb-clasping responses. *Brain Res. Rev.* **67,** 252–259 (2011).
20. Di Virgilio, G., Clarke, S., Pizzolato, G. & Schaffner, T. Cortical regions contributing to the anterior commissure in man. *Exp. Brain Res.* **124,** 1–7 (1999).
21. Javitt, D. C. & Freedman, R. Sensory Processing Dysfunction in the Personal Experience and Neuronal Machinery of Schizophrenia. *Am. J. Psychiatry* **172,** 17–31 (2014).

22. Lee, Y. & Davis, M. Role of the hippocampus, the bed nucleus of the stria terminalis, and the amygdala in the excitatory effect of corticotropin-releasing hormone on the acoustic startle reflex. *J. Neurosci. Off. J. Soc. Neurosci.* **17,** 6434–6446 (1997).
23. Hilakivi-Clarke, L. A. & Lister, R. G. The role of body weight in resident-intruder aggression. *Aggress. Behav.* **18,** 281–287 (1992).
24. Giusti, S. A. *et al.* Behavioral phenotyping of Nestin-Cre mice: Implications for genetic mouse models of psychiatric disorders. *J. Psychiatr. Res.* **55,** 87–95 (2014).
25. Kaur, M. *et al.* NIPBL expression levels in CdLS probands as a predictor of mutation type and phenotypic severity. *Am. J. Med. Genet. C Semin. Med. Genet.* **172,** 163–170 (2016).
26. Kawauchi, S. *et al.* Multiple Organ System Defects and Transcriptional Dysregulation in the Nipbl +/− Mouse, a Model of Cornelia de Lange Syndrome. *PLoS Genet.* **5,** (2009).
27. Remeseiro, S. *et al.* Reduction of Nipbl impairs cohesin loading locally and affects transcription but not cohesion-dependent functions in a mouse model of Cornelia de Lange Syndrome. *Biochim. Biophys. Acta BBA - Mol. Basis Dis.* **1832,** 2097–2102 (2013).
28. Borck, G. *et al.* Father-to-daughter transmission of Cornelia de Lange syndrome caused by a mutation in the 5′ untranslated region of the NIPBL Gene. *Hum. Mutat.* **27,** 731–735 (2006).
29. Liu, J. *et al.* Transcriptional Dysregulation in NIPBL and Cohesin Mutant Human Cells. *PLOS Biol.* **7,** e1000119 (2009).

30. Breuss, M. *et al.* Mutations in the murine homologue of TUBB5 cause microcephaly by perturbing cell cycle progression and inducing p53-associated apoptosis. *Development* **143,** 1126–1133 (2016).

31. Liu, H., Fan, G., Xu, K. & Wang, F. Changes in cerebellar functional connectivity and anatomical connectivity in schizophrenia: A combined resting-state functional MRI and diffusion tensor imaging study. *J. Magn. Reson. Imaging* **34,** 1430–1438 (2011).

32. Bottmer, C. *et al.* Reduced cerebellar volume and neurological soft signs in first-episode schizophrenia. *Psychiatry Res. Neuroimaging* **140,** 239–250 (2005).

33. Thomann, P. A. *et al.* Cerebellar substructures and neurological soft signs in first-episode schizophrenia. *Psychiatry Res. Neuroimaging* **173,** 83–87 (2009).

34. Andreasen, N. C., Paradiso, S. & O'Leary, D. S. 'Cognitive dysmetria' as an integrative theory of schizophrenia: a dysfunction in cortical-subcortical-cerebellar circuitry? *Schizophr. Bull.* **24,** 203–218 (1998).

35. Fusar-Poli, P. *et al.* Functional atlas of emotional faces processing: a voxel-based meta-analysis of 105 functional magnetic resonance imaging studies. *J. Psychiatry Neurosci. JPN* **34,** 418–432 (2009).

36. Critchley, H. Explicit and implicit neural mechanisms for processing of social information from facial expressions: A functional magnetic resonance imaging study. *Hum. Brain Mapp.* **9,** 93–105

37. Kana, R. K. *et al.* Aberrant functioning of the theory-of-mind network in children and adolescents with autism. *Mol. Autism* **6,** 59 (2015).

38. Goddyn, H., Leo, S., Meert, T. & D’Hooge, R. Differences in behavioural test battery performance between mice with hippocampal and cerebellar lesions. *Behav. Brain Res.* **173,** 138–147 (2006).
39. Lalonde, R., Bensoula, A. N. & Filali, M. Rotorod sensorimotor learning in cerebellar mutant mice. *Neurosci. Res.* **22,** 423–426 (1995).
40. Bardgett, M. E. *et al.* NMDA receptor blockade and hippocampal neuronal loss impair fear conditioning and position habit reversal in C57Bl/6 mice. *Brain Res. Bull.* **60,** 131–142 (2003).
41. Deacon, R. M. J., Bannerman, D. M., Kirby, B. P., Croucher, A. & Rawlins, J. N. P. Effects of cytotoxic hippocampal lesions in mice on a cognitive test battery. *Behav. Brain Res.* **133,** 57–68 (2002).
42. Torremans, A. *et al.* GSA: behavioral, histological, electrophysiological and neurochemical effects. *Physiol. Behav.* **84,** 251–264 (2005).
43. Bannerman, D. M., Lemaire, M., Beggs, S., Rawlins, J. N. & Iversen, S. D. Cytotoxic lesions of the hippocampus increase social investigation but do not impair social-recognition memory. *Exp. Brain Res.* **138,** 100–109 (2001).
44. Joyal, C. C., Strazielle, C. & Lalonde, R. Effects of dentate nucleus lesions on spatial and postural sensorimotor learning in rats. *Behav. Brain Res.* **122,** 131–137 (2001).
45. Fenlon, L. R. *et al.* Formation of functional areas in the cerebral cortex is disrupted in a mouse model of autism spectrum disorder. *Neural Develop.* **10,** 10 (2015).
46. Di Martino, A. *et al.* The autism brain imaging data exchange: towards a large-scale evaluation of the intrinsic brain architecture in autism. *Mol. Psychiatry* **19,** 659–667 (2014).

47. Ellegood, J. *et al.* Clustering autism - using neuroanatomical differences in 26 mouse models to gain insight into the heterogeneity. *Mol. Psychiatry* **20,** 118–125 (2015).
48. Yoon, J. H. *et al.* Association of dorsolateral prefrontal cortex dysfunction with disrupted coordinated brain activity in schizophrenia: relationship with impaired cognition, behavioral disorganization, and global function. *Am. J. Psychiatry* **165,** 1006–1014 (2008).
49. Lawrie, S. M. *et al.* Reduced frontotemporal functional connectivity in schizophrenia associated with auditory hallucinations. *Biol. Psychiatry* **51,** 1008–1011 (2002).
50. Jamain, S. *et al.* Reduced social interaction and ultrasonic communication in a mouse model of monogenic heritable autism. *Proc. Natl. Acad. Sci.* **105,** 1710–1715 (2008).
51. Tsai, P. T. *et al.* Autistic-like behaviour and cerebellar dysfunction in Purkinje cell Tsc1 mutant mice. *Nature* **488,** 647–651 (2012).
52. Katayama, Y. *et al.* CHD8 haploinsufficiency results in autistic-like phenotypes in mice. *Nature* **advance online publication,** (2016).
53. Kazdoba, T. M., Leach, P. T. & Crawley, J. N. Behavioral phenotypes of genetic mouse models of autism. *Genes Brain Behav.* **15,** 7–26 (2016).
54. Schmeisser, M. J. *et al.* Autistic-like behaviours and hyperactivity in mice lacking ProSAP1/Shank2. *Nature* **486,** 256–260 (2012).
55. Schoch, H. *et al.* Sociability Deficits and Altered Amygdala Circuits in Mice Lacking Pcdh10, an Autism Associated Gene. *Biol. Psychiatry* doi:10.1016/j.biopsych.2016.06.008
56. Horvitz, J. C. Mesolimbocortical and nigrostriatal dopamine responses to salient non-reward events. *Neuroscience* **96,** 651–656 (2000).

57. Arnsten, A. F. T. Stress signalling pathways that impair prefrontal cortex structure and function. *Nat. Rev. Neurosci.* **10,** 410–422 (2009).
58. Papaleo, F. *et al.* Genetic Dissection of the Role of Catechol-O-Methyltransferase in Cognition and Stress Reactivity in Mice. *J. Neurosci. Off. J. Soc. Neurosci.* **28,** 8709–8723 (2008).
59. Barkus, C. *et al.* What causes aberrant salience in schizophrenia? A role for impaired short-term habituation and the GRIA1 (GluA1) AMPA receptor subunit. *Mol. Psychiatry* **19,** 1060–1070 (2014).
60. El-Kordi, A. *et al.* Development of an autism severity score for mice using Nlgn4 null mutants as a construct-valid model of heritable monogenic autism. *Behav. Brain Res.* **251,** 41–49 (2013).
61. Milenkovic, M., Mielnik, C. A. & Ramsey, A. J. NMDA receptor-deficient mice display sexual dimorphism in the onset and severity of behavioural abnormalities. *Genes Brain Behav.* **13,** 850–862 (2014).
62. Beery, A. K. & Zucker, I. Sex bias in neuroscience and biomedical research. *Neurosci. Biobehav. Rev.* **35,** 565–572 (2011).
63. Abel, K. M., Drake, R. & Goldstein, J. M. Sex differences in schizophrenia. *Int. Rev. Psychiatry Abingdon Engl.* **22,** 417–428 (2010).
64. Werling, D. M. & Geschwind, D. H. Sex differences in autism spectrum disorders. *Curr. Opin. Neurol.* **26,** 146 (2013).
65. Fink, G., Sumner, B. E., Rosie, R., Grace, O. & Quinn, J. P. Estrogen control of central neurotransmission: effect on mood, mental state, and memory. *Cell. Mol. Neurobiol.* **16,** 325–344 (1996).

66. Crider, A. & Pillai, A. Estrogen Signaling as a Therapeutic Target in Neurodevelopmental Disorders. *J. Pharmacol. Exp. Ther.* **360,** 48–58 (2017).
67. Dias, C. *et al.* BCL11A Haploinsufficiency Causes an Intellectual Disability Syndrome and Dysregulates Transcription. *Am. J. Hum. Genet.* **99,** 253–274 (2016).
68. Bérubé, N. G. *et al.* The chromatin-remodeling protein ATRX is critical for neuronal survival during corticogenesis. *J. Clin. Invest.* **115,** 258–267 (2005).
69. Heath, H. *et al.* CTCF regulates cell cycle progression of αβ T cells in the thymus. *EMBO J.* **27,** 2839–2850 (2008).
70. D'Hooge, R. & De Deyn, P. P. Applications of the Morris water maze in the study of learning and memory. *Brain Res. Brain Res. Rev.* **36,** 60–90 (2001).
71. Valsamis, B. & Schmid, S. Habituation and Prepulse Inhibition of Acoustic Startle in Rodents. *J. Vis. Exp. JoVE* (2011). doi:10.3791/3446
72. Akdag, S. J. *et al.* The startle reflex in schizophrenia: habituation and personality correlates. *Schizophr. Res.* **64,** 165–173 (2003).
73. Koch, M. The neurobiology of startle. *Prog. Neurobiol.* **59,** 107–128 (1999).
74. Deacon, R. M. J. Digging and marble burying in mice: simple methods for in vivo identification of biological impacts. *Nat. Protoc.* **1,** 122–124 (2006).

Chapter 4

cussion

General overview

ID, ASD and SCZ are heterogeneous disorders with related etiology. Gene-mutation of factors regulating chromatin architecture can cause these disorders, indicating this mechanism of regulation is of particular importance to brain development. CTCF is a ubiquitous chromatin-organizing protein that mainly regulates gene expression through chromatin looping. Mutations in one copy of the *CTCF* gene were found to cause ID and ASD, and *CTCF* has also been associated with SCZ, demonstrating the important role for this factor in neurodevelopment. Despite this, there have been only a handful of studies investigating the function of CTCF in the brain.

The goal of this study was to investigate the role of CTCF in early brain development and potential consequences in the postnatal brain. Conditional whole-brain and MGE-specific *Ctcf* knockout mouse models were generated using the *NestinCre* and *Nkx2.1Cre* driver lines, respectively. This is the first study to show that CTCF is an important upstream regulator of cortical interneuron fate specification, which is highly relevant to disease, given that dysfunction of these neurons has been reported in ID, ASD, and SCZ. I also provide insight into the transcriptional dysregulation that mechanistically links altered chromatin higher order structure and neurodevelopmental disorders. In the second arm of this study, the outcome of *Ctcf* heterozygosity was examined in the mouse brain, which uniquely models the human ID syndrome. I characterized the behaviour and brain structure of these *Ctcf*-deficient mice, which phenotypically resemble those of other mouse models of ID, ASD and SCZ.

role of CTCF in MGE development

The deletion of *Ctcf* from the developing brain using the *NestinCre* driver line resulted in reduced expression of genes with ontology implicated in interneuron development. By deleting *Ctcf* specifically from the MGE using the *Nkx2.1Cre* driver, I create an elegant model in which we could explore the cell-autonomous effects of *Ctcf* loss from this region. In addition, as these conditional *Ctcf* mutants survive into the postnatal period, this allowed us to study the outcome of *Ctcf* loss on the final laminar position and subtype specification of the cortical interneurons.

As with whole-brain loss of *Ctcf,* the deletion of *Ctcf* from the MGE led to decreased expression of *Lhx6.* As the LHX6 transcription factor has been well-established as required for the generation of PV and SST cortical interneurons, it is unsurprising that we saw a corresponding decrease in the numbers of these interneuron subtypes in the P21 *Ctcf* conditional mutant. We also saw a decrease in the number of MGE-derived migrating cortical interneurons during development (E16.5), but by P21, there are a similar number of GABAergic cells in the cortex of the *Ctcf* conditional mutant. This is most likely explained by a combination of two things: i) *Lhx6* is known for regulating multiple factors involved in migration, so migration is impaired or inefficient, and ii) the MGE-derived cells partially adopt the default fate of CGE-derived interneurons, which are known to migrate later into the developing cortex. In support of this second explanation, the interneurons occupied more superficial laminar positions consistent with CGE-derived interneuron behaviour. Defaulting to a CGE-derived fate is closely linked to LHX6 function; interneurons from *Lhx6* and *Nkx2.1* mutants have been shown to not only occupy superficial laminar layers, but also to have CGE-like morphology, electrophysiology, and express CGE markers[1,2]. Together, this shows that CTCF is an important regulator of the transcriptional pathway that allows deviation from the default CGE-derived interneuron fate in order to generate MGE-derived PV and SST interneurons.

Transduction of *Lhx6* into *Ctcf*-null MGE cells was sufficient to rescue MGE-like laminar position and interneuron subtype, suggesting CTCF functions upstream of LHX6 in the MGE. Expression of NKX2.1 was unperturbed in the *Ctcf*-null brains, and we did not find any evidence of interaction between NKX2.1 and CTCF. One possibility is that in the absence of CTCF, chromatin architecture is not permissive for NKX2.1 binding at LHX6. Additional studies will be required to precisely uncover how CTCF affects chromatin structure and gene expression in the MGE.

I found that CTCF not only controls MGE versus CGE fate of cortical interneurons. When I deleted CTCF from the developing MGE, there was a concomitant increase in *Lhx8*, which encodes a transcription factor with shared and distinct functions from LHX6. LHX8 overlaps with LHX6 in some of its down-stream effectors, as demonstrated by the partial rescue of PV and SST interneuron numbers with *Lhx8* transduction into *Lhx6*-mutant MGE cells[2]. So one possibility is that *Lhx8* becomes over-activated as part of a compensatory mechanism with the loss of *Lhx6* in the *Ctcf* mutant MGE. However, re-expression of *Lhx6* did not normalize the level of *Lhx8* transcript, suggesting that *Lhx8* is regulated separately by CTCF.

I showed that CTCF regulates the dichotomy between Lhx6 and Lhx8 expression, but the mechanistic link between CTCF, Lhx6 and Lhx8 remains unknown. I found CTCF binding at the *Lhx8* gene. A few remaining questions are whether CTCF binds at the *Lhx8* gene to place it in a repressive loop in certain cells, and whether over-expression of *Lhx8* causes decreased *Lhx6* expression, as LIM proteins are known to regulate each other. It is possible that deregulation of *Lhx8* with loss of CTCF may be the upstream cause of *Lhx6* inactivation. Since GABAergic striatal neurons co-express *Lhx6* and *Lhx8,* it is unlikely that LHX8 would directly inhibit *Lhx6*, but may act through another factor. There are no models of LHX8 over-expression reported in the literature. It would be interesting to further characterize the consequences of its over-expression, namely whether the increased number of basal forebrain projection neurons persists post-natally.

I observed an increase in the number of basal forebrain projection neurons, suggesting that the imbalance between *Lhx6* and *Lhx8* in the *Ctcf*-null MGE results in some MGE cells becoming re-specified to basal forebrain projection neurons. This likely occurs at the expense of cortical interneurons, however as the total number of basal forebrain projection neurons represents a small population, even large increases in the numbers of these cells is not likely to be sufficient to significantly impact the total number of cortical interneurons by our quantification methods, representing a limitation of the current model.

Future studies in the MGE may examine how a decreased amount of CTCF may alter chromatin organization, or make its three dimensional structure less stable, and more vulnerable to secondary environmental or genetic insults. The idea that the developmental cascade specifying the MGE may be more vulnerable to stressors is easy to reconcile with the hypothesis that it is a deviation from the default transcriptional profile which would specify CGE fate. There have been a few reports investigating the transcriptional profiles of MGE cells, with the goal of understanding the large diversity of cells generated in this transient organ[3,4]. Future studies may compare CGE and MGE transcriptional profiles and chromatin organization.

lications to disease treatment

There has been interest in using GABAergic interneurons as a cell-based therapy in human neurologic disease[21]. Studies in mice show that upon transplantation into a mature host brain, GABAergic interneurons retain the ability to laminate into appropriate layers and functionally integrate into circuits[22,23]. In models of epilepsy, the transplantation of MGE progenitors into the mature hippocampus or visual cortex reduced seizure frequency and severity about 3-4 weeks after surgery[24–26] and these benefits persisted even 6 months after transplantation[24]. Given that cortical interneuron dysfunction and imbalances in excitation-inhibition are implicated in ID, SCZ, and ASD (section 1.3.5), there has been a great momentum to understand how to differentiate these cells *in vitro* from pluripotent cells. Understanding the development of the transplanted cells is required to prevent possible inappropriate differentiation, proliferation or migration of grafts. Our results designate CTCF as a novel regulator of interneuron genesis, and therefore can contribute to future efforts to improve the *in vitro* generation of interneurons from stem cells.

Recently, protocols were developed for deriving functionally mature cortical interneurons from human induced pluripotent stem cells (hiPSCs) and human embryonic stem cells (hESCs) [27,28]. In addition to potential use as grafts, development of cortical interneurons from hiPSCs or hESCs permits the generation of large homogeneous populations of cells that can be used for modeling neurological disorders and testing novel drugs *in vitro*[29].

One difficulty with deriving cortical interneurons is the lengthy maturation time the cells must undergo[29]. Optimizing levels of CTCF protein levels may be used to push MGE-derived cells down a desired lineage, and may help decrease human interneuron maturation times by more quickly inducing chromatin conformations required for specifying interneuron cell fate.

itations of study of CTCF in MGE

It has been difficult to study the role of CTCF in gene regulation because its deletion causes cell death in so many tissues. We circumvented cell death in the *NestinCre*-mediated *Ctcf* knockout embryos by concomitant deletion of *Puma*, but these mice still died at birth. Mice survived longer with the loss of *Ctcf* from the MGE, but eventually succumbed to hypothyroidism, likely due to *Nkx2.1Cre* expression in the thyroid. We presume that CTCF deletion from the thyroid results in extensive cell death, as with other tissues[11,70,71]. This limited our study of these mice to weaning age. The adult pattern of cortical interneuron laminar positioning is well established by this time-point, but networks are not fully matured until about P30[2], therefore we could not test the functionality of *Ctcf*-null cortical interneurons. In future studies, this limitation could be overcome by testing transplanted *Ctcf*-null MGE cells in wildtype mouse brain, by performing *in utero* electroporation of the MGE with *Ctcf* shRNA, or by treating *Nkx2.1Cre Ctcf*-null mice with thyroxine.

dity of the *Ctcf*$^{\text{Nestinhet}}$ mice as a model of the associated human syndrome and SCZ

There are several well-established rodent models of SCZ that have allowed the establishment of the murine behaviours which best represent symptoms of SCZ including

1) spontaneous locomotor hyperactivity, which is thought to emulate the delusions/ hallucinations seen in humans; 2) sensorimotor gating deficits; 3) reduced re-learning, which represents cognitive inflexibility or impairment; 4) Deficits in social interaction. A similar constellation of behaviours contributes to the face validity of ASD mouse models to the human disorder, including social deficits and repetitive behaviours[30]. Additional associated behaviours are often present, and can include cognitive inflexibility, anxiety, hyperactivity, and altered sensory reactivity.

Table 1 summarizes the behavioural differences identified in *Ctcf*$^{\mathrm{Nestinhet}}$ mice. *Ctcf*$^{\mathrm{Nestinhet}}$ mice have hyperactivity and impaired spatial learning. In addition, male *Ctcf*$^{\mathrm{Nestinhet}}$ mice had decreased anxiety and altered social behaviour. Spontaneous locomotor hyperactivity is often seen in SCZ mouse models (section 1.4.1). Impaired spatial learning is typically associated with mouse models of ID, and decreased sociability is phenotypic of ASD and SCZ models (section 1.4.1). Therefore *Ctcf*$^{\mathrm{Nestinhet}}$ mice do show face validity to the associated human syndrome. One surprise is that we did not see an increase in repetitive behaviours, which is robustly observed in ASD mouse models. However, not all patients with CTCF mutation are described as autistic, and one possibility is that stereotypies are not a predominant feature of the human syndrome.

male brain is more susceptible to neurological perturbation

We observed more severe and additional behaviour defects in male *Ctcf*$^{\mathrm{Nestinhet}}$ mice than females. This is consistent with others who have found that male mice tend to be more sensitive to neurological perturbation and have more robust impairments[31,32]. This is why female mice are commonly excluded from behavioural and neurobiological studies (reviewed in [33]).

Table 1: Summary of *Ctcf*^{Nestinhet} behaviours

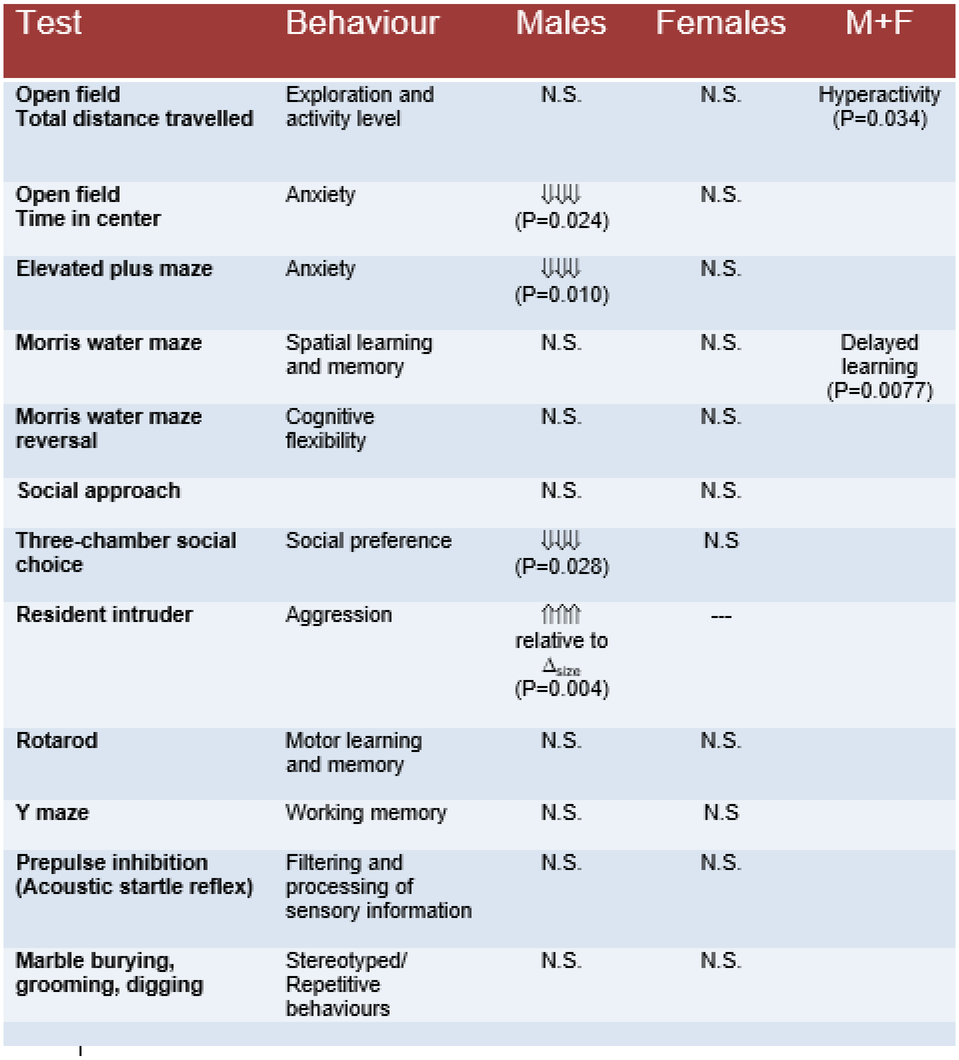

Test	Behaviour	Males	Females	M+F
Open field **Total distance travelled**	Exploration and activity level	N.S.	N.S.	Hyperactivity (P=0.034)
Open field **Time in center**	Anxiety	⇓⇓⇓ (P=0.024)	N.S.	
Elevated plus maze	Anxiety	⇓⇓⇓ (P=0.010)	N.S.	
Morris water maze	Spatial learning and memory	N.S.	N.S.	Delayed learning (P=0.0077)
Morris water maze reversal	Cognitive flexibility	N.S.	N.S.	
Social approach		N.S.	N.S.	
Three-chamber social choice	Social preference	⇓⇓⇓ (P=0.028)	N.S	
Resident intruder	Aggression	⇑⇑⇑ relative to Δ_{size} (P=0.004)	---	
Rotarod	Motor learning and memory	N.S.	N.S.	
Y maze	Working memory	N.S.	N.S	
Prepulse inhibition (Acoustic startle reflex)	Filtering and processing of sensory information	N.S.	N.S.	
Marble burying, grooming, digging	Stereotyped/ Repetitive behaviours	N.S.	N.S.	

Both SCZ and ASD have higher incidence in males[34,35]. Estrogen has been suggested as having protective effects on the brain[36], particularly from neurodevelopmental insults, through its influence on gene expression and cell excitability (reviewed in [37]). We observed a sociability deficit in male *Ctcf*$^{\text{Nestinhet}}$ mice but not females. In SCZ, it has been reported that negative symptoms (such as social withdrawal) are less severe in females[38]. In regards to the association of *CTCF* with SCZ, it remains unclear whether the association was stronger in males than females[17]. Males and females with syndrome-causing mutations in the *CTCF* gene have been identified at similar rates[6,13,14].

phenotype of *Ctcf*$^{\text{Nestinhet}}$ mice resemble other mutant mouse models of chromatin factors

Upon reviewing the literature, we identified other mice with a similar profiles to *Ctcf*$^{\text{Nestinhet}}$ mice, which surprisingly are implicated in chromatin regulation. *Ctcf*$^{\text{Nestinhet}}$ mice share many behavioural deficits with mice heterozygous for *Bcl11a* deletion, which functions in the Baf swi/snf chromatin-remodelling complex, suggesting there may be overlap in the transcriptional networks regulated by CTCF and BCL11A[39]. In humans, *BCL11A* gene mutation causes Dias-Logan syndrome, which has microcephaly and ID as core features, with 30% of patients also having ASD. Interestingly, some of the patients with this syndrome are reported to have cerebellar vermis hypoplasia, hypoplasia of the corpus callosum and decreased white matter volume[39], some of which are features of the *Ctcf*$^{\text{Nestinhet}}$ mice on MRI. When normalized for brain volume, there were decreases in *Bcl11a +/-* mice in the volumes of the hippocampus (all areas except the dentate gyrus), corpus callosum, amygdaloid nuclei, ventral midline thalamic nuclei, and parts of the cerebellum, which has extensive overlap with what we observe in *Ctcf*$^{\text{Nestinhet}}$ mice. This overlap in the human syndrome, the mouse model behaviour, and the brain structure suggests that CTCF and BCL11A likely regulate the same transcriptional networks.

Mutation of *BCL11B,* the homolog of *BCL11A,* also known as *CTIP2,* causes immunodeficiency and ID[40], and has been implicated in postnatal development of the dentate gyrus[41]. Forebrain ablation of *Bcl11b* in mice using *Emx1Cre* resulted in a reduction in granular cell number, resulting in a smaller dentate gyrus[41]. These mice had impaired spatial learning and memory, and hyperactivity. In addition, a patient with *BCL11B* mutation had agenesis of the corpus callosum (the largest white matter structure in the brain). In *Ctcf*$^{\text{Nestinhet}}$ mice, we observed decreased volumes of the anterior commissure, a white matter tract. but there was an increased volume in the dentate gyrus of the hippocampi. However it is possible that there would be more overlap of *Ctcf*$^{\text{Nestinhet}}$ mice with mice that are heterozygous for *Bcl11b* in the forebrain, instead of those with complete ablation. In support of this, complete ablation of *Ctcf* from the postnatal hippocampus causes widespread apoptosis at 14 weeks, a very different phenotype from that observed in *Ctcf*$^{\text{Nestinhet}}$ mice.

Mice mutant for the *Cbp* gene, which is associated with Rubinstein-Taybi syndrome, have many behavioural abnormalities[42], some of which overlap with *Ctcf*$^{\text{Nestinhet}}$ mice. The *Cbp* mutant mouse behaviours include repetitive behaviours, hyperactivity, social deficits, decreased anxiety, impaired nest building, increased aggression, impaired motor function and impaired long-term memory[42]. With the exception of spatial learning, which was not assessed in these mice, they have all the features of *Ctcf*$^{\text{Nestinhet}}$ male mice and more. Notably, mice heterozygous for *p300* deletion, despite also being a model of Rubinstein-Taybi syndrome, do not share these same behaviours[43]. This suggests that like BCL11A, the transcriptional targets of CBP also likely overlap with those of CTCF. This reaffirms the newer consensus opinion about CTCF, which is that its function in promoting enhancer-promoter interactions is more relevant than its role as a genetic insulator. Future studies should compare the transcriptomes from brain-relevant samples of these mutant mice. There is also a possibility that there may be cooperation between CBP and CTCF in gene regulation.

n structure of the *Ctcf*$^{\text{Nestinhet}}$ mice and further evidence for the cerebellum in cognition

MRI revealed volume changes in multiple limbic structures of the *Ctcf*$^{\text{Nestinhet}}$ brain. These structures may be involved in emotional processing and social functioning. We also measured a decrease in the volumes of the deep cerebellar nuclei, and an increase in the anterior lobe of the cerebellum. Although traditionally associated with balance, motor control and motor learning, the cerebellum now has an emerging role in cognition; the same processing that allows for the cerebellum to automate motor tasks is relevant to automating thoughts and implicit cognitive processes[47].

The cerebellum regulates the rest of the brain though the cerebello-thalamo-cortical pathway, and defects in this circuit at both the cerebellum and thalamus have been implicated in the cognitive dysmetria (difficulty in processing, prioritizing and responding to information) observed in SCZ[48–51]. Liu et al [48] found evidence for damage to cerebellum itself in 10 schizophrenia patients compared to controls. In ASD, deficits in the ability to implicitly process non-verbal and social cues may be related to cerebellar defects, as functional MRI has demonstrated cerebellar activity during the processing of emotional facial expressions[52,53]. Links between ASD and the cerebellum have been reviewed extensively, and include altered cerebellar volumes and Purkinje cell numbers in subjects ASD compared to controls [47,54,55]. Theory-of-mind tasks have noted functional hypoconnectivity in ASD between medial cortex and cerebellum[56]. In addition, individuals with ASD do not activate the left cerebellum like controls, when implicitly processing emotional facial expressions[57].

An ASD mouse model in which *Tsc1* is deleted from cerebellar Purkinje cells leads to abnormal social interaction, impaired MWM reversal, and repetitive behaviour[58]. Cerebellum-lesioned mice have increased latencies to target in MWM, and this has been correlated with size of the lesion[59]. Cerebellum-lesioned rodents show tapered reductions in latency to target platform compared to control, reminiscent to *Ctcf*$^{\text{Nestinhet}}$ mice, and show no or mild defects in target location memory retention[59–63]. Specific lesion of the cerebellar dentate nuclei bilaterally in rats can cause this spatial learning deficit pattern[62]. Thus the pattern of learning deficit observed *Ctcf*$^{\text{Nestinhet}}$ mice may be more consistent with impairments in cerebellar function than with that of hippocampus[59,64,65]. This likely reflects a role for the dentate nuclei in the cognitive processes in MWM acquisition, without affecting memory retention.

I observed increases in the volume of the hippocampal dentate gyrus in the *Ctcf*$^{\text{Nestinhet}}$ mice. This could be caused by an increase in grey matter in this region, but will require further elucidation in the future. It may represent a compensation for having impaired spatial learning due to cerebellar defects, as increased grey matter volumes in the hippocampus have been associated with improved spatial sense[66]. Alternatively, increased dentate gyrus volume may result from altered densities of cell subpopulations as a direct result of decreased CTCF.

re investigation of GABAergic neurons in *Ctcf*$^{\text{Nestinhet}}$ mice

Despite the role for *Ctcf* in the development of interneurons, we did not investigate the numbers and positioning of cortical interneurons in the *Ctcf* haploinsufficiency model, which may provide relevant insight into the mechanistic links of CTCF to human ID, ASD and SCZ. We expect that cortical interneuron development and/ or function is abnormal with loss of one functional copy of *Ctcf*.

It would also be interesting to determine whether there is an increase in the number of GABAergic basal forebrain projection neurons in the *Ctcf* haploinsufficiency model. Clinical and animal studies have linked the basal forebrain with abnormal aggression (reviewed in [67]). In addition, the valence of aggressive behaviour in the resident-intruder paradigm has been linked to GABAergic projection neurons from the basal forebrain to the lateral habenula[68]. It is possible that the abnormal aggression observed in the *Ctcf*$^{\mathrm{Nestinhet}}$ mice is related to an increased number of GABAergic basal forebrain projection neurons. In addition, rats with higher numbers of basal forebrain GABAergic projection neurons perform worse on spatial learning tasks[69], an impairment we observed in the *Ctcf*$^{\mathrm{Nestinhet}}$ mice.

itation of the *Ctcf* haploinsufficiency mouse model

Our study of mice heterozygous for *Ctcf* in the brain was complicated by effects of the *NestinCre* transgene. The *NestinCre* driver mice have mild hypopituitarism and postnatal growth retardation, due to insertion of the human growth hormone gene with the *NestinCre*, which down-regulates the mouse growth hormone gene and causes decreased levels of *Igf-1*[72]. Male *NestinCre* mouse behaviour is grossly normal, but it has been reported that the *NestinCre* mice spend less time freezing in contextual and cued fear conditioning paradigms[73]. The *NestinCre* mice also spent significantly less time in the open arms of the elevated plus maze, suggesting the decreased freezing time is not due to decreased anxiety, but due to impaired fear memory acquisition. Of note, spatial memory acquisition was not significantly different in *NestinCre* mice. In addition, mice with increased hypothalamic growth hormone receptor signaling, like *NestinCre* mice, typically have reduced anxiety, which is inconsistent with the findings of Giusti et al [73]. Therefore, it is difficult to reconcile these and our findings.

Despite having grossly normal behaviour, in our study we observed increased hind-limb clasping due to the *NestinCre* transgene, which suggests neurological function is abnormal. Due to previous extensive behavioural phenotyping of the *NestinCre* mice, we did not use them as a behavioural control in our study, which in hindsight may limit the interpretation of some of the findings. We also did not use the *NestinCre* mice as a control for the structural MRI study, which is another limitation. Others have reported that *NestinCre* mice have reduced brain volumes similar to our *Ctcf* haploinsufficiency model but no other brain structure abnormalities were reported[74].

4.11 Implications

De novo, disrupting mutations in regulators of chromatin architecture are frequent causes of ASD and severe ID[5–7], suggesting that chromatin structure is an important regulatory mechanism of gene expression particularly in the brain. CdLS and Mediator-related syndromes were described as “transcriptomopathies”[8,9], that is a disease caused by global alteration of gene expression. As these complexes are also involved in chromatin looping, the syndromes caused by *CTCF* mutations likely have altered transcriptome as a shared etiology (reviewed in [10]). Although the ASD/ ID syndromes caused by mutation of the individual genes are distinct, there are multiple shared features and the commonly affected molecular pathways remain poorly understood. Therefore, characterizing the transcriptional pathways that are altered with CTCF loss from the brain is an important step in understanding this group of disorders. Previous work characterizing the transcriptional pathways regulated by CTCF in the brain have implicated it in neuroprogenitor survival through PUMA regulation[11], and neuron connectivity through the activation of *Pcdh* gene clusters[12]. My study advances our understanding by i) identifying a role for CTCF in MGE development, and ii) generating a mouse model of *Ctcf* loss with behavioural and brain structural changes congruent with *CTCF*-related disorders that can be used for further study.

CTCF has been associated with SCZ[17], which shares etiology with ASD[18,19]. This finding has not yet been replicated, but the dysregulation of interneuron development, the hyponnectivity, and the behaviour profile of *Ctcf* mutant mice in our study are consistent with a possible role in SCZ. It is possible that disrupting mutations of *CTCF* cause ASD/ID whereas polymorphisms influencing small or regional/timing-specific changes in expression of *CTCF* predispose to SCZ, along with other environmental and genetic factors. Intriguingly, maternal immune activation (MIA), commonly utilized to generate a SCZ rat model, caused altered expression of genes implicated in cortical interneuron migration[20], implying the transcriptional pathways regulating these cells may be particularly vulnerable. I am the first to show that CTCF is a required upstream regulator in cortical interneuron development.

I generated a mouse model of *Ctcf* loss that provides an opportunity to further study ASD, SCZ and ID. I found that early transcriptional compensation restores CTCF levels in the adult brain of this model system. Importantly, I observed brain structural changes in the cerebellum and the limbic system of the *Ctcf*$^{\mathrm{Nestinhet}}$ mice, implicating these structures are important in these human conditions. Further, this signifies that decreased CTCF levels in the embryonic brain are sufficient to cause structural and behavioural changes. Future studies could utilize this mouse model to characterize the abnormalities in the transcriptome and development of the embryonic precursors of these brain structures.

4.12 References

1. Butt, S. J. B. *et al.* The Requirement of Nkx2-1 in the Temporal Specification of Cortical Interneuron Subtypes. *Neuron* **59,** 722–732 (2008).
2. Vogt, D. *et al.* Lhx6 Directly Regulates Arx and CXCR7 to Determine Cortical Interneuron Fate and Laminar Position. *Neuron* **82,** 350–364 (2014).
3. Chen, Y.-J. J. *et al.* Single-cell RNA sequencing identifies distinct mouse medial ganglionic eminence cell types. *Sci. Rep.* **7,** (2017).
4. Zechel, S., Zajac, P., Lönnerberg, P., Ibáñez, C. F. & Linnarsson, S. Topographical transcriptome mapping of the mouse medial ganglionic eminence by spatially resolved RNA-seq. *Genome Biol.* **15,** 486 (2014).
5. O'Roak, B. J. *et al.* Recurrent de novo mutations implicate novel genes underlying simplex autism risk. *Nat. Commun.* **5,** 5595 (2014).
6. Iossifov, I. *et al.* The contribution of de novo coding mutations to autism spectrum disorder. *Nature* **515,** 216–221 (2014).
7. Jin, S. C. *et al.* Contribution of rare inherited and de novo variants in 2,871 congenital heart disease probands. *Nat. Genet.* **49,** 1593–1601 (2017).
8. Kawauchi, S. *et al.* Using mouse and zebrafish models to understand the etiology of developmental defects in Cornelia de Lange Syndrome. *Am. J. Med. Genet. C Semin. Med. Genet.* **172,** 138–145 (2016).

9. Kline, A. D. *et al.* Cornelia de Lange syndrome and molecular implications of the cohesin complex: Abstracts from the 7th biennial scientific and educational symposium 2016. *Am. J. Med. Genet. A.* **173,** 1172–1185 (2017).
10. Davis, L., Onn, I. & Elliott, E. The emerging roles for the chromatin structure regulators CTCF and cohesin in neurodevelopment and behavior. *Cell. Mol. Life Sci. CMLS* (2017). doi:10.1007/s00018-017-2706-7
11. Watson, L. A. *et al.* Dual Effect of CTCF Loss on Neuroprogenitor Differentiation and Survival. *J. Neurosci.* **34,** 2860–2870 (2014).
12. Hirayama, T., Tarusawa, E., Yoshimura, Y., Galjart, N. & Yagi, T. CTCF is required for neural development and stochastic expression of clustered Pcdh genes in neurons. *Cell Rep.* **2,** 345–357 (2012).
13. Gregor, A. *et al.* De novo mutations in the genome organizer CTCF cause intellectual disability. *Am. J. Hum. Genet.* **93,** 124–131 (2013).
14. Bastaki, F. *et al.* Identification of a novel CTCF mutation responsible for syndromic intellectual disability – a case report. *BMC Med. Genet.* **18,** 68 (2017).
15. Kawauchi, S. *et al.* Multiple Organ System Defects and Transcriptional Dysregulation in the Nipbl +/− Mouse, a Model of Cornelia de Lange Syndrome. *PLoS Genet.* **5,** (2009).
16. Gomez-Velazquez, M. *et al.* CTCF counter-regulates cardiomyocyte development and maturation programs in the embryonic heart. *PLoS Genet.* **13,** e1006985 (2017).
17. Juraeva, D. *et al.* Integrated Pathway-Based Approach Identifies Association between Genomic Regions at CTCF and CACNB2 and Schizophrenia. *PLOS Genet* **10,** e1004345 (2014).

18. de Lacy, N. & King, B. H. Revisiting the relationship between autism and schizophrenia: toward an integrated neurobiology. *Annu. Rev. Clin. Psychol.* **9,** 555–587 (2013).
19. Fromer, M. *et al.* De novo mutations in schizophrenia implicate synaptic networks. *Nature* **506,** 179 (2014).
20. Oskvig, D. B., Elkahloun, A. G., Johnson, K. R., Phillips, T. M. & Herkenham, M. Maternal immune activation by LPS selectively alters specific gene expression profiles of interneuron migration and oxidative stress in the fetus without triggering a fetal immune response. *Brain. Behav. Immun.* **26,** 623–634 (2012).
21. Chohan, M. O. & Moore, H. Interneuron Progenitor Transplantation to Treat CNS Dysfunction. *Front. Neural Circuits* 64 (2016). doi:10.3389/fncir.2016.00064
22. Alvarez-Dolado, M. *et al.* Cortical Inhibition Modified by Embryonic Neural Precursors Grafted into the Postnatal Brain. *J. Neurosci.* **26,** 7380–7389 (2006).
23. Hsieh, J.-Y. & Baraban, S. C. Medial Ganglionic Eminence Progenitors Transplanted into Hippocampus Integrate in a Functional and Subtype-Appropriate Manner. *eNeuro* **4,** (2017).
24. Casalia, M. L., Howard, M. A. & Baraban, S. C. Persistent seizure control in epileptic mice transplanted with gamma-aminobutyric acid progenitors. *Ann. Neurol.* **82,** 530–542 (2017).
25. Hammad, M. *et al.* Transplantation of GABAergic Interneurons into the Neonatal Primary Visual Cortex Reduces Absence Seizures in Stargazer Mice. *Cereb. Cortex N. Y. N 1991* **25,** 2970–2979 (2015).

26. Henderson, K. W. *et al.* Long-term seizure suppression and optogenetic analyses of synaptic connectivity in epileptic mice with hippocampal grafts of GABAergic interneurons. *J. Neurosci. Off. J. Soc. Neurosci.* **34,** 13492–13504 (2014).
27. Maroof, A. M. *et al.* Directed differentiation and functional maturation of cortical interneurons from human embryonic stem cells. *Cell Stem Cell* **12,** 559–572 (2013).
28. Nicholas, C. R. *et al.* Functional maturation of hPSC-derived forebrain interneurons requires an extended timeline and mimics human neural development. *Cell Stem Cell* **12,** 573–586 (2013).
29. Marín, O. Human cortical interneurons take their time. *Cell Stem Cell* **12,** 497–499 (2013).
30. Kazdoba, T. M., Leach, P. T. & Crawley, J. N. Behavioral phenotypes of genetic mouse models of autism. *Genes Brain Behav.* **15,** 7–26 (2016).
31. El-Kordi, A. *et al.* Development of an autism severity score for mice using Nlgn4 null mutants as a construct-valid model of heritable monogenic autism. *Behav. Brain Res.* **251,** 41–49 (2013).
32. Milenkovic, M., Mielnik, C. A. & Ramsey, A. J. NMDA receptor-deficient mice display sexual dimorphism in the onset and severity of behavioural abnormalities. *Genes Brain Behav.* **13,** 850–862 (2014).
33. Beery, A. K. & Zucker, I. Sex bias in neuroscience and biomedical research. *Neurosci. Biobehav. Rev.* **35,** 565–572 (2011).
34. Abel, K. M., Drake, R. & Goldstein, J. M. Sex differences in schizophrenia. *Int. Rev. Psychiatry Abingdon Engl.* **22,** 417–428 (2010).

35. Werling, D. M. & Geschwind, D. H. Sex differences in autism spectrum disorders. *Curr. Opin. Neurol.* **26,** 146 (2013).

36. Fink, G., Sumner, B. E., Rosie, R., Grace, O. & Quinn, J. P. Estrogen control of central neurotransmission: effect on mood, mental state, and memory. *Cell. Mol. Neurobiol.* **16,** 325–344 (1996).

37. Crider, A. & Pillai, A. Estrogen Signaling as a Therapeutic Target in Neurodevelopmental Disorders. *J. Pharmacol. Exp. Ther.* **360,** 48–58 (2017).

38. Lindamer, L. A. *et al.* Gender differences in characteristics and service use of public mental health patients with schizophrenia. *Psychiatr. Serv. Wash. DC* **54,** 1407–1409 (2003).

39. Dias, C. *et al.* BCL11A Haploinsufficiency Causes an Intellectual Disability Syndrome and Dysregulates Transcription. *Am. J. Hum. Genet.* **99,** 253–274 (2016).

40. Punwani, D. *et al.* Multisystem Anomalies in Severe Combined Immunodeficiency with Mutant BCL11B. *N. Engl. J. Med.* **375,** 2165–2176 (2016).

41. Simon, R. *et al.* A dual function of Bcl11b/Ctip2 in hippocampal neurogenesis. *EMBO J.* **31,** 2922–2936 (2012).

42. Zheng, F. *et al.* Mutation of the CH1 Domain in the Histone Acetyltransferase CREBBP Results in Autism-Relevant Behaviors in Mice. *PLOS ONE* **11,** e0146366 (2016).

43. Viosca, J., Lopez-Atalaya, J. P., Olivares, R., Eckner, R. & Barco, A. Syndromic features and mild cognitive impairment in mice with genetic reduction on p300 activity: Differential contribution of p300 and CBP to Rubinstein–Taybi syndrome etiology. *Neurobiol. Dis.* **37,** 186–194 (2010).

44. Di Martino, A. *et al.* The autism brain imaging data exchange: towards a large-scale evaluation of the intrinsic brain architecture in autism. *Mol. Psychiatry* **19,** 659–667 (2014).
45. Yoon, J. H. *et al.* Association of dorsolateral prefrontal cortex dysfunction with disrupted coordinated brain activity in schizophrenia: relationship with impaired cognition, behavioral disorganization, and global function. *Am. J. Psychiatry* **165,** 1006–1014 (2008).
46. Lawrie, S. M. *et al.* Reduced frontotemporal functional connectivity in schizophrenia associated with auditory hallucinations. *Biol. Psychiatry* **51,** 1008–1011 (2002).
47. D'Angelo, E. & Casali, S. Seeking a unified framework for cerebellar function and dysfunction: from circuit operations to cognition. *Front. Neural Circuits* **6,** (2013).
48. Liu, H., Fan, G., Xu, K. & Wang, F. Changes in cerebellar functional connectivity and anatomical connectivity in schizophrenia: A combined resting-state functional MRI and diffusion tensor imaging study. *J. Magn. Reson. Imaging* **34,** 1430–1438 (2011).
49. Bottmer, C. *et al.* Reduced cerebellar volume and neurological soft signs in first-episode schizophrenia. *Psychiatry Res. Neuroimaging* **140,** 239–250 (2005).
50. Thomann, P. A. *et al.* Cerebellar substructures and neurological soft signs in first-episode schizophrenia. *Psychiatry Res. Neuroimaging* **173,** 83–87 (2009).
51. Andreasen, N. C., Paradiso, S. & O'Leary, D. S. 'Cognitive dysmetria' as an integrative theory of schizophrenia: a dysfunction in cortical-subcortical-cerebellar circuitry? *Schizophr. Bull.* **24,** 203–218 (1998).

52. Fusar-Poli, P. *et al.* Functional atlas of emotional faces processing: a voxel-based meta-analysis of 105 functional magnetic resonance imaging studies. *J. Psychiatry Neurosci. JPN* **34,** 418–432 (2009).
53. Critchley, H. Explicit and implicit neural mechanisms for processing of social information from facial expressions: A functional magnetic resonance imaging study. *Hum. Brain Mapp.* **9,** 93–105
54. Hashimoto, T. Development of the brainstem and cerebellum in autistic patients. *J. Autism Dev. Disord.* **25,** 1–18 (1995).
55. Bauman, M. L. Neuroanatomic observations of the brain in autism: a review and future directions. *Int. J. Dev. Neurosci.* **23,** 183–187
56. Kana, R. K. *et al.* Aberrant functioning of the theory-of-mind network in children and adolescents with autism. *Mol. Autism* **6,** 59 (2015).
57. Critchley, H. D. The functional neuroanatomy of social behaviour. *Brain* **123,** 2203–2212
58. Tsai, P. T. *et al.* Autistic-like behaviour and cerebellar dysfunction in Purkinje cell Tsc1 mutant mice. *Nature* **488,** 647–651 (2012).
59. Goddyn, H., Leo, S., Meert, T. & D'Hooge, R. Differences in behavioural test battery performance between mice with hippocampal and cerebellar lesions. *Behav. Brain Res.* **173,** 138–147 (2006).
60. Gandhi, C. C., Kelly1, R. M., Wiley, R. G. & Walsh, T. J. Impaired acquisition of a Morris water maze task following selective destruction of cerebellar purkinje cells with OX7-saporin. *Behav. Brain Res.* **109,** 37–47 (2000).

61. Joyal, C. C. *et al*. Effects of midline and lateral cerebellar lesions on motor coordination and spatial orientation. *Brain Res.* **739,** 1–11 (1996).
62. Joyal, C. C., Strazielle, C. & Lalonde, R. Effects of dentate nucleus lesions on spatial and postural sensorimotor learning in rats. *Behav. Brain Res.* **122,** 131–137 (2001).
63. Petrosini, L., Molinari, M. & Dell'Anna, M. E. Cerebellar Contribution to Spatial Event Processing: Morris Water Maze and T-maze. *Eur. J. Neurosci.* **8,** 1882–1896 (1996).
64. Deacon, R. M. J., Bannerman, D. M., Kirby, B. P., Croucher, A. & Rawlins, J. N. P. Effects of cytotoxic hippocampal lesions in mice on a cognitive test battery. *Behav. Brain Res.* **133,** 57–68 (2002).
65. Torremans, A. *et al.* GSA: behavioral, histological, electrophysiological and neurochemical effects. *Physiol. Behav.* **84,** 251–264 (2005).
66. Maguire, E. A., Woollett, K. & Spiers, H. J. London taxi drivers and bus drivers: a structural MRI and neuropsychological analysis. *Hippocampus* **16,** 1091–1101 (2006).
67. Takahashi, A. & Miczek, K. A. Neurogenetics of aggressive behavior: studies in rodents. *Curr. Top. Behav. Neurosci.* **17,** 3–44 (2014).
68. Golden, S. A. *et al.* Basal forebrain projections to the lateral habenula modulate aggression reward. *Nature* **534,** 688 (2016).
69. Bañuelos, C. *et al.* Age-related changes in rostral basal forebrain cholinergic and GABAergic projection neurons: relationship with spatial impairment. *Neurobiol. Aging* **34,** 845–862 (2013).

70. Soshnikova, N., Montavon, T., Leleu, M., Galjart, N. & Duboule, D. Functional analysis of CTCF during mammalian limb development. *Dev. Cell* **19,** 819–830 (2010).

71. Sams, D. S. *et al.* Neuronal CTCF Is Necessary for Basal and Experience-Dependent Gene Regulation, Memory Formation, and Genomic Structure of BDNF and Arc. *Cell Rep.* **17,** 2418–2430 (2016).

72. Declercq, J. *et al.* Metabolic and Behavioural Phenotypes in Nestin-Cre Mice Are Caused by Hypothalamic Expression of Human Growth Hormone. *PLOS ONE* **10,** e0135502 (2015).

73. Giusti, S. A. *et al.* Behavioral phenotyping of Nestin-Cre mice: Implications for genetic mouse models of psychiatric disorders. *J. Psychiatr. Res.* **55,** 87–95 (2014).

74. Breuss, M. *et al.* Mutations in the murine homologue of TUBB5 cause microcephaly by perturbing cell cycle progression and inducing p53-associated apoptosis. *Development* **143,** 1126–1133 (2016).

Curriculum Vitae

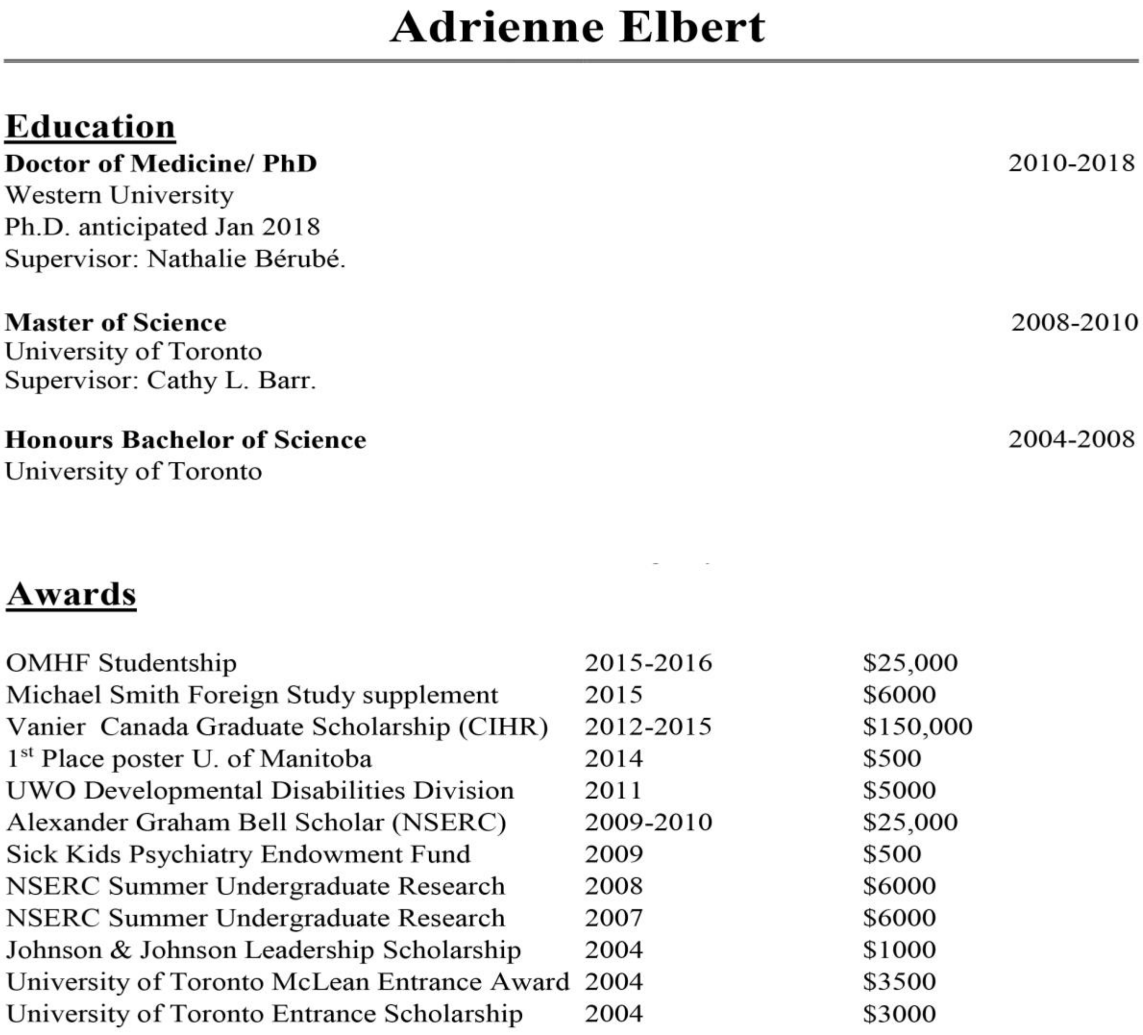

Adrienne Elbert

Education

Doctor of Medicine/ PhD 2010-2018
Western University
Ph.D. anticipated Jan 2018
Supervisor: Nathalie Bérubé.

Master of Science 2008-2010
University of Toronto
Supervisor: Cathy L. Barr.

Honours Bachelor of Science 2004-2008
University of Toronto

Awards

OMHF Studentship	2015-2016	$25,000
Michael Smith Foreign Study supplement	2015	$6000
Vanier Canada Graduate Scholarship (CIHR)	2012-2015	$150,000
1st Place poster U. of Manitoba	2014	$500
UWO Developmental Disabilities Division	2011	$5000
Alexander Graham Bell Scholar (NSERC)	2009-2010	$25,000
Sick Kids Psychiatry Endowment Fund	2009	$500
NSERC Summer Undergraduate Research	2008	$6000
NSERC Summer Undergraduate Research	2007	$6000
Johnson & Johnson Leadership Scholarship	2004	$1000
University of Toronto McLean Entrance Award	2004	$3500
University of Toronto Entrance Scholarship	2004	$3000

Teaching Experience

Jan 2010- Apr 2010 and Jan 2009- Apr 2009: Human genetics small group teaching assistant (U of T). Ran teaching session and small group problems for groups of 25 students.

Research Experience

PhD Thesis: Chromatin organizer CTCF in forebrain development and behaviour. Biochemistry Dept., and Collaborative Program in Developmental Biology, Western University. Children's Hospital, LHSC. Supervisor: Dr. Nathalie Bérubé.

Foreign study during PhD: MSFSS awarded to join Cardoso Lab in Marseille and learn to perform *in utero* electroporation in mice. Institut de neurobiologie de la méditerranée. Supervisor: Dr. Carlos Cardoso.

MSc Thesis: Identification of Genes and Putative Regulatory Variants contributing to Reading Disabilities & ADHD. Institute of Medical Sciences and the Neuroscience Program, University of Toronto. Toronto Western Research Institute and Sick Kids Hospital. Supervisor: Dr. Cathy Barr.

NSERC Undergraduate Summer Project: Testing the involvement of CD36 in maintaining poly-unsaturated fatty acid levels in the mouse brain. Dept. of Nutritional Sciences, University of Toronto. Supervisor: Dr. Richard Bazinet.

Honours Thesis: Autosomal Recessive Mutations in Novel Gene CC2D2A cause Mental Retardation with Retinitis Pigmentosa. Psychiatry Dept., University of Toronto. Centre for Addiction and Mental Health. Supervisor: Dr. John Vincent.

NSERC Undergraduate Summer Project: Developmental constraints: Inducing an extra segment in *Drosophila melanogaster*. Dept. of Cell and Systems Biology, University of Toronto. Supervisor: Dr. Ellie Larsen.

Presentations

Ctcf loss results in fate change of MGE-derived interneurons

March 16-20, 2016: Canadian Developmental Biology Meeting (poster) Banff, Alberta
July 19-24, 2014: Brain Development Meeting (poster) ISDN, NeuroDevNet. Montreal, Quebec
May 21st 2014: Pediatric Research Day (poster)
Children's Hospital, London ON
May 5th 2014: SONA meeting (poster)
Western University, London ON
Mar 18th 2014: London Health Research day (poster)
London Convention Centre, London ON

Ctcf is required for cortical interneuron migration through the regulation of Lhx6

May 30th 2013: Developmental Biology Research Day (London ON) (poster)
Mar 19th 2013: London Health Research day (poster)
London Convention Centre, London ON
May 29th 2013: Pediatric Research Day (Oral presentation)

Investigation of DCDC2 for functionally relevant polymorphisms associated with Reading Disabilities and/or Attention Deficit Hyperactivity Disorder (poster)

May 5th 2010: Institute of Medical Sciences Scientific Day
Medical Sciences Building, University of Toronto

Investigation of chr. 6 genes for functional risk variants in Reading Disabilities and ADHD

Jun 17th 2010: University of Toronto Dept. of Psych Harvey Stancer Day Metro Toronto
Convention Centre, Toronto, Ontario (poster)

Reading Disabilities and ADHD: Candidate Genes on chr6 (poster)

Nov 4-8, 2009: XVII World Congress on Psychiatric Genetics
Manchester Grand Hyatt, San Diego, California
Jun 25th 2009: University of Toronto Dept. of Psychiatry Harvey Stancer Day
Metro Toronto Convention Centre, Toronto, Ontario
Apr 16th 2009: University of Toronto Neuroscience Program Day
Medical Sciences Building, University of Toronto
May 5th 2009: Institute of Medical Sciences Scientific Day
Medical Sciences Building, University of Toronto
May 13th 2009: Toronto Western Hospital Research Day

Publications

The CTCF chromatin organizer dictates cortical GABAergic interneuron fate. **Elbert A.**, Vogt D., Watson L.A., Jiang Y., Brûlé E., Rowland M. E., Rubenstein J. L. R. and Bérubé N.G. 2017. (Submitted to Nature Communications- NCOMMS-17-26776).

Brain dysmorphology and sexually dimorphic behaviour impairments induced by embryonic CTCF haploinsufficiency. **Elbert A.**, Levy M., Watson L.A., Schmid, S., Lerch, J, Bérubé N.G, 2017. (In Preparation).

GnRH Neuron-Specific Ablation of Gαq/11 Results in Only Partial Inactivation of the Neuroendocrine-Reproductive Axis in Both Male and Female Mice: In Vivo Evidence for Kiss1rCoupled Gαq/11-Independent GnRH Secretion. Babwah AV, Navarro VM, Ahow M, Pampillo M, Nash C, Fayazi M, Calder M, **Elbert A**, Urbanski HF, Wettschureck N, Offermanns S, Carroll RS, Bhattacharya M, Tobet SA, Kaiser UB. J Neurosci. 2015 Sep 16;35(37):12903-16.

Implantation failure in female Kiss1-/- mice is independent of their hypogonadic state and can be partially rescued by leukemia inhibitory factor. Calder M, Chan YM, Raj R, Pampillo M, **Elbert A**, Noonan M, Gillio-Meina C, Caligioni C, Bérubé NG, Bhattacharya M, Watson AJ, Seminara SB, Babwah AV. Endocrinology. 2014 Aug;155(8):3065-78.

Dual effect of CTCF loss on neuroprogenitor differentiation and survival. Watson LA, Wang X, **Elbert A**, Kernohan KD, Galjart N, Bérubé NG. J Neurosci. 2014 Feb 19;34(8):2860-70.

Genetic variation in the KIAA0319 5' region as a possible contributor to dyslexia. **Elbert A**, Lovett MW, Cate-Carter T, Pitch A, Kerr EN, Barr CL. Behav Genet. 2011 Jan;41(1):77-89.

Genetic ablation of CD36 does not alter mouse brain polyunsaturated fatty acid concentrations. Song BJ, **Elbert A**, Rahman T, Orr SK, Chen CT, Febbraio M, Bazinet RP. Lipids. 2010 Apr;45(4):291-9.